Finite Element Modelling of Skew Slab with edge supports

A Thesis report submitted in the partial fulfilment of requirement for the award of the degree of

MASTERS OF CIVIL ENGINEERING

IN

STRUCTURES

Submitted By

Sanjay Kumar

Roll No. 820922004

Under the supervision of

Dr. Naveen Kwatra

Associate Professor & Head
Department of Civil Engineering
Thapar University, Patiala

DEPARTMENT OF CIVIL ENGINEERING

THAPAR UNIVERSITY,

PATIALA-147004, (INDIA)

July-2013

DECLARATION

I hereby declare that the work which is presented in this Thesis report entitled "FINITE ELEMENT MODELLING OF SKEW SLAB WITH EDGE SUPPORTS" in partial fulfillment of requirements for the award of the **MASTERs DEGREE** in **CIVIL ENGINEERING,** submitted in the **CIVIL ENGINEERING DEPARTMENT, THAPAR UNIVERSITY, PATIALA,** is an authentic record of the initial work carried out by him under the supervision of **Dr. Naveen Kwatra, Associate Professor & Head,** DEPARTMENT OF CIVIL ENGINEERING , THAPAR UNIVERSITY, PATIALA.

The matter embodied in this report has not been submitted in part or full to any other university or institute for the award of any degree.

Date: 15/7/2013

Sanjay Kumar.
(Sanjay Kumar)

This is to certify that the above declaration made by the student concerned is correct to the best of my knowledge and belief.

15/7/13
(Dr. NAVEEN KWATRA)

Associate Professor & Head
Deptt. Of Civil Engineering,
Thapar University, Patiala

(Dr. S. K. Mohapatra)

Dean Academic Affairs
Thapar University,
Patiala.

15/7/13
`(Dr. NAVEEN KWATRA)

Associate Professor & Head,
Deptt. Of Civil Engineering,
Thapar University, Patiala

ACKNOWLEDGEMENT

First and foremost, I would like to express my deepest appreciation to my thesis supervisor, Associate Professor & Head of the Civil Engineering Department of this institute **Dr. Naveen Kwatra** for their gracious efforts and keen pursuits, which has remained as a valuable asset for the successful instrument of my Thesis Report. His dynamism and diligent enthusiasm has been highly instrumental in keeping my spirit high. His flawless and forthright suggestions blended with an innate intelligent application have crowned my task a success.

I would like to express my gratitude to my family, for their unconditional support and prayers at all times and constant encouragement during the entire course of my thesis work.I am also like to offer my sincere thanks to all faculty, teaching and non-teaching of Civil Engineering (CED) TU, Patiala for their assistance. Thank you.

Sanjay kumar

M.E CIVIL STRUCTURES

ROLL NO 820922004

ABSTRACT

Newly designed bridges are often skew. This is due to space constraints in congested urban areas. Skew bridges allow a large variety of solutions in roadway alignments. This contributes to a small environmental impact for new road construction projects. It can also be needed due to geographical constraints such as mountainous terrains. However, the force flow in skew bridges is much more complicated than in right-angle bridges. Analytical calculations alone do not provide sufficient accuracy for structural design. Numerical analysis needs to be performed, in which a skew bridge can be modelled in several ways with different degrees of sophistication.

The study reveals that the construction of simply supported skew slabs may be recommended only if the short diagonal of the slab is greater than its span otherwise it shows some uplifts at acute corners. The study deals with "Finite Element modelling of the RCC Skew slab with edge supports" with the help of ATENA. The ATENA is new FEM based software which helps in FEM modeling the RCC structure.

The behavior of the simply supported skew slab under point load applied at the centre depends on the ratio of short diagonal to its span. Skew slabs with ratio of short diagonal to span less than unity show lifting of acute corners whereas slabs with ratio of short diagonal to span greater than unity do not. This is because the reactions act at the obtuse corner only when the ratio of short diagonal to its span less than unity and it is well within supports when ratio of short diagonal to span is greater than unity.

In the present work FE modeling of the skew slab specimen with edge supports has been done and the results obtained are compared with experimental result of the skew slab without edge beam. By introducing edge supports in the skew slab the load carrying capacity has been almost increase by 2.5 times.

TABLE OF CONTENTS

LIST OF TABLES

LIST OF FIGURES

CHAPTER-1, INTRODUCTION

1.1 GENERAL DESCRIPTION

Reinforced concrete skew slabs are widely used in bridge construction when the roads cross the streams and canals at angles other than 90 degrees. They are also used in floor system of reinforced concrete building as well as load bearing brick buildings where the floors and roofs are skewed for architectural reasons or space limitations.

Due to increasing population in India, the demand for more roads and highways are increasing and more of them would require more intersections of roads and highways. To maintain steady flow of traffic in these intersections it will be necessary that they be designed with grade separation, which indicates that more skew slab and deck bridges will be constructed in future.

Skew slab bridges may be required to maintain the geometry of the road or keep the road straight at crossing or for any other reason. In the present work Finite Element modelling of RCC skew slab has been done in ATENA. Various researchers have used yield criterion for normal and skew slabs, for predicting the collapse load. An analytical model has been developed for calculating load and deflection in ATENA. Results of the analytical work (ATENA) have been confirmed by experimental work. The study of the skew slabs simply supported on two opposite rigid supports has revealed the following facts;

Skew slabs simply supported on two opposite side span can be divided into two types depending on the shape and the behavior of slabs.

i. Skew slab with ratio of short diagonal to span less than unity,
ii. Skew slab with ratio of short diagonal to span greater than unity,

The behavior of the simply supported skew slab under point load applied at the centre depends on the ratio of short diagonal to its span. Skew slabs with ratio of short diagonal to span less than unity show lifting of acute corners whereas slabs with ratio of short diagonal to span greater than unity do not. This is because the reactions act at the obtuse corner only when the ratio of short diagonal to its span less than unity and it is well within supports when ratio of short diagonal to span is greater than unity[(1)]. In this study edge supports has been considered with the skew slabs to minimize the uplift.

1.2 BACKGROUND

Newly designed bridges are often skew. This is due to space constraints in congested urban areas. Skew bridges allow a large variety of solutions in roadway alignments. This contributes to a small environmental impact for new road construction projects. It can also be needed due to geographical constraints such as mountainous terrains. However, the force flow in skew bridges is much more complicated than in right-angle bridges. Analytical calculations alone do not provide sufficient accuracy for structural design. Numerical analysis needs to be performed, in which a skew bridge can be modelled in several ways with different degrees of sophistication.

In right-angle bridges the load path goes straight towards the support in the direction of the span. In skew bridges this is not the case. For a solid slab skew bridge the load tends to take a short cut to the obtuse corners of the bridge. In bridge decks supported by longitudinal girders this effect occurs too, although less pronounced. This change in direction of the load path in very skew bridges brings about the following special characteristics.

- Significant torsional moments in the deck slab
- Decrease in longitudinal moment
- Increase in transverse moment
- Concentration of reaction forces and negative moments at the obtuse corners
- Small reactions and a possibility of uplift reaction forces at the acute corners

These special characteristics of skew bridges make their analysis and design more intricate than right bridges. [(2)]

Significant research efforts have been devoted to the application of finite elements in the analysis of reinforced concrete since the emergence of the finite element method in the 1950s. While many achievements have been accomplished in research environments, few of these achievements have been implemented in practical applications for structural engineers in the design office. While much analytical work has been focused on the application of nonlinear constitutive modeling of reinforced concrete, most software packages currently implemented offer only linear elastic finite element capabilities. The following review details the progression from the conception of finite element based slab design to the current state of the art. Much of the work cited deals primarily with the modeling and analysis of slab systems by the finite element method, without explicitly discussing reinforcement design. However, the primary

purpose of the finite element model is the determination of design forces and moments, and once these quantities have been accurately determined, the resulting design becomes a function of the active design code.[(2)]

It can be seen that large skew angles always reduce the longitudinal bending moment and increases the torsion moment at the obtuse corner of the bridge and the transverse bending in the deck. This might be due to the fact that some of the wheels of trucks on skew bridges are closer to the supports than on right bridges. Another reason may be that in short spans with large skew angle bridges, the slab tends to bend along a direction perpendicular to the abutments. This action can transfer part of the load from deck slabs directly to the supports, rather than through the girders as in right bridges

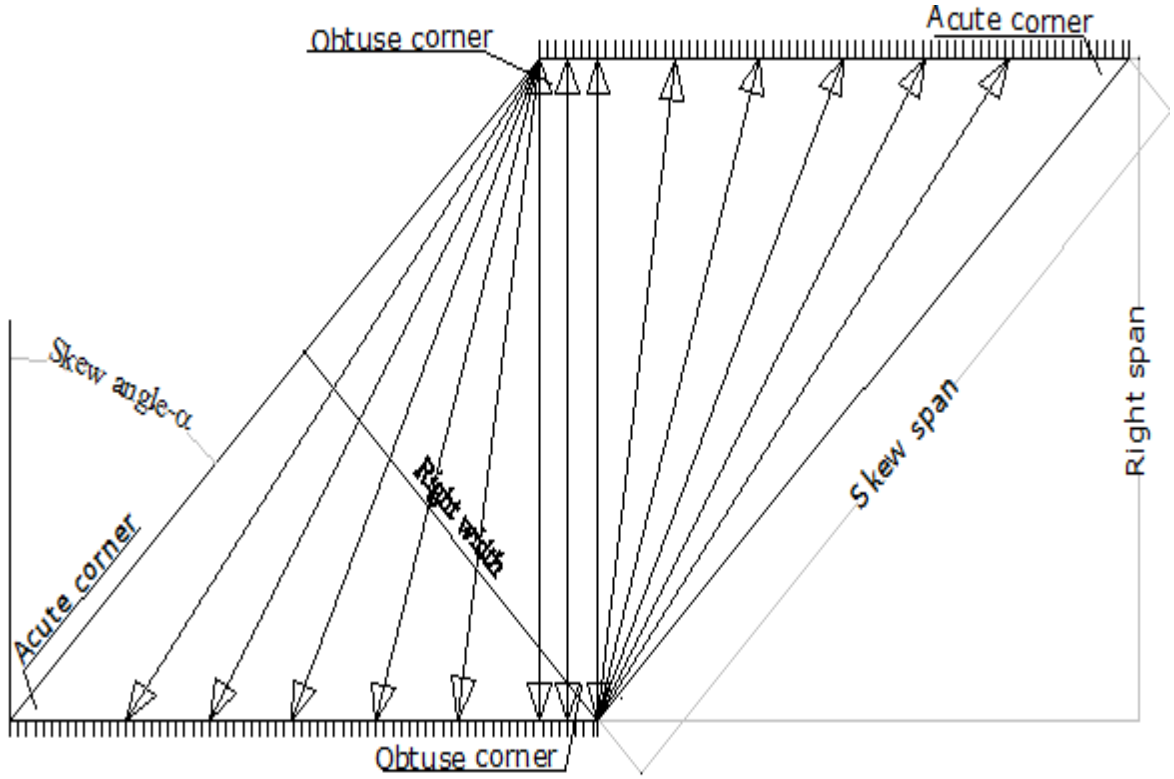

Figure 1.1 Load path of skew bridge [2]

1.3 METHODS OF ANALYSIS OF SKEW SLAB

The analytical treatment of the behavior of skew plates is rather involved complexity as compared to rectangular plates, because of irregular behavior at the corners. Reinforced concrete

skew slabs because of its own non-linear behavior add further to the complexity of the problem. There exist some numerical methods of elastic analysis of skew orthotropic plates and slabs. The finite element method is the most powerful and versatile tool for the analysis of complex structures. However, alternative finite strip method is equally powerful, efficient and requires fewer efforts in the preparation of input data files. The skew slabs are designed by same theories of bending and shear as are used for beam.[(2)] The following methods of analysis are available:

- Method of Grillage analogy
- Finite strip method
- Finite element method

1.3.1 METHOD OF GRILLAGE ANALOGY

Grillage analogy is one of the most popular computer-aided methods used for analyzing bridge decks. The method consists of representing the actual decking system of the bridge by an equivalent grillage of beams. The dispersed bending and torsional stiffness of the decking system are assumed, for the purpose of analysis, to be concentrated in these beams. The stiffness of the beams is chosen so that the prototype bridge deck and the equivalent grillage of beams are subjected to identical deformations under loading. The method is applicable to bridge decks with simple as well as complex configurations with almost the same ease and confidence. The method is easy to comprehend and use. The analysis is relatively inexpensive and has been proved to be reliably accurate for a wide variety of bridges. The grillage representation helps in giving a feel of the structural behavior of the bridge and the manner in which the loading is distributed and eventually taken to the supports. The grillage analogy method, which is a computer-oriented technique, is increasingly being used in the analysis and design of bridges. The method is also suitable in cases where bridge exhibits complicating features such as heavy skew, edge stiffening and isolated supports. The method is versatile in nature and the contribution of kerb beams and the effect of differential sinking of girder ends over yielding bearings (such as neoprene bearing) can also be taken into account and large variety of bridge decks can be analyzed with sufficient practical accuracy.

The method consists of ‘converting’ the bridge deck structure into a network of rigidly connected beams at discrete nodes i.e. idealizing the bridge by an equivalent grillage. The deformations at the two ends of a beam element are related to the bending and torsional moments through their

bending and torsional stiffness. Bridge deck is analyzed by the method of Grillage Analogy. There are four steps to be followed for obtaining design responses

i. Idealization of physical deck into equivalent grillage;
ii. Evaluation of equivalent elastic inertias of members of grillage;
iii. Analyse the structure; and
iv. Interpretation of results.

The method of grillage analysis involves the idealization of the bridge deck as a plane grillage of discrete inter-connected beams. It is difficult to make precise general rules for choosing a grillage mesh and much depends upon the nature of the deck to be analysed, its support conditions, accuracy required, quantum of computing facility available etc. and only a set of guidelines can be suggested for setting grid lines. It may be noted that such idealization of the deck is not without pitfalls and the grid lines adopted in once case may not be efficient in another similar case and the experience and judgment of the designer will always play a major role. [(3)]

1.3.2 FINITE STRIP METHOD

In the finite strip method the structure is divided into a set of finite strips of the length *L* (*L* is width of the slab) and an arbitrary width *b*. The unknowns are displacements *u* and *v* (in the *x* and *y* directions) along the nodal line *r* which connects two adjacent strips. It is assumed that the present approach has considerable advantage over the finite element method for certain class of problems. For analyzing reinforced concrete skew slabs with various boundary conditions and loadings, the finite strip method has proven to be the most efficient numerical method. It uses a series of orthogonal functions in the longitudinal direction; Y, combined with the conventional finite element polynomial shape function in the transverse direction; X, to simulate all the displacement components of the structure. In this way, the number of dimensions of the analysis is reduced by at least one. Consequently, computer time, storage and input data requirements are reduced significantly.

Cheung Y. K. first studied the finite strip method for analysis of simply supported bridge deck Structure, in 1968. Powell and Ogden also suggested the finite strip method for rectangular slab type bridge decks independently, in 1969. Since then, considerable research and development on that method have been carried out in many countries. Among them, the main subjects related to the finite strip analysis in structural engineering may be listed as follows; [(3)]

- A finite strip method for plastic collapse analysis of compressed plate and plate assemblage, 1983.
- Compound finite strip method for analysis of plates continuous over intermediate flexible beams and columns using a direct stiffness methodology since 1983.
- Post-buckling behavior and geometrically nonlinear analysis of plate structures since 1981-1985.
- Material nonlinear analysis of steel structures since 1986.
- Material nonlinear analysis of reinforced concrete slabs 1988.
- Large-deflection elastic-plastic analysis of plate structures 1989.

1.3.3 FINITE ELEMENT METHOD

The finite element method has been an obvious choice for the modeling and analysis of reinforced concrete systems for many years. Finite elements have the unique capability to conform to virtually any geometry that could be physically implemented. Thus, the finite element method has gained acceptance as an appropriate tool for the analysis of flat plates, especially those with highly irregular or unusual geometries where the direct design and equivalent frame techniques are not valid. In irregular slabs such as these, the finite element method can be shown to accurately solve for the distribution of stress where numerous approximations and assumptions would be invoked if the yield line or strip design technique were applied.

An additional benefit of a finite element approach to slab design is that engineers no longer need to develop multiple models to design a structure for various types of behavior. By integrating the slab model with the three-dimensional frame, the combined effects of gravity and lateral loading conditions can be assessed together. The interaction of the slab and columns is accurately simulated, providing favorable results to approximations of connection stiffness. An integrated approach to analysis and design thus emerges.

Significant research efforts have been devoted to the application of finite elements in the analysis of reinforced concrete since the emergence of the finite element method in the 1950s. While many achievements have been accomplished in research environments, few of these achievements have been implemented in practical applications for structural engineers in the design office. While much analytical work has been focused on the application of nonlinear

constitutive modeling of reinforced concrete, most software packages currently implemented offer only linear elastic finite element capabilities.

The following review details the progression from the conception of finite element based flat plate design to the current state of the art. Much of the work cited deals primarily with the modeling and analysis of flat plate systems by the finite element method, without explicitly discussing reinforcement design. However, the primary purpose of the finite element model is the determination of design forces and moments, and once these quantities have been accurately determined, the resulting design becomes a function of the active design code

1.4 OBJECTIVE

The main objective of this study is to investigate the effects of edge supports on behaviour of skew slab using finite element techniques. In the present investigation, the nonlinear response of RCC skew Slab under the point loads with incremental load pattern has been studied with the intent to investigate the relative importance of edge supports in the behaviour of skew slab. This will include the variation in load displacement graph, load and uplifts graph, the crack patterns, propagation of the cracks, the crack width and the effect of size of the finite element mesh on the analytical results and the effect of the nonlinear behavior of concrete and steel on the response of control Slab and the deformed slab.

The following will be the main objectives of the study:

- To study the response and load-carrying capacity of RCC skew slab with edge supports using non-linear finite element analysis.
- To model the skew slab specimen with angle 16.49^0 and aspect ratio i.e. ratio of supported length and span along the traffic 0.49, 0.65.
- Verify FEM-Design's results of internal forces and crack propagation.
- To compare the results of the F.E model slab results with the experimental results.

1.5 SCOPE OF THE WORK

In the present study of FE modelling of the RCC skew slab under the incremental loads has been analyzed using ATENA software and the results so obtained have been compared with available

experimental and analytical results taken from report ("*Finite Element Modelling of Reinforced Cement Concrete Skew Slabs Madhu Sharma*) [(1)]

Two specimen of skew slab with edge supports has been modeled with skew angle 16.49^0.

1. Length of short diagonal of skew slab less than its span measured along the traffic.
2. Length of short diagonal of skew slab greater than its span measured along the traffic.

The skew slab is analyzed using ATENA software up to the failure and the load deformation curves are plotted and the cracking behaviour is monitored. The skew slabs have been analyzed and results have been compared with the experimental results.

The following parameters are proposed to be measured:

i) Nonlinear load-deflection behaviour.

ii) Study of crack patterns at different load steps.

iii) Level/type of damage and location of damage.

1.6 IMPORTANCE OF FINITE ELEMENT MODELLING

To model the complex behaviour of reinforced concrete analytically in its non-linear zone is difficult. This has led engineers in the past to rely heavily on empirical formulas which were derived from numerous experiments for the design of reinforced concrete structures. The Finite Element method makes it possible to take into account non-linear response. The FE method is an analytical tool which is able to model RCC structure and is able to calculate the non-linear behaviour of the structural members is Finite element method. For structural design and assessment of reinforced concrete members, the non-linear finite element (FE) analysis has become an important tool. The method can be used to study the behaviour of reinforced and pre stressed concrete structures including both force and stress redistribution.

With the advent of digital computers and powerful methods of analysis, such as the finite element method many efforts to develop analytical solutions which would obviate the need for experiments have been undertaken by investigators. The finite element method has thus become a powerful computational tool, which allows complex analyses of the nonlinear response of RC structures to be carried out in a routine fashion [3].

FEM is useful for obtaining the load deflection behaviour and its crack patterns in various loading conditions. The finite element method has a number of advantage, they include the ability to:

a. Model irregularly shaped bodies and composed of several different materials.
b. Handle general load condition and unlimited numbers and kind of boundary conditions.
c. Include Dynamic effects.
d. Handle nonlinear behavior existing with large deformation and non linear materials.

1.7 ORGANIZATION OF THE THESIS

Keeping in view the above objective, the thesis is divided into five chapters, The thesis is organized as par detail given below:

Chapter 1: Introduces to the topic of thesis in brief.

Chapter 2: Discusses the literature review i.e. the work done by various researchers in the field of FE modelling of RCC skew slabs and structural members .

Chapter 3: Deals with the details of the structure modelled in Atena in its first part. Second part comprises of FEM modelling, theory related to the ATENA, material modelling and analytical programming procedure steps involved in modelling of the RCC skew slabs. It also deals with the description of the material behaviour of concrete, reinforced steel bars.

Chapter 4: The results from the analysis, comparison between the analytical and the experimental results, results comparison between the cracking behaviour of the skew slab.

Chapter 5: Finally, salient conclusions and recommendations of the present study are given in this chapter followed by the references.

CHAPTER 2, REVIEW OF LITRATURE

2.1 GENERAL

In order to contextualize the current work, related works from literature is discussed. In addition a thorough review of literatures on various aspects nonlinear FE analysis of RC skew slab bridge and other factors that is load distribution, shear and reaction distribution, effect of skew angle in bridges is presented. This chapter gives a comprehensive review of the work carried out by various researches in the field of normal and skew slabs.

2.2 LATERAL LOAD DISTRIBUTION USING FINITE ELEMENT ANALYSIS

Many studies of skewed bridges using finite element analysis have been made in the past years especially on live load distributions in the transverse direction. For instance,

Mohammad, Khaleel and Rafik (1990), conducted finite-element analysis to determine moments in continuous right and skew slab-and-girder bridges due to live loads. They analyzed 112 continuous bridges, each having five pretensioned I girders. The spans vary between 24.4 and 36.6 m and are spaced between 1.8 and 2.7 m on center. The skew angle varies between 0 and 60°. The finite element analysis makes use of a skew stiffened plate which consists of two thin shell elements and one beam element. The two thin shell elements are connected to the beam element by rigid links. The element used to model the reinforced concrete deck slab is an 8 node isoperimetric thin shell element with six degrees of freedom at each node. In this study it is concluded that larger skew angle significantly reduces the design longitudinal moment. The reduction of maximum positive and negative moments in the interior girders is less than 6% for skewness of less than 30° and as much as 29% when skew angle is 60°. The reduction of the maximum positive or negative bending moments in the exterior girders is less than 10% for angles of skew less than 45° and as much as 20% when skew angle is 60°.[(5)]

Mabsout et al. (1997), compared four finite-element modeling methods to determine load distribution factors for a one-span, two-lane, simply supported, composite steel girder bridge. In the first method, the concrete slab was modeled with quadrilateral shell elements, and the steel girders were idealized as space frame members. The centroid of each girder coincided with the

centroid of the concrete slab. In the second model, the concrete slab was modeled with quadrilateral shell elements and eccentrically and rigidly connected to space frame members, which represented the girders. In the third method, the concrete slab and steel girder web were modeled with quadrilateral shell elements. Girder flanges were modeled as space frame elements, and flange-to-deck eccentricity as modeled by imposing a rigid link. In the fourth method, the concrete slab was modeled with isotropic, eight-node brick elements; the steel girder flanges and webs were modeled with quadrilateral shell elements. All of the four finite-element models produced similar load distribution factors. The results indicated that the concrete slab could be modeled with sufficient accuracy as quadrilateral shell elements and the girders as concentric space frame elements. [(6)]

Khaloo and Mirzabozorg(2003), have also conducted three-dimensional analysis for skew simply supported bridges of concrete decks with five concrete I-section precast prestressed girders using ANSYS. Span lengths, skew angles, girder spacing, and arrangements of internal transverse diaphragms were the basic variables. In all models two end diaphragms and different arrangements of internal transverse diaphragms are considered. They analyzed Bridges with three span lengths of 25, 30, and 35 m. Girder spacings of 1.8, 2.4 and 2.7 m and skew angles of 0^o, 30^o, 45^o, and 60° are chosen in the skew bridge models. Three different arrangements for internal transverse diaphragms are considered. In the first pattern the models do not include any internal transverse diaphragms. In the second pattern, internal transverse diaphragms are parallel to the axis of the support, and in the third pattern internal transverse diaphragms are perpendicular to the longitudinal girders. In their study, they showed that the skew angle of the deck is the most influential factor on load distribution. The load distribution factors of skew bridges are always less than those of right bridges. The load distribution factor of external girders reduces by 24% for a skew angle of 60° as compared with right bridges. In addition the study showed the sensitivity of load distribution factors of internal girders with respect to skew angle. For decks with a skew angle of 60° the distribution factors decrease by 26.3% as compared with right bridges. However, for decks with a skew angle up to 30°, this effect is insignificant. In this study for system without internal transverse diaphragms, the load distribution factors of external girders are not influenced significantly when skew angle increases; however, these factors decrease up to 18% in internal girders. When the transverse diaphragms are parallel to the axis of

the support, load distribution factors of external girders decrease up to 19% and those of the internal girders are approximately constant when skew angle increases. When the internal transverse diaphragms are perpendicular to the girders, distribution factors of both internal and external girders decreases as skew angles increases and are more sensitive than the other two systems with respect to skew angles. In general, for large skew angles, the effect of internal diaphragms parallel to the supporting lines is insignificant. Also, in various skew angles, the effect of spacing between internal transverse diaphragms perpendicular to longitudinal girders is insignificant. [(7)]

Huang, Shenton, and Chajes (2004), carried out field testes and theoretical analyses using finite element methods for two span continuous slab-on-steel girder composite Bridge with a skew angle of 60°. The main objectives of this study were to experimentally evaluate the load distribution for the highly skewed bridge, compare the predictions resulting from the AASHTO formulas with the field test results, and verify the theoretical analyses using the finite element method with the field test results. A three-dimensional finite element model of the bridge was developed using the commercial program ANSYS. In the numerical model, the influence of the transverse diaphragms and diaphragm stiffness was analyzed by considering three different cases: diaphragms with the stiffness calculated from the real cross frames, diaphragms with one-half the calculated stiffness, and finally, no transverse diaphragms at all. The effect of end diaphragms is revealed at the pinned ends of the girder. Without diaphragms, the strain at the support was exactly zero. However, for the case with diaphragms at the pinned ends of girders at the acute corner side of the bridge, positive strains appeared, and at the pinned ends of girders at the obtuse corner side of the bridge, negative strains appeared. Due to these negative strains at the pinned ends, positive strains at the middle of the span are reduced. Results of this research also showed that the strains in the girders away from the load decreased and the strains in the girders under the load increased when the stiffness of the diaphragms was reduced. However, comparing the case with the full stiffness to the case with half the stiffness, the difference in the peak strains is not significant. That mean, the peak strains change more slowly as the stiffness of the diaphragm increases, showing that the influence of the diaphragms is not linear. This study additionally showed that, the analytical results are in good agreement with the measured data.

The numerical model is slightly stiffer than the real structure; i.e., the model predicts smaller strains than recorded in the girders farthest from the load. [(8)]

Maher Shaker Qaqish,(2006), This research is concerned of studying the variation of bending moments in the longitudinal and transverse directions in the concrete slab of skew bridges. The superstructure used is composed of prestressed concrete beams 26 m length spaced at 2.2 m centre to centre with cast in situ concrete slab 20 cm depth supported by 5 cm precast concrete slab to save scaffolding. The total width of deck slab is 10.5 m with 5 prestress concrete elements AASHTO type IV. The skew angle used is 35^0 and the method used in the analysis of deck slab is finite element method. A finite element model was carried out for prestressed precast beams and cast in situ slab bridge. This structural model was subjected to 1.8 AASHTO truck loading, 1.8 AASHTO equivalent distributed loading and abnormal loading. These results for transverse and longitudinal moments were compared with the result obtained from AASHTO specification. This comparison shows that applying AASHTO specification for slab bridge deck is safe and economical. [(9)]

Menassa, Mabsout, Tarhini and Frederick (2007), have conducted FEA for simply supported, one-span, multilane skew reinforced concrete slab bridges. Four span lengths were considered in this parametric study as 7.2, 10.8, 13.8, and 16.2 m with corresponding solid slab thicknesses of 450, 525, 600, and 675 mm respectively. One, two, three, and four lane bridges without shoulders at both free edges were investigated. The effect of skewness is studied by combining the spans and lanes considered with skew angles varying between 0^o and 50° by increments of 10^o. Right bridges, zero skew angles, served as a reference for comparison with skewed bridges. The general FEA program, SAP2000 (1998), was used to generate the three-dimensional (3D) finite-element models. The concrete slabs were modeled using quadrilateral shell elements with 6 degree of freedom at each node. From this study, they concluded the following:

1. The ratio between the FEA longitudinal moments for skewed and straight bridges was almost one for bridges with skew angle less than 20°. This ratio decreased to 0.75 for bridges with skew angles between 30^o and 40°, and further decreased to 0.5 as the skew angle of the bridge increased to 50°
2. This decrease in the longitudinal moment ratio is offset by an increase by up to 75% in the maximum transverse moment ratio as the skew angle increases from 0^o to 50°.

3. The ratio between the FEA maximum live-load deflection for skewed bridges and right bridges decreases in a pattern consistent with that of the longitudinal moment. This ratio decreases from one for skew angles less than 10° to 0.6 for skew angles between 40° and 50°. The above research finally recommends that engineers should perform three-dimensional finite-element analysis when the skew angle is greater than 20°. [(10)]

Trilok Gupta and Anurag Misra (2007), studied the effect of skew on the behavior of T beam bridges of short to medium range of spans where the span and width are of the same order. The study was carried out for two lane T-Beam girder bridges of 8m, 16m, 24m and 32m right spans and 0^0, 10^0, 20^0, 30^0, 40^0, 50^0 and 60^0 skew angles using grillage analogy method. This research has concluded the following.

a. The maximum support reaction is occurred at the support near obtuse corner with the exception of 0^0 skew angle, for which the maximum reaction was occurred at the support of the middle girder.

b. For skewness of greater than 30^o, the minimum reaction force is negative (uplift reaction). For large span bridges, this negative reaction starts at 20^o skewness and increases with the angle of skew. [(11)]

2.2.1 DESIGN BASED ON LINEAR AND NON LINEAR ANALYSIS

Sawko and Cope (1969), considered the application of finite elements to the case of skew bridge decks. The benefits of the finite element method with respect to model testing, finite difference methods, and the grillage approach were presented. The application of finite elements to orthotropic skew decks, with longitudinal stiffness greater than transverse stiffness, was detailed and shown to provide accurate results. This work also emphasized the importance of Poisson ratio effects, citing that neglect of Poisson ratio effects can lead to underestimation of maximum longitudinal moments by as much as 6% and transverse moments by as much as 16%.[(12)]

Cusens and Besser (1980), investigated a skew bridge deck with particular focus on the obtuse corners and boundaries in determination of shear forces in the slab. The slab evaluated contained a 45^0 skew angle, and was modeled as simply supported with one end restrained with semi-infinite rigidity and the other end with several discrete elastic supports. They found that the

Kirchoff boundary conditions introduce physically significant corner and edge forces near obtuse corners, distributing a large shear force close to the edge. Also, elastic bearings were recommended in the regions near obtuse corners in order to provide a more even distribution of reaction forces. Significant reversals in bending moment were detected near obtuse corners as well as the largest values of torsional moment. [(13)]

Barzegar and Maddipudi (1994), extended many of the common nonlinear finite element reinforced concrete techniques with respect to the simulation of reinforcement in three-dimensional solid elements. Instead of either a smeared or layered approach, a model for spatially embedded reinforcement independent of the finite element nodal coordinates was presented by which an entire reinforcement cage is automatically mapped into a mesh of solid isoparametric concrete elements. This technique was shown to be not only applicable to straight reinforcing bars, but also readily applicable to prestressed systems in which the strand geometry can be approximated using a piecewise linear tendon distribution. [(14)]

James A. Kankam and Habib J. Dagher, (1995), has developed a program (NARCOS) for nonlinear analysis of RC skewed slab bridge. The program is based is based on a layering formulation in which the cross section is devided into steel and concrete layers,with nonlinear material properties.concrete layers simulated with four- node plane stress and midlin plate element ; steel layers are modelled with plane stress element. Transverse shear deformation are considered. Interlayer compatibility is satisfied by constraining in-plane displacements along common interfaces to be same for the adjacent layers. An efficient alogrithm is used for assembly of the stiffness matrix and solution of the equilibrium equations. Comparison with experimental and other analytical results indicates the efficiency of procedure embodied in the program. The program is used to analyze different models of skewd slab bridge in order to assess the relative merits of two different methods of designing such bridge. Bridge design with increased reinforcement at the obtuse corner have a higher crack-intiation load and a higher ultimate strength than bridges designed with uniform reinforcement in the slab.

The main objective of the research to describes the nonlinear finite element analysis of skewed slab bridge to obtain the effects of steel redistribution near the obtuse corners on the service ability and ultimate strength of these bridges. The nonlinear analysis was carried out with a

specially written finite element program called NARCOS.comparision of NARCOS results with analytical and experimental results of other reseachers indicates that NARCOS has a high level of accuracy.comparision of results obtained for the two models of skewed slab bridge whose design is based on linear finite element analysis in which more reinforcement is placed near the obtuse corner than near the acute corner has ahigher crack intiation load than a corrosponding bridge designed with uniform reinforcement even though the total amount of steel in the two bridges may be practically the same.a skewed slab bridge with more reinforcement near the obtuse corner has a higher ultimate strength than a corrosponding bridge design with uniform reinforcement. [(15)]

Denton and Burgoyne (1996), Wood- Armer had derived equations for the design of reinforced concrete slabs subject to complex loadings. The equations insure that the capacity of a slab is not exceeded in flexure by an imposed loading, whilst minimizing the total amount of reinforcement required. This equation leads to a conservative estimate of structure capacity where steel is not distributed optimally. The optimality condition is a constraint in design problems that is not relevant to assessment problems and its use can lead to adequate structures being condemned as unsafe.

Denton- Burgoyne have conducted a analysis which was based on the same fundamental principal as those set by hillerbourg, which were extended by Wood & Armer in the derivation of Wood-Armer equations. It was assumes that the reinforcement arrangement is already known. The methodology provides a systematic approch to assess whether a reinforced concrete slab has sufficient capacity to withstand an imposed loading,quantified by determination of the factor of safety on that loading.

However by adopting the alternative methodology based on the same fundamental principal, a more accurate assesment of the stuctural capacity unde an imposed field of moments can be achived. In most of the cases, this approch will lead to a higher assessed capaciy for bridges previously analysed using the Wood-Armer equations and found to requires a load restictions. [(16)]

Bruce W.Golley (1998), made an excellent contribution to understanding the behavior of continuous skew bridges, and presented valuable empirical formulas to predict reaction and shear distributions under dead and live loads. The demonstration carried out through model tests and

finite element analysis the critical nature of obtuse corners in both single span and multispan bridges. The supports reactions calculated under simulated truck loading during tests and verified by finite element modeling. The concluded observations

1. In the case of bridge model 1 with skew angle 0^0 to $14.1^{0.}$ The maximum reaction at simply supported end of the loaded long span increased from 10.4 KN. In rectangular bridge model 1 maximum reaction occurred at interior beam.
2. In the case of bridge model 2 with skew angle 45^0 an increase of about 36%. In skewed bridge model 2 the maximum reaction occurred at the outside beam at an obtuse corner.

An elastic analysis carried out using finite element program LUSAS (LUSAS 1994). The bridge deck was modeled as an equivalent thick orthotropic plate using 504 8- node curved quadrilateral elements. The obtuse corners satisfied the shear provision of the ASTROADS Bridge design code under a force of 756 KN. It was determined that an upward force of applied at bearing would cause a yield line to develop at corner. It can be seen that maximum reaction at obtuse corners is 2.3 times the maximum reaction at the acute corner. Also found that maximum reaction occurs at obtuse corners of single and multi-span skew bridges. The failure of obtuse corners occurs due to the direction of the transverse reinforcement in the top and the bottom of slab. The transverse reinforcement placed in the skew direction. Earlier investigations also shown that when transverse reinforcement placed normal to the bridge centerline, that significantly increase the bridge stiffness, but it also prevents or reduces considerably the possibility of cracking at the obtuse corners. [(17)]

Phuvoravan and Sotelino, (2005), has proposed a new finite element analysis procedure for nonlinear analysis of reinforced concrete slab. The proposed element combines a four nodes Kirchhoff shell element for concrete with two node Euler beam elements for the steel reinforcement bars. The connectivity between reinforcement beam element and concrete shell element was achieved by means of rigid link and by using the transformation method for rigid link; beam nodes were eliminated from the final mesh of the structure. The new finite element was then, verified with experimental result and it was shown there exist good agreement between the analysis result and the values; obtained from the experimental result. [(18)]

Hossain and Olufemi, (2005) has developed finite element prediction process for the development of charts for accurate peak load determination of simply supported, reinforced

concrete slabs under uniformly distributed loading. Through a series of parametric studies using a simple concrete model, the simulation of tests on four simply supported slabs was used as a basis for establishing a set of optimum parameter values and computational conditions, which guarantees acceptable solution. The reliability of the established parameter values for prediction purposes was verified by the direct simulation of 11 other slabs. Following the successful reliability check, the finite element model was used for analyzing 270 "computer model" slabs, from which charts were developed. These charts serve for quick and reliable peak load determination of arbitrary simply supported slabs. A comparative study of the direct finite element and chart predictions, with values from analytical and design methods, reveals the superiority of the charts over the latter methods, with accuracy comparable to that of the optimized finite element model. The chart prediction is noted to be accurate to within 4% of test results. A strategy for displacement determination is also established, with the same degree of success and the paper discusses possible practical applications of the developed finite element system.

The 3D degenerated, layered shell element formulation, having five degrees of freedom at each node is used in the finite element discretization and parametric studies are carried out with reduced, selective and full integration schemes. Reinforcing steel is represented with a layer of equivalent thickness, with nonlinear uniaxial strength and rigidity properties. Geometric nonlinearity is taken into account using the total Lagrangian approach.

A plasticity formulation based concrete material model, having a dual criterion for yielding and crushing, in terms of stresses and strains respectively, is adopted. The perfectly plastic or strain hardening plasticity model for concrete is given a one-dimensional representation. Plasticity formulation incorporates concepts such as yield criterion, flow and hardening rules, and as in this case, crushing condition. The yield function is assumed to be a modified Drucker Prager surface

Finite element idealization The slabs are idealised with the 3D degenerated, 9-noded Heterosis elements, with each node having five degrees of freedom. A symmetric quarter of the slab is discretized into nine elements. For slabs with irregular reinforcement spacing, the averaged spacing is used to calculate the idealised amount of reinforcement in the elements. The concrete depth is discretized into 10 layers of equal thickness. [(19)]

Sharma M. (2011), In the present work, F.E. model for skew slabs with any degree of skew angle and aspect ratio developed using ATENA. The non-linear response of RCC skew slab specimens using FE Modelling under the incremental loading has been carried out with the intention to study the relative importance of several factors in the non-linear finite element analysis of RC skew slabs It has been noticed that the skew slabs using bridges with short diagonal less than its span causes lifting of acute corners under loading, whereas other does not. The study of skew slabs simply supported on two opposite rigid supports revealed the following fact.

Skew slab simply supported on two opposite sides can be divided into two types depending on the shape and behavior of slabs.

1. Skew slab with ratio of short diagonal to span less than unity.
2. Skew slab with ratio of short diagonal to span greater than unity.

Skew slabs with ratio of short diagonal to its span less than unity shows lifting of acute corners therefore these are not recommended for the construction and it is suggested that skew slabs with ratio of short diagonal greater than unity should be constructed and preferred by selection of suitable geometrical parameters.

The results of FE model of the skew slabs have found to be higher by 5% of the experimental results. So it can be concluded that FE model results holds good with the experimental results though they are on slightly higher side. [(1)]

2.2.2 YIELD LINE THEORY OF SLAB

Jain and kennedy, (1973) has developed the yield criterion for reinforced concrete slabs being used in predicting the collapse load in yield line theory. The orthotropic reinforcement was considered in the slab panel to obtain the yield criterion. [(20)]

Bauer, D. Redwood, R.G., (1986) the authors have presented a numerical methods based on the virtual work approach of the yield line theory. The method consists of computing the yield load of a plate based on the geometry of an assumed collapse mechanism defined by means of nodes planes and lines. In addition, it can be used for the yield line analysis of plate with complex shapes, assumed mechanism and with any loading. Algorithms for the calculations of the work done by the external loads on the plate and internal work dissipated by the yield lines in the assumed mechanism are also described. [(21)]

Valentine Quintas, (2003) has suggested a generalized yield line method to determine the collapse load for reinforced concrete slabs. The yield line method, initially proposed by Johansen was modified to predict the true yield line pattern and collapse load. It was shown that if the assumed yield line pattern is correct, and then it would accompanied by only bending moment acting along the assumed yield line. The former approach was called as "Normal moment method". It was suggested that if the yield line pattern is not known in advance, torsional moments must be considered to be acting along with bending moment on the assumed yield line.

In this paper two methods are proposed that, without invalidating previous ones, really correspond to the two different ways of performing yield line analysis and therefore facilitate a better comprehension of the general problem of the failure of slabs. These methods are the nearly abandoned

- ''normal moment method''
- ''skew moment method.''

In ''normal moment method'' only bending moments are supposed to act at yield lines. In ''skew moment method,'' twisting moments in addition to bending moments act along yield lines. The ''normal moment method'' is general only if yield patterns are ''correct,'' that is, they are composed by possible yield lines. If yield lines are ''incorrect,'' or not possible, yield line analysis can only be performed, in general, by means of ''skew moment method.'' As shown in this paper, many of the classical solutions of yield line analysis correspond to incorrect yield patterns. This work demonstrates that Johansen's ''nodal force theory''—or ''equilibrium method''—and ''work method'' are only partial applications of ''skew moment method.'' This generalization of yield line analysis allows defining new equilibrium conditions not included in classical yield lines theory and permits obtaining more accurate solutions.

If the yield pattern is correct, in ''normal moment method'' we first obtain the relationship between the bending moment acting alone at yield lines of each region—and a shear if applicable—and the loads. Since the unknown *Mab* has been eliminated, the geometry of the correct yield pattern can be obtained directly by equating moments at each side of each yield line. The bending moment corresponding to that correct yield pattern is then supposed to be the yield bending moment *Mp* . In ''skew moment method,'' we must fulfill the two equilibrium conditions 1 and 2 at the yield mechanism, in order to obtain a relation between the internal

forces and the geometrical parameters of the yield pattern. The geometrical parameters that define the correct yield pattern are obtained making zero all twisting moments at every internal yield line.In the usual process of designing a slab the value of the yield load p of the slab is known, and therefore the aim of yield analysis is to obtain the values of yield bending moments *Mp*1 and *Mp*2 that appear at the failure state of the slab. This can be done by following two equilibrium conditions:

1. At each region of the yield mechanism of a slab, internal forces acting at yield lines must balance loads and reactions.

2. Internal forces must be in equilibrium at each side of a yield line.

These two conditions can be performed using directly equilibrium equations or, alternatively, applying the principle of virtual work to the whole mechanism of the slab supposing that internal forces that act at each side of each yield line are equal and, therefore, fulfilling simultaneously the equilibrium conditions 1 and 2. The results must be identical as principle of virtual work is only a way of using equilibrium equations. In this way we can always obtain a relation between internal forces and the geometrical parameters of the yield pattern of the slab. The following step is to find the values of those parameters that approach best the real yield pattern. This can be done by two basic methods: the ‘‘normal moment method’’ and the ‘‘skew moment method.’’

In the ‘‘normal moment method,’’ it is assumed from the beginning that only a constant bending moment *Ma* acts at yield lines, plus shear forces if *Ma* is not a local maximum. In ‘‘skew moment method’’ a constant moment, *Ma,* and a constant twisting moment, *Mab* , whose resultant is a ‘‘skew moment’’ are assumed to act at yield lines, plus shear forces if applicable. As their application is very different for ‘‘correct’’ and ‘‘incorrect’’ yield patterns, the two methods will be separately considered depending on the nature of the yield pattern concerned. [(22)]

Johansen K.W., this book has described yield patterns in reinforced cement concrete skew slab depending on the length of short diagonal greater or lesser than the length of free edge and its fixity at supports. He has also given two possible yield patterns for simply supported skew slabs. It is mentioned that the reactions are located inside the supports and a positive yield line is generated through the centre and parallel to the supports when a point load is applied at the centre of the slab, with length of free edge less than the short diagonal. Whereas in skew slabs

with length of free edge greater than the short diagonal the slab rotates about the axis passing through the obtuse corner and at an angle from the short diagonal equal to acute angle of the slab. The positive yield line is generated through the centre parallel to these axis of rotation when load is applied at the centre of the slab and the reactions act at the obtuse corners. [(23)]

2.3 GAPS IN RESEARCH AREA

Many experimental and analytical works has been done by many researchers in the area of finite element modelling and nonlinear FE analysis of RC skew slab bridges. These works contain extensive treatment of constitutive relations and failure theories, modeling of reinforcement and bond, concrete cracking formulations, shear transfer, load distribution, skew angle effects, numerical optimization, and dynamic analysis of reinforced concrete systems from a finite element perspective. Additionally, much research has been conducted concerning the general application of computers to reinforced concrete. Topics studied include the general optimization of design of reinforced concrete systems using computers, the general development of programming tools and resources suited to analyze and design reinforced concrete structures, and numerical advances in the modeling of multiscale behavior.

Several commercial software packages offer the capability to design slabs using finite elements. Some of these programs include ANSYS, NARCOS, SAFE, RAM Concept (formerly ADAPT Floor), and STAAD. Finite element–based skew slab design in NARCOS is based on the layering formulation incorporating transverse shear deformation. Finite element-based slab design in SAFE, as well as RAM Concept, is based on element force results, while finite element-based slab design in STAAD is based on element stresses, using the conventional Wood and Armer approach. The exact procedures that these software use to compute design moments are not disclosed in the cited technical reference documentation.

This research is concerned with the finite element modelling of the RCC skew slab with edge supports. Various researches have been conducted based on softwares which give the results for the skew slab with girders in bridges. However as per the current scenario of the construction field individual skew slab analysis is required to provide this slab and based on the space availability.

So for no research has been conducted on the skew slab resting on the flexible supports. In this study it has been tried to find out the detail analysis of the simply supported skew slab with edge

supports and compared with analytical and experimental values of skew slab without edge supports.

2.4 CLOSURE

The literature review has suggested that use of a finite element modelling of the RCC skew slab . So it has been decided to use ATENA for the FE modelling. With the help of this software study of RC skew slab with edge supports has been done. ATENA also helps in FE modelling and meshing inside the surface of element. It gives the load deflection curve and gives the values of stresses and strains, crack width of the elements of the slab at every step.

CHAPTER - 3, FINITE ELEMENT MODELLING OF RCC SKEW SLAB WITH EDGE SUPPORTS

3.1 GENERAL

Over the last one or two decade numerical simulation of reinforced concrete structures and structural elements has become a major research area. A successful numerical simulation demands choosing suitable elements, formulating proper material models and selecting proper solution method. This chapter is intended to give a description of the structure that is to be FE modeled and analyzed to obtain the load deflection and uplifts curve analytically. In first part of the chapter the RC skew slabs (experimentally and analytically analyzed) "*Finite Element Modelling of Reinforced Cement Concrete Skew Slab*" *by Madhu Sharma* is described in detail. This chapter also discusses the theory related to ATENA and information about finite elements currently implemented in ATENA in its second part. All the necessary steps to create these models are explained in detail and the steps taken to generate the analytical load-deformation response of the model are discussed.

3.2 GENERAL DESCRIPTION OF STRUCTURE

Skew slab has been modelled with skew angle and aspect ratio i.e. ratio of supported length and span along the traffic, 0.49 and 0.65 under central concentrated load and self weight.
Skew slab have been divided into two types, depending on the length of short diagonal of skew slab being less or greater than its span measured along the traffic. Two specimens has been analyzed, i.e.

1. Skew slab with ratio of short diagonal to span less than unity.
2. Skew slab with ratio of short diagonal to span greater than unity.

An analytical model for skew slabs resting over rigid supports for any degree of skew angle and aspect ratio has been developed. It has been noticed that the skew slab bridges with short diagonal less than span show lifting of acute corners, and therefore cannot be recommended for construction. It is also found that skew slab bridge with any skew angle can be constructed if its short diagonal is kept more than the span. [(24)]

3.3 SLAB SPECIMENS

In order to validate the analytical results of proposed approach, the six skew slabs have been modelled with skew angle of $16.49^{0,}$ and with aspect ratio of 0.49 and 0.65 to keep the short diagonal of skew slabs less than the span in one case and greater than the span in other. M 25 concrete have been used along with reinforcement 8 mm diameter bars @100 mm c/c and distribution steel of 8 mm diameter bars @125 mm c/c laid over main reinforcement at right angles to it or parallel to the supports. Thicknesses of slabs have been kept 70 mm with clear cover 10 mm.

3.3.1 TEST SPECIMEN -1, SKEW SLAB WITH SHORT DIAGONAL LESS THAN ITS SPAN

Skew slab Specimen -1 three skew slab specimens with edge supports has been modelled with skew angle of 16.49^{0}, the support length and span was kept as 1200 mm and 2470 mm respectively with M 25 grade concrete. The schematic diagram of specimen is shown figure-3.1 Thickness of slab has been kept as 70 mm. Length of short diagonal of the slab is 2420 mm which is less than span 2470 mm. slab has been reinforced with main reinforcement of 8 mm diameter for steel bars @ 100 mm c/c at the bottom face of the slab at right angles to the supports i.e. along x-direction and distribution reinforcement of also 8 mm diameter tor steel bars @ 125 mm c/c laid over main reinforcement, parallel to the supports i.e. along y- direction.

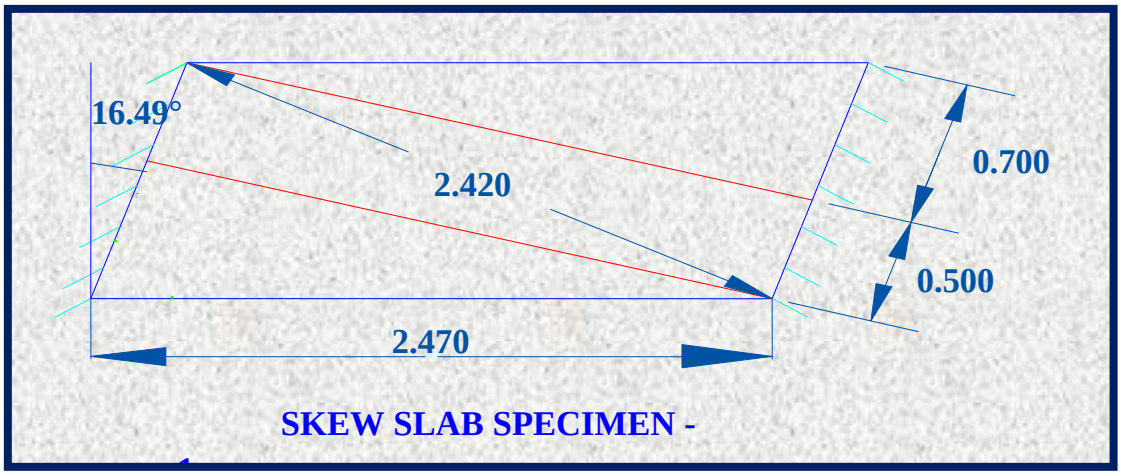

Figure 3.1, Skew slab with short diagonal less than span (L< *l*) [(24)]

The size of edge beams are taken as 150 x 150, 150 x 130, 150 x 100 for specimen-1 of skew slab.

Length of short diagonal, L = 2420 mm < span, *l* = 2470 mm

3.3.2 TEST SPECIMEN -2, SKEW SLAB WITH SHORT DIAGONAL GREATER THAN ITS SPAN

Skew slab specimen-2 three skew slab specimens has been modelled with skew angle of 16.49^0, the supports length and span was kept as 1600 mm and 2470 mm respectively with M 25 grade concrete. The schematic diagram of specimen is shown in figure 3.2.Thickness of slab has been kept as 70 mm. Length of short diagonal of the slab is 2530 mm which is greater than the span 2470 mm. Slab has been reinforced with main reinforcement of 8 mm diameter tor steel bar @ 100 mm c/c at the bottom face of slab at right angle to the supports i.e. along x- direction and distribution reinforcement of also 8 mm diameter tor steel bar @ 125 mm c/c laid over main reinforcement , parallel to the supports i.e. along y- direction.

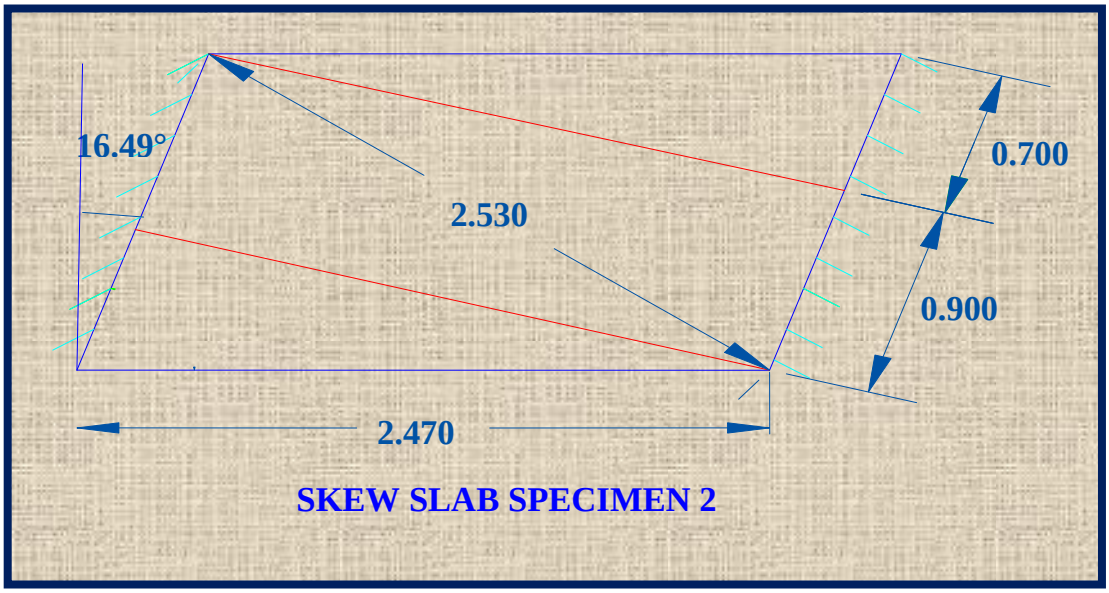

Figure 3.2 Skew slab with short diagonal greater than span (L> *l*) [(24)]

The size of edge beams are varying 150 x 150, 150 x 130, 150 x 100 for specimen-2 of skew slab. Short diagonal, L = 2530 mm > span = 2470 mm

3.3.3 REINFORCEMENT DETAIL

Detail reinforcement provided is as given in figure 3.4

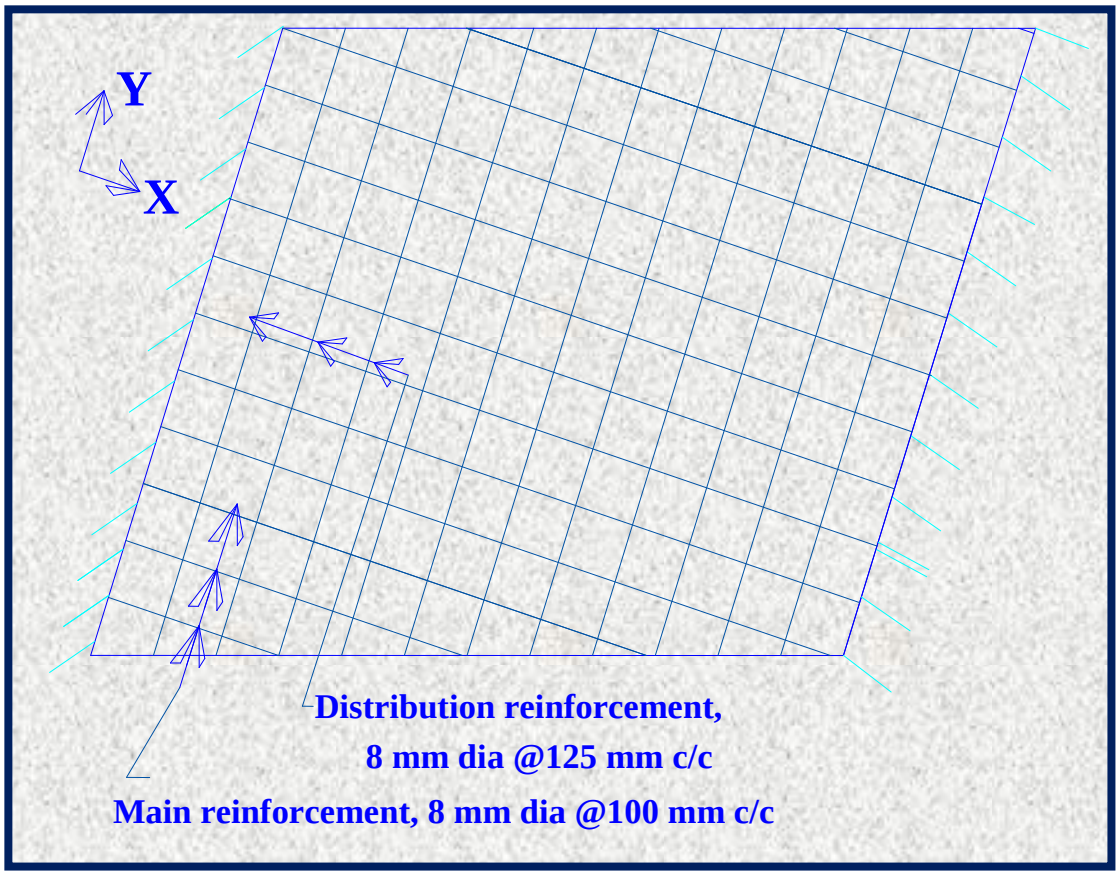

Figure 3.3 Reinforcement detail of test specimen [(24)]

3.4 INTRODUCTION TO FE MODELLING

If the finite element method is to be a useful tool in the design of reinforced concrete plate structures, accurate modeling is a prerequisite. Accurate modeling involves understanding the important relationships between the physical world and the analytical simulation. As Clough states, "Depending on the validity of the assumptions made in reducing the physical problem to a numerical algorithm, the computer output may provide a detailed picture of the true physical behavior or it may not even remotely resemble it.The behavior of RC structures is distinctly nonlinear, because of several factors:

- Nonlinear material behavior of concrete and steel and their interaction through bond and Dowel action;

- Cracking of concrete;
- Time dependent effects such as creep, shrinkage, temperature and load history. In dealing with these problems in an analytical setting several nonlinear solution algorithms are now available.

3.5 FINITE ELEMENT METHOD

The finite element method (FEM) or finite element analysis is a numerical technique for finding approximate solutions of partial differential equations (PDE) as well as of integral equations. The solution approach is based either on eliminating the differential equation completely (steady state problems), or rendering the PDE into an approximating system of ordinary differential equations, which are then numerically integrated using standard techniques.

In solving partial differential equations, the primary challenge is to create an equation that approximates the equation to be studied, but is numerically stable, meaning that errors in the input data and intermediate calculations do not accumulate and cause the resulting output to be meaningless. The Finite Element Method is a good choice for solving partial differential equations over complex domains. To summarize in general terms how the finite element method works we will succinctly list these steps now;

1.Discretize the Continuum. The first step is to divide the continuum or solution region into elements. A variety of element shapes may be used, and different element shapes may be employed in the same solution region. Indeed, when analyzing an elastic structure that has different types of components such as plates and beams, it is not only desirable but also necessary to use different elements in the same solution. Although the number and the type of elements in a given problem are matters of engineering judgment, the analyst can rely on the experience of others for guidelines.

2. Select Interpolation Functions. The next step is to assign nodes to each element and then choose the interpolation function to represent the variation of the field variable over the element. The field variable may be a scalar, a vector, or a higher-order tensor. Often, polynomials are selected as interpolation functions for the field variable because they are easy to integrate and differentiate. The degree of the polynomial chosen depends on the number of nodes assigned to

the element, the nature and number of unknowns at each node, and certain continuity requirements imposed at the nodes and along the element boundaries. The magnitude of the field variable as well as the magnitude of its derivatives may be the unknowns at the nodes.

3. Find the Element Properties. Once the finite element model has been established (that is, once the elements and their interpolation functions have been selected), we are ready to determine the matrix equations expressing the properties of the individual elements. For this task we may use one of the three approaches just mentioned: the direct approach, the variational approach, or the weighted residuals approach.

4. Assemble the Element Properties to Obtain the System Equations. To find the properties of the overall system modeled by the network of elements we must "assemble" all the element properties. In other words, we combine the matrix equations expressing the behavior of the elements and form the matrix equations expressing the behavior of the entire system. The matrix equations for the system have the same form as the equations for an individual element except that they contain many more terms because they include all nodes. The basis for the assembly procedure stems from the fact that at a node, where elements are interconnected, the value of the field variable is the same for each element sharing that node. A unique feature of the finite element method is that the system equations are generated by assembly of the individual *element* equations. In contrast, in the finite difference method the system equations are generated by writing nodal equations.

5. Impose the Boundary Conditions. Before the system equations are ready for solution they must be modified to account for the boundary conditions of the problem. At this stage we impose known nodal values of the dependent variables or nodal loads.

6. Solve the System Equations. The assembly process gives a set of simultaneous equations that we solve to obtain the unknown nodal values of the problem. If the problem describes steady or equilibrium behavior, then we must solve a set of linear or nonlinear algebraic equations. There are standard solution techniques for solving these equations. If the problem is unsteady, the nodal unknowns are a function of time, and we must solve a set of linear or nonlinear ordinary differential equations.

7. Make Additional Computations If Desired. Many times we use the solution of the system equations to calculate other important parameters. For example, in a structural problem the nodal unknowns are displacement components. From these displacements we calculate element strains and stresses. Similarly, in a heat-conduction problem the nodal unknowns are temperatures, and from these we calculate element heat fluxes.

3.5.1 APPLICATION OF FINITE ELEMENT METHOD

- FEM helps in solving complex elasticity and structural analysis problem in civil engineering.
- FEM helps tremendously in producing stiffness and strength visualizations and also in minimizing weight, materials, and costs.
- FEM allows detailed visualization of where structures bend or twist, and indicates the distribution of stresses and displacements.
- FEM software provides a wide range of simulation options for controlling the complexity of both modeling and analysis of a system. Similarly, the desired level of accuracy required and associated computational time requirements can be managed simultaneously to address most engineering applications.
- FEM allows entire designs to be constructed, refined, and optimized before the design is manufactured.
- FEM is the most powerful design tool which significantly improved both the standard of engineering designs and the methodology of the design process in many civil engineering applications.

In summary, benefits of FEM include increased accuracy, enhanced design and better insight into critical design parameters, virtual prototyping, fewer hardware prototypes, a faster and less expensive design cycle, increased productivity, and increased revenue. [(25)]

3.6 FINITE ELEMENT MODELLING

The basic concept of FEM modelling is the subdivision of the mathematical model into disjoint (non-overlapping) components of simple geometry. The response of each element is expressed in terms of a finite number of degrees of freedom characterized as the value of an unknown function, or functions or at a set of nodal points. The response of the mathematical model is then

considered to be the discrete Model obtained by connecting or assembling the collection of all elements.

Within the framework of the finite element method reinforced concrete can be represented either by superimposition of the material models for the constituent parts (i.e., for concrete, for reinforcing steel or by a constitutive law for the composite concrete, embedded steel considered as a continuum.

The finite element method is well suited for superimposition of the material models for the constituent parts of a composite material. Several constitutive models covering these effects are implemented in the computer code ATENA, which is a finite element package designed for computer simulation of concrete structures. The graphical user interface in ATENA provides an efficient and powerful environment for solving many anchoring problems. ATENA enables virtual testing of structures using computers, which is the present trend in the research and development world. Material models of this type can be employed for virtually all kinds of reinforced concrete structural members. Depending on the type of material modelling to be solved in ATENA, concrete can be represented by solid brick elements; the reinforcement is modelled by bar elements (discrete representation). Geometry and shape of any mathematical element help in proper placement of the nodal points and materials properties helps in using proper modelling.

3.7 MATERIAL MODELS

The program system ATENA offers a variety of material models for different materials and purposes. The most important material models in ATENA for RCC structure are concrete and reinforcement. These advanced models take into account all the important aspects of real material behaviour in tension and compression [26].

3.7.1 MODELLING OF CONCRETE

A. Geometry of the Concrete

Element geometric modelling of concrete has been done using 3D solid brick element with 8 up to 20 nodes in ATENA, shown in Figure 3.4

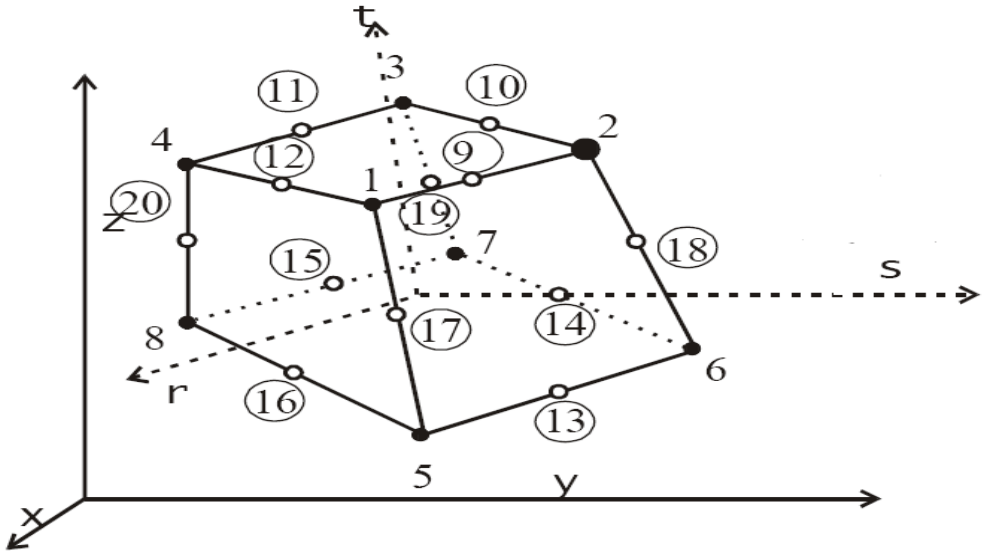

Figure 3.4 Geometry of Brick element

B. Element Properties

3D solid brick element having three degree of freedom at each node: translations in the nodal x, y and z directions. This is an isoparametric elements integrated by Gauss integration at integration points. This element is capable of plastic deformation, cracking in three orthogonal directions, and crushing. The most important aspect of this element is the treatment of non-linear material properties.

3.7.2 MODELLING OF REINFORCEMENT

A Geometry of the reinforcement

Reinforcement modelling could be discrete or smeared. In our work, a discrete modelling of reinforcement has been done. The reinforcement has been modelled using bar elements in ATENA.

B Element Properties

Reinforcement steel is a 3D bar element, which has three degrees of freedom at each node; translations in the nodal x, y and z direction. Bar element is a uniaxial tension-compression

element. The stress is assumed to be uniform over the entire element. Also plasticity, creep, swelling, large deflection and stress-stiffening capabilities are included in the element.

3.8 STRESS-STRAIN RELATIONS FOR CONCRETE [26]

Concrete exhibits a large number of micro-cracks, especially, at the interface between coarser aggregates and mortar, even before subjected to any load. The presence of these micro-cracks has a great effect on the mechanical behaviour of concrete, since their propagation during loading contributes to the nonlinear behaviour at low stress levels and causes volume expansion near failure. Many of these micro-cracks are caused by segregation, shrinkage or thermal expansion of the mortar. Some micro-cracks may develop during loading because of the difference in stiffness between aggregates and mortar. Since the aggregate-mortar interface has a significantly lower tensile strength than mortar, it constitutes the weakest link in the composite system. This is the primary reason for the low tensile strength of concrete. The response of a structure under load depends to a large extent on the stress-strain relation of the constituent materials and the magnitude of stress. Since concrete is used mostly in compression, the stress-strain relation in compression is of primary interest [26].

3.8.1 EQUIVALENT UNIAXIAL LAW

The nonlinear behaviour of concrete in the biaxial stress state is described by means of the so called effective stress σ_c^{ef}, and the equivalent uni-axial strain ε^{eq}. The effective stress is in most cases a principal stress. The equivalent uni-axial strain is introduced in order to eliminate the Poisson's effect in the plane stress state.

$$\varepsilon_{eq} = \sigma_{ci} / E_{ci}$$

The equivalent uni-axial strain can be considered as the strain, that would be produced by the stress σci in a uni-axial test with modulus associated Eci with the direction *i*. Within this assumption, the nonlinearity representing damage is caused only by the governing stress σci. The complete equivalent uni-axial stress-strain diagram for concrete is shown in Figure 3.5.

The numbers of the diagram parts in Figure 3.5 (material state numbers) are used in the results of the analysis to indicate the state of damage of concrete.

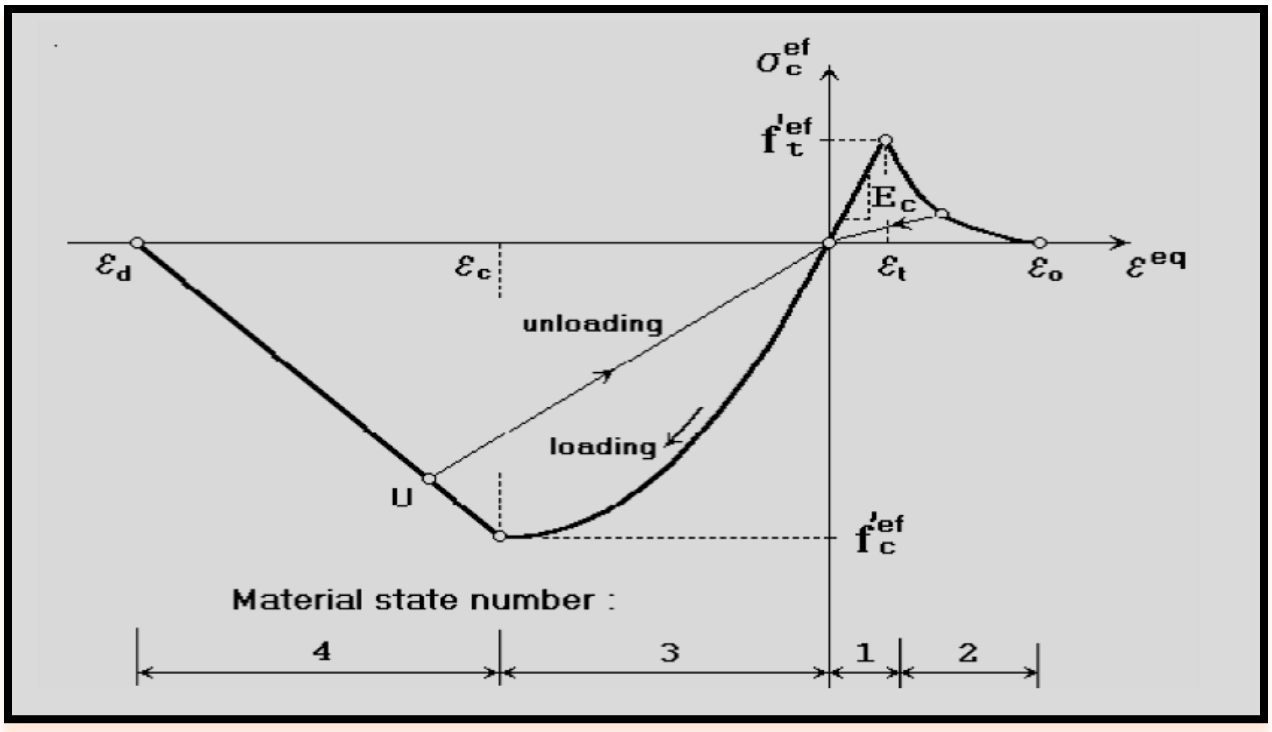

Figure 3.5 Uniaxial stress strain law of concrete [(26)]

Unloading is a linear function to the origin. An example of the unloading point *U* is shown in Figure 3.5. Thus, the relation between stress σ_{cef} and strain ε_{eq} is not unique and depends on a load history. A change from loading to unloading occurs, when the increment of the effective strain changes the sign. If subsequent reloading occurs the linear unloading path is followed until the last loading point *U* is reached again. Then, the loading function is resumed.

The peak values of stress in compression f_{cef} and in tension f_{tef} are calculated according to the biaxial stress state. Thus, the equivalent uni-axial stress-strain law reflects the biaxial stress state.

3.8.2 BIAXIAL STRESS FAILURE CRITERION OF CONCRETE

A. Compressive Failure

A biaxial stress failure criterion according to KUPFER et al. (1969) is used as shown in Figure 3.6. In the compression-compression stress state the failure function is

$$f_{cef} = [(1+3.65a)/(1+a)_2]f_c;\ a = (\sigma_{c1}/\sigma_{c2}) \qquad (3.1)$$

Where σ_{c1}, σ_{c2} are the principal stresses in concrete and f_c is the uni-axial cylinder strength. In the biaxial stress state, the strength of concrete is predicted under the assumption of a proportional stress path.

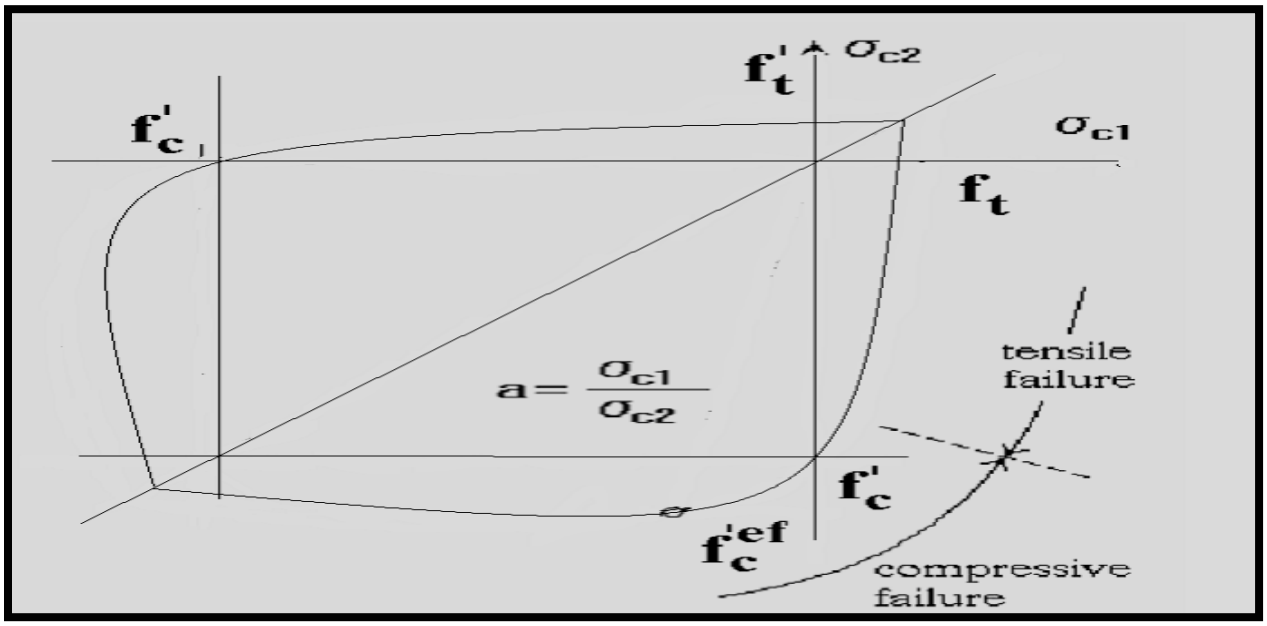

Figure 3.6 Biaxial failure functions of concrete [(26)]

In the tension-compression state, the failure function continues linearly from the point $\sigma_{c1} = 0$, $\sigma_{c2} = f_c$, into the tension-compression region with the linearly decreasing strength:

$f_{cef} = f_{c\,rec}$, $r_{ec} = [1+ 5.3278(\sigma_{c1}/ f_c)]$ (3.2)

Where r_{ec} is the reduction factor of the compressive strength in the principal direction 2 due to the tensile stress in the principal direction 1.

B Tensile failures

In the tension-tension state, the tensile strength is constant and equal to the uniaxial tensile strength f‟ t. In the tension-compression state, the tensile strength is reduced by the relation:

$f_{tef} = f_t r_{et}$ (3.3)

Where ret is the reduction factor of the tensile strength in the direction 1 due to the compressive stress in the direction 2. The reduction function has one of the following forms.

$r_{et} = 1 – 0.8 (\sigma_{c2}/ f_c)$ (3.4)

$r_{et} = [A + (A – 1) B]/ AB; B = Kx + A; x = \sigma_{c2}/ f_c$ (3.5)

The relation in Eq. (3.4) is the linear decrease of the tensile strength and (3.5) is the hyperbolic decrease. Two predefined shapes of the hyperbola are given by the position of an intermediate point *r, x*.

Constants *K* and *A* define the shape of the hyperbola. The values of the constants for the two positions of the intermediate point are given in the following table.

Type	point		Parameters	
	R	X	A	X
A	0.5	0.4	0.75	1.125
B	0.5	0.2	1.0625	6.0208

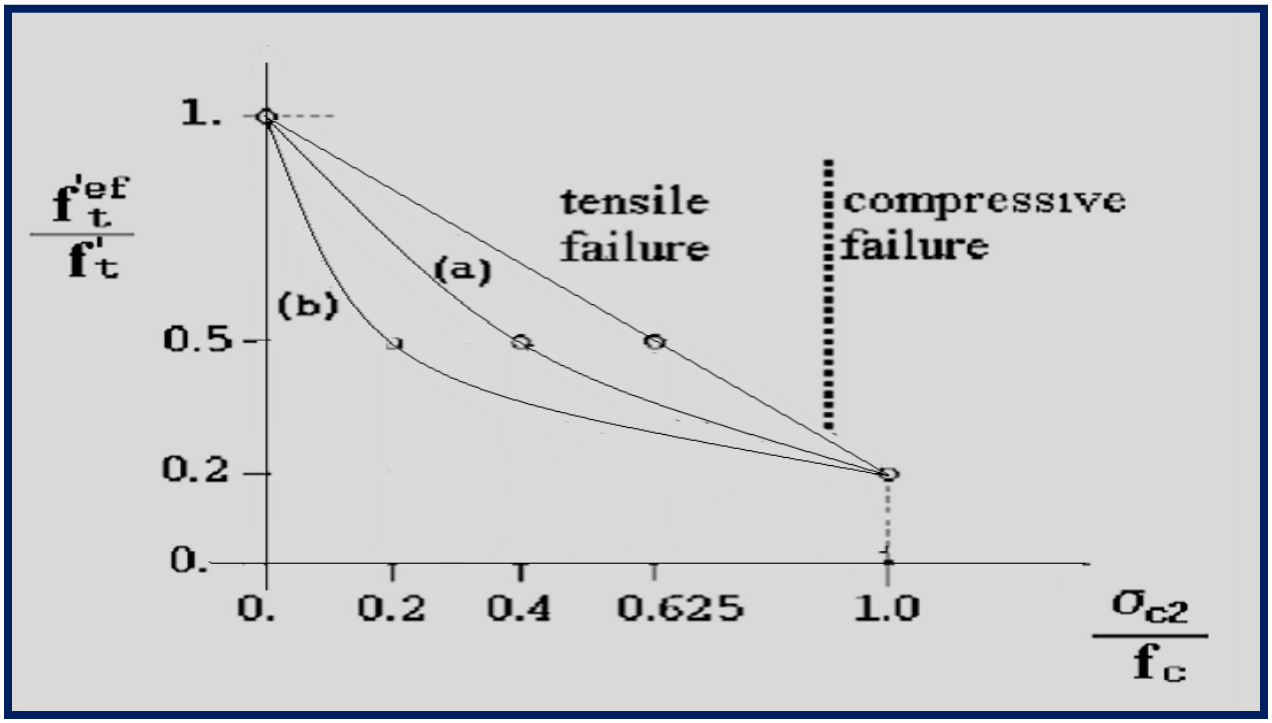

Figure 3.7 Tension Compression failure function of Concrete [(26)]

3.8.3 TENSION BEFORE CRACKING

The behaviour of concrete in tension without cracks is assumed linear elastic. E_c *is* the initial elastic modulus of concrete, f_{tef} is the effective tensile strength derived from the biaxial failure function already describe above.

$$\sigma cef = Ec\ \varepsilon eq,\ 0 < \sigma c < ftef$$

3.8.4 TENSION AFTER CRACKING

A fictitious crack model is based on a crack-opening law and fracture energy. This formulation is suitable for modelling of crack propagation in concrete. It is used in combination with the crack band. It is a region (band) of material, which represents a discrete failure plane in the finite element analysis. In A fictitious crack model is based on a crack-opening law and fracture energy. This formulation is suitable for modelling of crack propagation in concrete. It is used in combination with the crack band. It is a region tension it is a crack, in compression it is a plane of crushing. In reality these failure regions have some dimension. However, since according to the experiments, the dimensions of the failure regions are independent on the structural size, they are assumed as fictitious planes. In case of tensile cracks, this approach is known as rack the "crack band theory", **(*BAZANT OH 1983*).** Here is the same concept used also for the compression failure. The purpose of the failure band is to eliminate two deficiencies, which occur in connection with the application of the finite element model: element size effect and element orientation effect.

A. Element size effect.

The direction of the failure planes is assumed to be normal to the principal stresses in tension and compression, respectively. The failure bands (for tension Lt and for compression Lc) are defined as projections of the finite element dimensions on the failure planes.

B. Element Orientation Effect.

The element orientation effect is reduced, by further increasing of the failure band for skew meshes, by the following formula (proposed by (***CERVENKA et al. 1995*).**

$L_t = \gamma L_t$, $L_c = \gamma L_c$

$\gamma = 1 + (\gamma_{max} - 1)\ (\theta / 45),\ \theta\ \varepsilon\ (\theta / 45)$ (3.6)

An angle θ is the minimal angle (min (θ_1, θ_2)) between the direction of the normal to the failure plane and element sides. In case of a general quadrilateral element the element sides" directions are calculated as average side directions for the two opposite edges. The above formula is a linear interpolation between the factor γ=1.0 for the direction parallel with element sides, and γ=γ max, for the direction inclined at 45^o. The recommended (and default) value of γ max =1.5.

3.9 BEHAVIOUR OF CRACKED CONCRETE [26]

3.9.1 DESCRIPTION OF A CRACKED SECTION

The nonlinear response of concrete is often dominated by progressive cracking which results in localized failure. The structural member has cracked at discrete locations where the concrete tensile strength is exceeded.At the cracked section all tension is carried by the steel reinforcement. Tensile stresses are, however, present in the concrete between the cracks, since some tension is transferred from steel to concrete through bond. The magnitude and distribution of bond stresses between the cracks determines the distribution of tensile stresses in the concrete and the reinforcing steel between the cracks.

Additional cracks can form between the initial cracks, if the tensile stress exceeds the concrete tensile strength between previously formed cracks. The final cracking state is reached when a tensile force of sufficient magnitude to form an additional crack between two existing cracks can no longer be transferred by bond from steel to concrete. As the concrete reaches its tensile strength, primary cracks form. The number and the extent of cracks are controlled by the size and placement of the reinforcing steel. At the primary cracks the concrete stress drops to zero and the steel carries the entire tensile force. The concrete between the cracks, however, still carries some tensile stress, which decreases with increasing load magnitude. This drop in concrete tensile stress with increasing load is associated with the breakdown of bond between reinforcing steel and concrete. At this stage a secondary system of internal cracks, called bond cracks, develops around the reinforcing steel, which begins to slip relative to the surrounding concrete.

Since cracking is the major source of material nonlinearity in the serviceability range of reinforced concrete structures, realistic cracking models need to be developed in order to accurately predict the load-deformation behaviour of reinforced concrete members. The selection of a cracking model depends on the purpose of the finite element analysis. If overall load-deflection behaviour is of primary interest, without much concern for crack patterns and estimation of local stresses, the "smeared" crack model is probably the best choice. If detailed local behaviour is of interest, the adoption of a "discrete" crack model might be necessary. Unless special connecting elements and double nodes are introduced in the finite element discretization of the structure, the well established smeared crack model results in perfect bond between steel and concrete, because of the inherent continuity of the displacement field.

3.9.2 MODELLING OF CRACKS IN CONCRETE

The process of crack formation can be divided into three stages, Figure 3.8. The un-cracked stage is before a tensile strength is reached. The crack formation takes place in the process zone of a potential crack with decreasing tensile stress on a crack face due to a bridging effect. Finally, after a complete release of the stress, the crack opening continues without the stress.

The tension failure of concrete is characterized by a gradual growth of cracks, which join together and eventually disconnect larger parts of the structure. It is usually assumed that cracking formation is a brittle process and that the strength in tension loading direction abruptly goes to zero after such cracks have formed.Therefore, the formation of cracks is undoubtedly one of the most important non-linear phenomenons, which governs the behaviour of the concrete structures. In the finite element analysis of concrete structures, two principally different approaches have been employed for crack modelling. These are (a) discrete crack modelling (b) smeared crack modellingThe discrete approach is physically attractive but this approach suffers from few drawbacks, such as**,** it employs a continuous change in nodal connectivity, which does not fit in the nature of finite element displacement method; the crack is considered to follow a predefined path along the element edges and excessive computational efforts are required. The second approach is the smeared crack approach. In this approach the cracks are assumed to be smeared out in a continuous fashion.

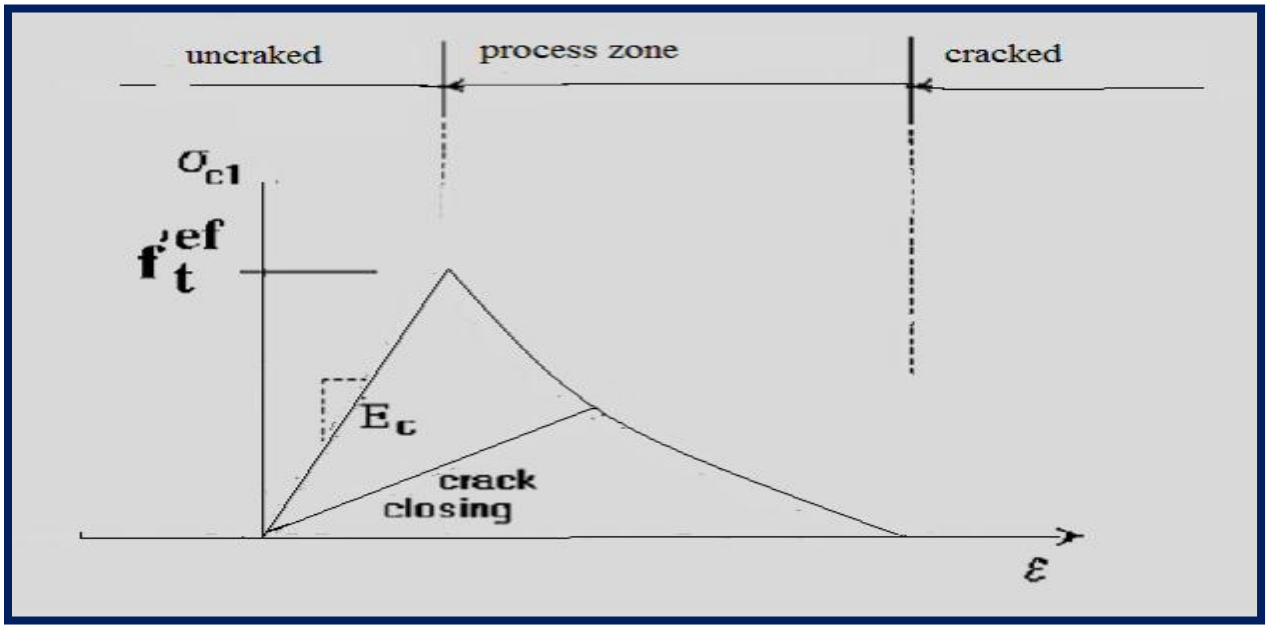

Figure 3.8 Stages of crack opening [(25)]

Within the smeared concept two options are available for crack models: the fixed crack model and the rotated crack model. In both models the crack is formed when the principal stress exceeds the tensile strength. It is assumed that the cracks are uniformly distributed within the material volume. This is reflected in the constitutive model by an introduction of orthotropy.

A. Fixed Crack Model

In the fixed crack model (***CERVENKA 1985, DARWIN 1974***) the crack direction is given by the principal stress direction at the moment of the crack initiation. During further loading this direction is fixed and represents the material axis of the orthotropy.

The principal stress and strain directions coincide in the un-cracked concrete, because of the assumption of isotropy in the concrete component. After cracking the orthotropy is introduced. The weak material axis m1 is normal to the crack direction; the strong axis *m2* is parallel with the cracks. In a general case the principal strain axes ε1 and ε2 rotate and need not to coincide with the axes of the orthotropy *m1* and *m2*. This produces a shear stress on the crack face as shown in Figure. 3.9. The stress components σc1 and σc2 denote, respectively, the stresses normal and parallel to the crack plane and, due to shear stress, they are not the principal stresses.

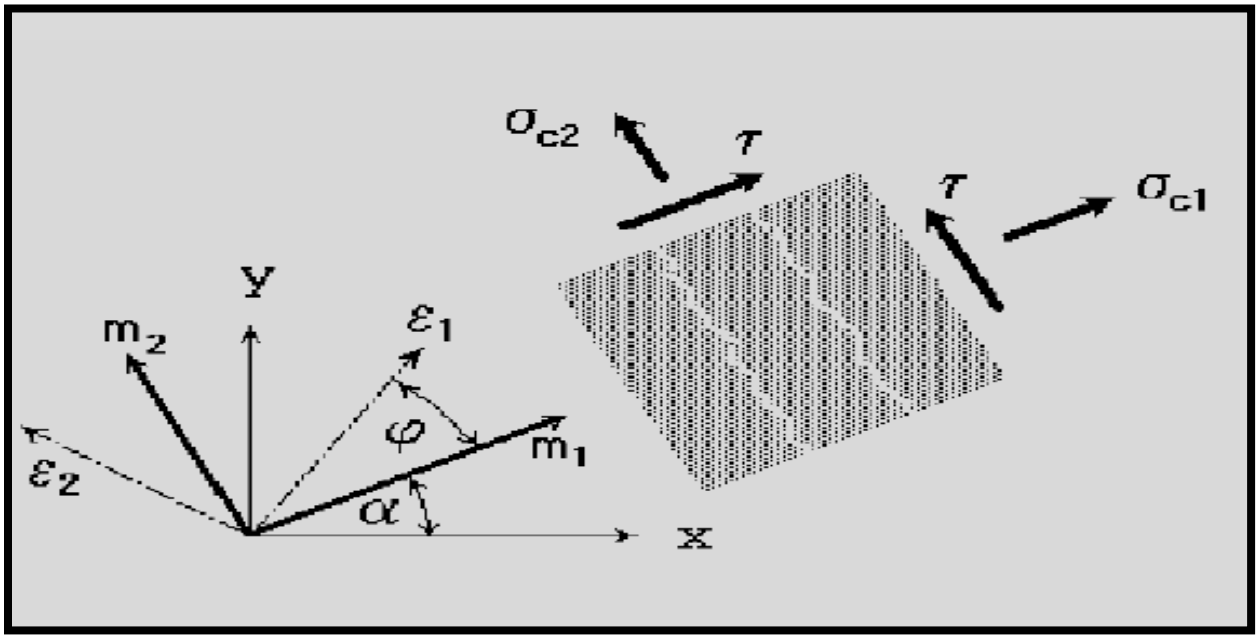

Figure 3.9 Fixed crack model Stress and strain state [26]

B. Rotated Crack Model

In the rotated crack model, the direction of the principal stress coincides with the direction of the principal strain. Thus, no shear strain occurs on the crack plane and only two normal stress components must be defined, as shown in Figure 3.10.

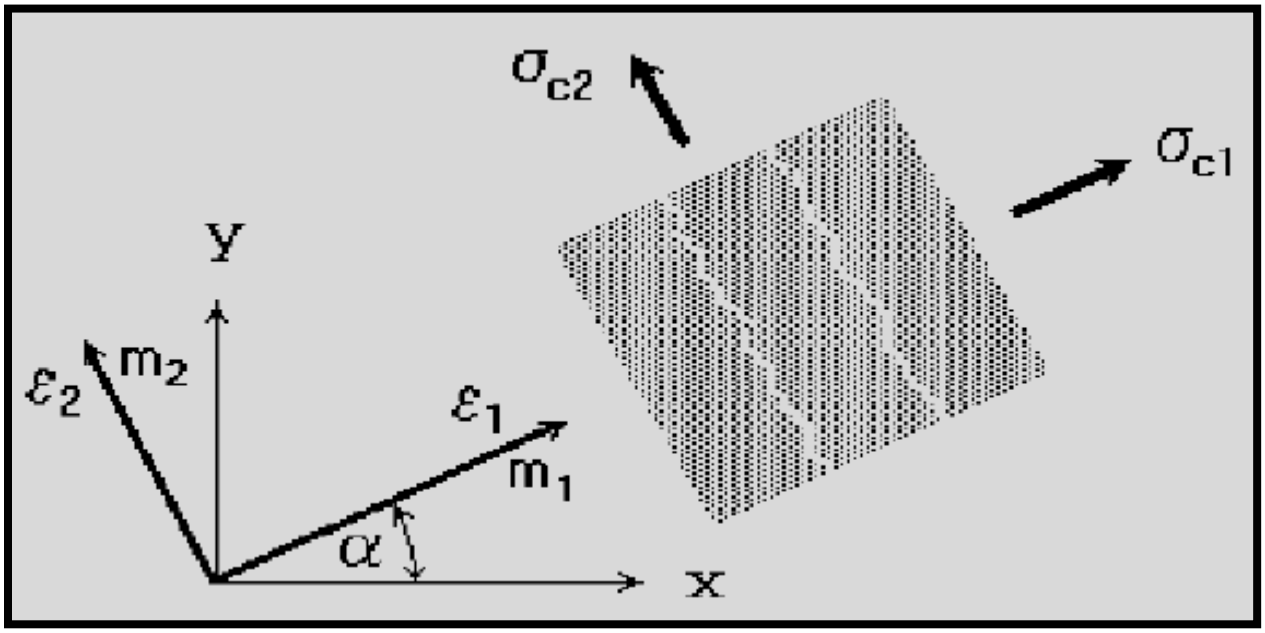

Figure 3.10 Rotated crack model. Stress and strain state [26]

If the principal strain axes rotate during the loading the direction of the cracks rotates, too. In order to ensure the co-axiality of the principal strain axes with the material axes the tangent shear modulus *Gt* is calculated according to CRISFIELD 1989 as

$G_t = (\sigma_{c1} - \sigma_{c2}) / 2\,(\varepsilon_1 - \varepsilon_2)$

3.10 STRESS-STRAIN LAWS FOR REINFORCEMENT [26]

3.10.1 INTRODUCTION

Reinforcement can be modelled in two distinct forms: discrete and smeared. Discrete reinforcement is in form of reinforcing bars and is modelled by truss elements. The smeared reinforcement is a component of composite material and can be considered either as a single (only one-constituent) material in the element under consideration or as one of the more such

constituents. The former case can be a special mesh element (layer), while the later can be an element with concrete containing one or more reinforcements. In both cases the state of uniaxial stress is assumed and the same formulation of stress-strain law is used in all types of reinforcement.

3.10.2 BILINEAR LAW

The bilinear law, elastic-perfectly plastic, is assumed as shown in Figure 3.11

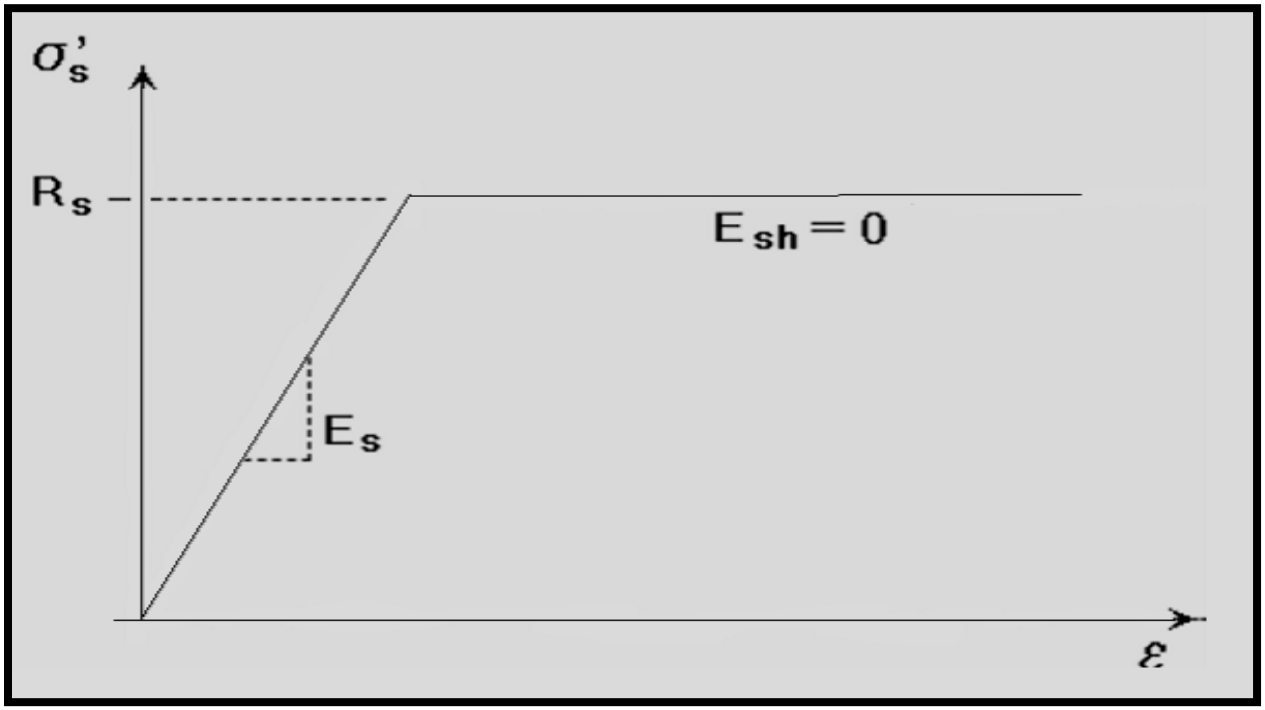

Figure 3.11 the bilinear stress-strain law for reinforcement [26]

The initial elastic part has the elastic modulus of steel E_s. The second line represents the plasticity of the steel with hardening and its slope is the hardening modulus E_{sh}. In case of perfect plasticity E_{sh} =0. Limit strain ε_L represents limited ductility of steel.

3.10.3 MULTI-LINEAR LAW

The multi-linear law consists of four lines as shown in Figure 3.12. This law allows modelling of all four stages of steel behaviour: elastic state, yield plateau, hardening and fracture. The multi-line is defined by four points, which can be specified by input.

The above described stress-strain laws can be used for the discrete as well as the smeared reinforcement. The smeared reinforcement requires two additional parameters: the reinforcing ratio *p* and the direction angle β as shown in Figure. 3.12. Where ρ = (Area of steel/ Area of

concrete). The spacing *s* of the smeared reinforcement is assumed infinitely small. The stress in the smeared reinforcement is evaluated in the cracks; therefore it should include also a part of stress due to tension stiffening. $\sigma_{scr} = \sigma_s + \sigma_{ts}$

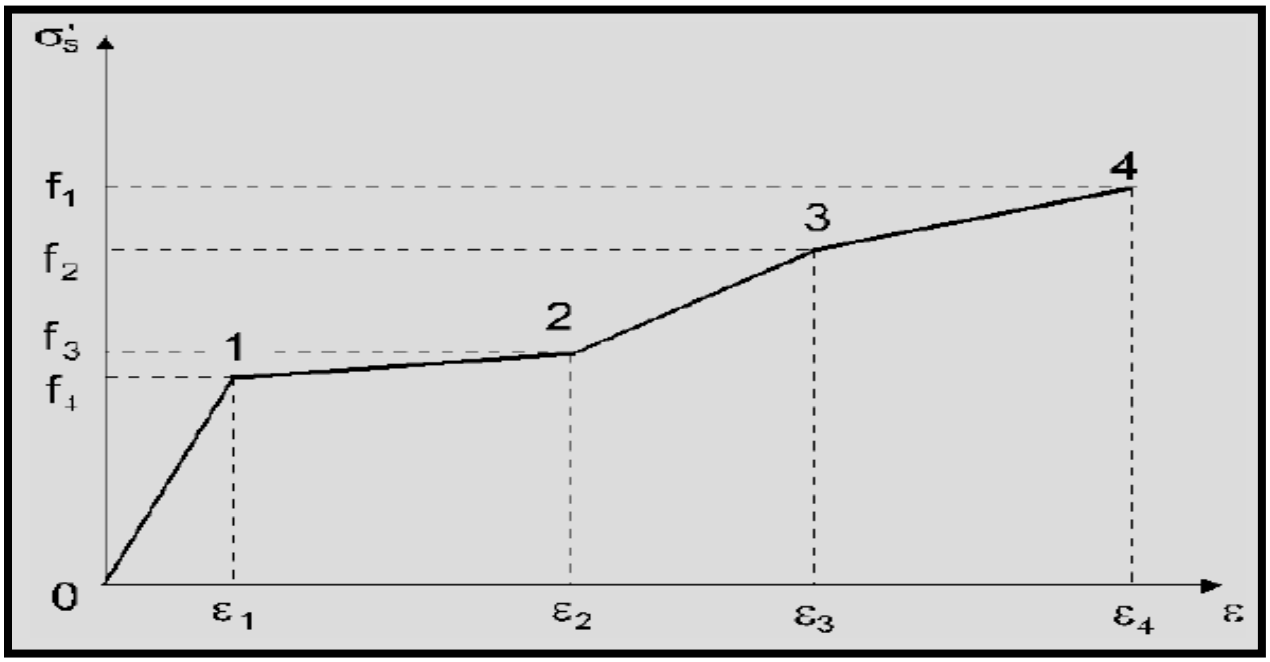

Figure, 3.12 the multi-linear stress-strain law for reinforcement [26]

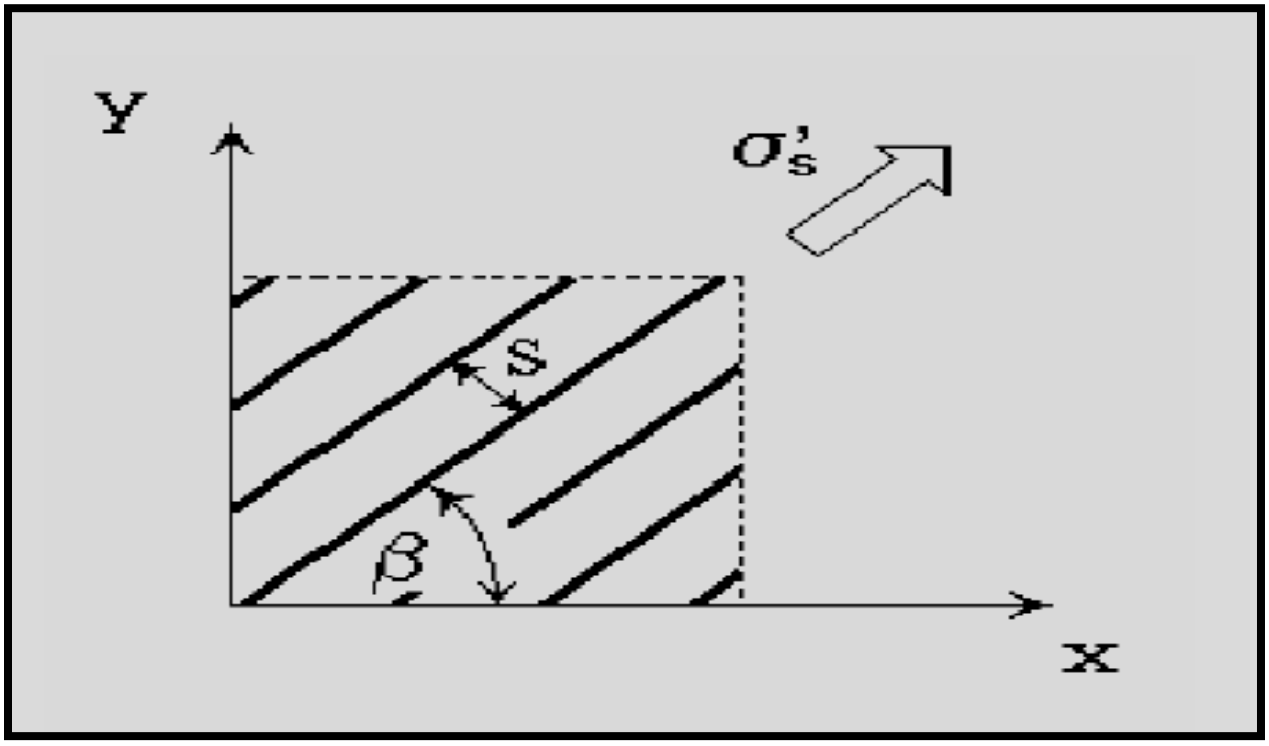

Figure, 3.13 Smeared reinforcement [26]

Where σ_s is the steel stress between the cracks (the steel stress in smeared reinforcement), σ_{scr} is the steel stress in a crack. If no tension stiffening is specified $\sigma_{ts} = 0$ and $\sigma_{scr} = \sigma_s$. In case of the discrete reinforcement the steel stress is always σ_s.

Once we understand the finite element modelling, the next step is the analytical programming. The main objective of this analytical program is to get the result of under reinforced concrete skew slabs and compare with the experimental results. In the analytical programming, first we select the materials and its properties and create geometry of the skew slab. The skew slabs are tested up to its failure point and the ultimate load deflection values are plotted as graphs. For modelling the control member in ATENA, concrete, reinforcement bars of different diameters, steel plates, is used as materials.

3.11 MATERIAL PROPERTIES

Concrete, reinforcement steel, steel plates have been used to model the RCC Skew slab. The specification and the properties of these materials are as under:

A. Concrete

In ATENA, concrete material is modelled as a 3D nonlinear cementitious2. The physical properties of 3D nonlinear cementitious2 material are given in Table 3.1. The values are calculated as per IS code 456:2000 and remaining are the default values.

Table 3.1 Material Properties of Concrete[1]

Properties	Values
Elastic Modulus (Fresh Concrete)	21981 Mpa
Poisson Ratio	0.2
Tensile Strength	3.94 Mpa
Compressive Strength	31.78 Mpa
Specific Fracture Energy	6.020 E -05 MN/ m
Critical Compressive Displacement	5000E – 04
Plastic Strain at compressive Strength	8.701 E -04
Reduction of Compressive strength	0.8
Fail Surface eccentricity	0.520
Specific Material weight	0.024 MN/ mE + 3

Coefficient of thermal expansion	1.2 E -05 1/K
Fixed Crack Model Cofficient	1

B. Reinforcement Bars

HYSD steel of grade Fe-415 of 8 mm diameter are used as main reinforcement and 8 mm bars are also used as distribution reinforcement. The properties of these bars are shown in Table 3.2.

Table 3.2 Material Properties of reinforcement [1]

Properties	Values
Elastic modulus	200000 Mpa
yield strength	624 Mpa
specific material weight	0.0785 MN/ mE +3
coefficient of thermel expansion	1.2 E - 05 1/K

C. Steel Plate

The function of the steel plate in the ATENA is for support and for loading. Here, the property of steel plate is same as the reinforcement bar except its yield strength. The HYSD steel of grade Fe-415 was used for steel plate

3.12 FE MODELLING OF RCC SKEW SLAB IN ATENA

3.12.1 INTRODUCTION

The ATENA program, which is determined for nonlinear finite element analysis of structures, offers tools specially designed for computer simulation of concrete and reinforced concrete structural behavior.ATENA program system consists of a solution core and several user interfaces. The solution core offers capabilities for variety of structural analysis tasks, such as: stress and failure analysis, transport of heat and humidity, time dependent problems (creep, dynamics), and their interactions. Solution core offers a wide range of 2D and 3D continuum models, libraries of finite elements, material models and solution methods. User interfaces are

specialized on certain functions and thus one user interface need not necessarily provide access to all features of ATENA solution core. This limitation is made on order to maintain a transparent and user friendly user environment in all specific applications of ATENA.

ATENA 3D program is designed for 3D nonlinear analysis of solids with special tools for reinforced concrete structures. However, structures from other materials, such as soils, metals etc. can be treated as well. The program has three main functions:

A. Preprocessing
B. Run
C. Postprocessing

A Pre-processing. Input of geometrical objects (concrete, reinforcement, interfaces, etc.), loading and boundary conditions, meshing and solution parameters.

B Analysis. It makes possible a real time monitoring of results during calculations.

C Post-processing. Access to a wide range of graphical and numerical results.

Procedure: In pre-processing window following steps are performed:-

Step1 Geometry of FE model is created .It has been presented in Figure 3.19 & 3.21.

Step2 Material properties are assigned to the various elements of the skew slab specimen.

Step3 Structural element, various supports, loadings and monitoring points are defined. (Figure 3.19 & 3.21)

Step4 Finite element meshing parameters are given and meshing of the model is generated accordingly.

Step5 Various analysis steps are defined. The FE non-linear analysis is done in Run window. The FE non-linear static analysis calculates the effects of steady loading conditions on a structure. A static analysis can, however, include steady inertia loads (such as gravity and rotational velocity), and time-varying loads that can be approximated as static equivalent. Static analysis is used to determine the displacements, stresses, strains, and forces in structures or components by loads.

Step6: When the FE non linear static analysis is completed the, the results are shown in third part of the ATENA i.e. Post processing. The stress- strain values at every step, crack pattern and

cracks propagation at every step shown help in to analyze the behaviour of the elements at every step of load deflection.

3.12.2 METHODS FOR NON-LINEAR SOLUTION [26]

The best part of the ATENA is the simpler way of solving the non-linear structural behaviour through finite element method and its incremental loading criteria. Different methods are available in ATENA for solving non-linear equations such as, linear method, Newton-Raphson Method, Modified Newton-Raphson method, Arc Length methods are used in ATENA. Among these the Newton-Raphson Method and Modified Newton-Raphson Method are more commonly used methods. In our present study, Newton-Raphson method is used for solving the simultaneous equations. It is an iterative process of solving the non-linear equations.

One approach to non-linear solutions is to break the load into a series of load increments. The load increments can be applied either over several load steps or over several sub steps within a load step. At the completion of each incremental solution, the program adjusts the stiffness matrix to reflect the nonlinear changes in structural stiffness before proceeding to the next load increment. . The ATENA program overcomes this difficulty by using Full Newton-Raphson method, or Modified Newton-Raphson method, which drive the solution to equilibrium convergence (within some tolerance limit) at the end of each load increment. In Full Newton-Raphson method, it obtains the following set of non-linear equations:

$K(p)\,\Delta p = q - f(p)$

where: q is the vector of total applied joint loads,

$f(p)$is the vector of internal joint forces,

Δp is the deformation increment due to loading increment,

p are the deformations of structure prior to load increment,

$K(p)$ is the stiffness matrix, relating loading increments to deformation increments.

Figure 3.17 illustrates the use of Newton-Raphson equilibrium iterations in nonlinear analysis. Before each solution, the Newton-Raphson method evaluates the out-of -balance load vector, which is the difference between the restoring, forces (the loads corresponding to the element stresses) and the applied loads. The program then performs a linear solution, using the out-of -

balance loads, and checks for convergence. If convergence criteria are not satisfied, the out-of-balance load vector is re-evaluated, the stiffness matrix is updated, and a new solution is obtained. This iterative procedure continues until the problem converges. But sometimes, the most time consuming part of the Full Newton-Raphson method solution is the re-calculation of the stiffness matrix $K\,(pi-1)$ at each iteration. In many cases this is not necessary and we can use matrix $K\,(p_0)$ from the first iteration of the step. This is the basic idea of the so-called Modified Newton-Raphson method. It produces very significant time saving, but on the other hand, it also exhibits worse convergence of the solution procedure. The simplification adopted in the Modified Newton-Raphson method can be mathematically expressed by:

$$K\,(pi-1) = K\,(p_0)$$

The modified Newton-Raphson method is shown in Figure 3.17. Comparing Figure3.16 and Figure3.17, it is apparent that the Modified Newton-Raphson method converges more slowly than the original Full Newton-Raphson method. On the other hand a single iteration costs less computing time, because it is necessary to assemble and eliminate the stiffness matrix only once. In practice a careful balance of the two methods is usually adopted in order to produce the best performance for a particular case. Usually, it is recommended to start a solution with the original Newton-Raphson method and later, i.e. near extreme points, switch to the modified procedure to avoid divergence.

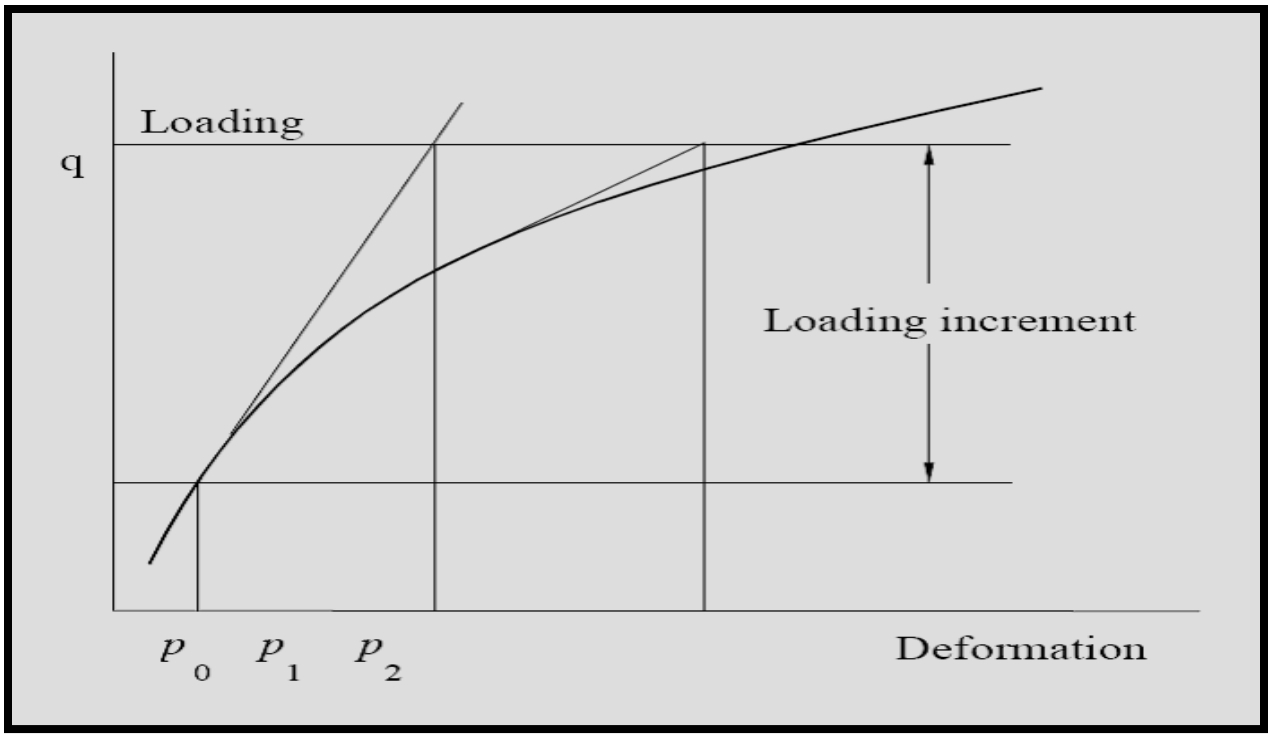

Figure 3.16 Full Newton-Raphson Method [26]

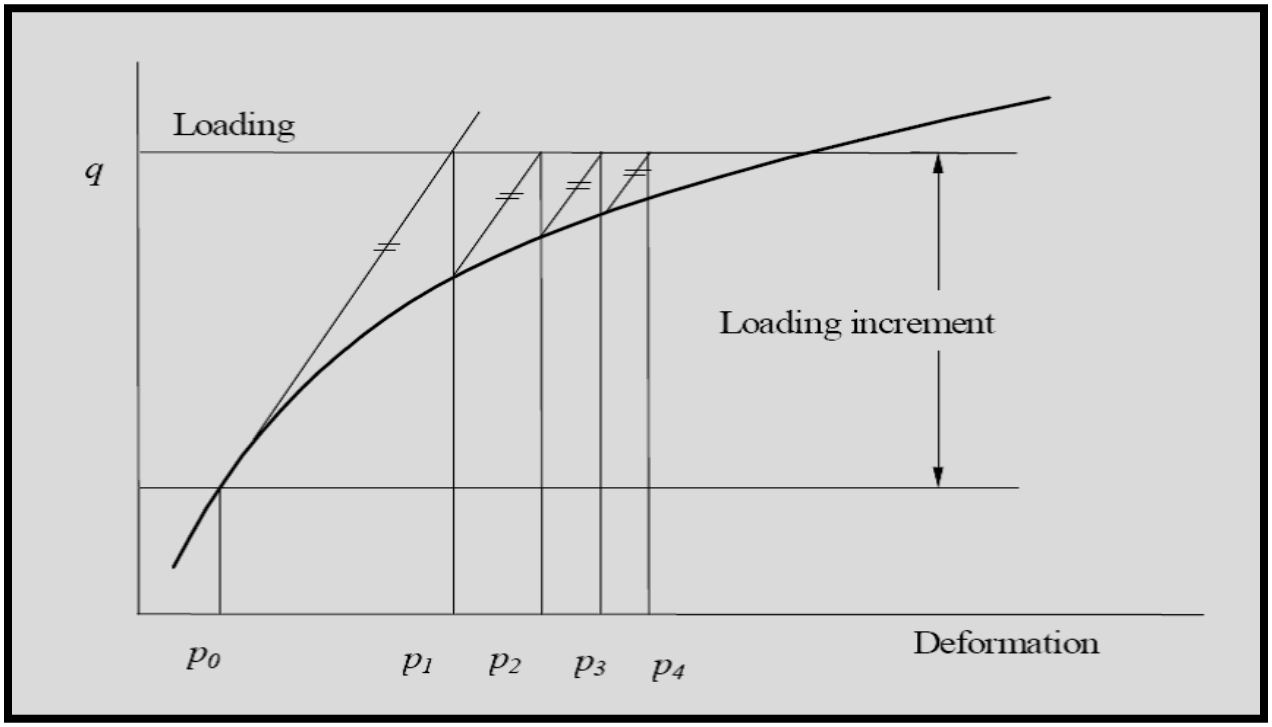

Figure 3.17 Modified Newton-Raphson Method [26]

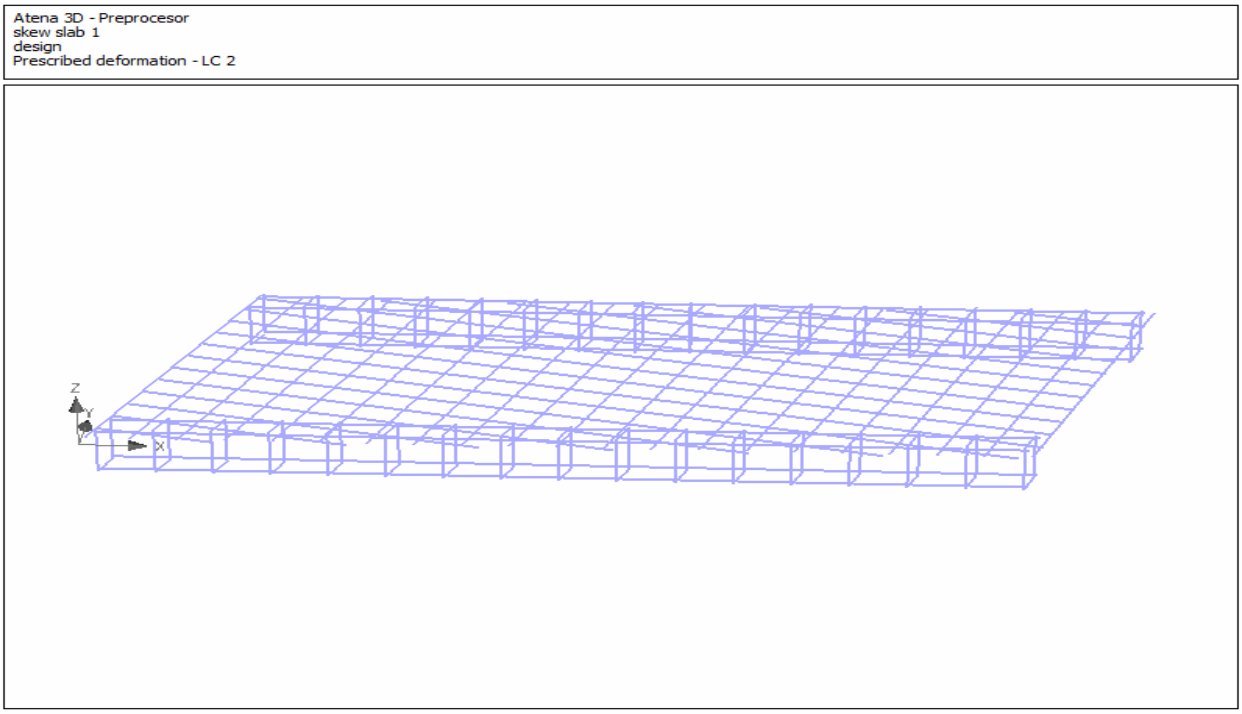

Figure 3.18, reinforcement in skew slab specimen 1

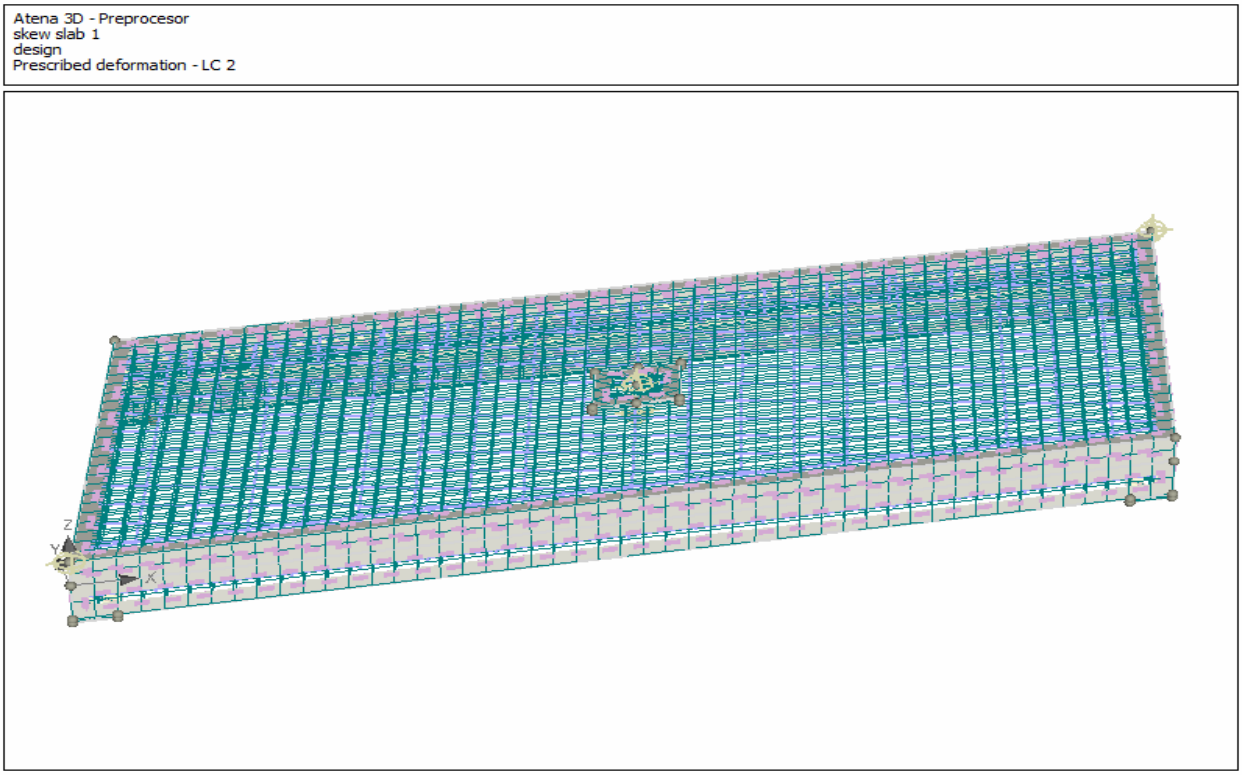

Figure 3.19, Modelling of skew slab specimen 1 with edge beam

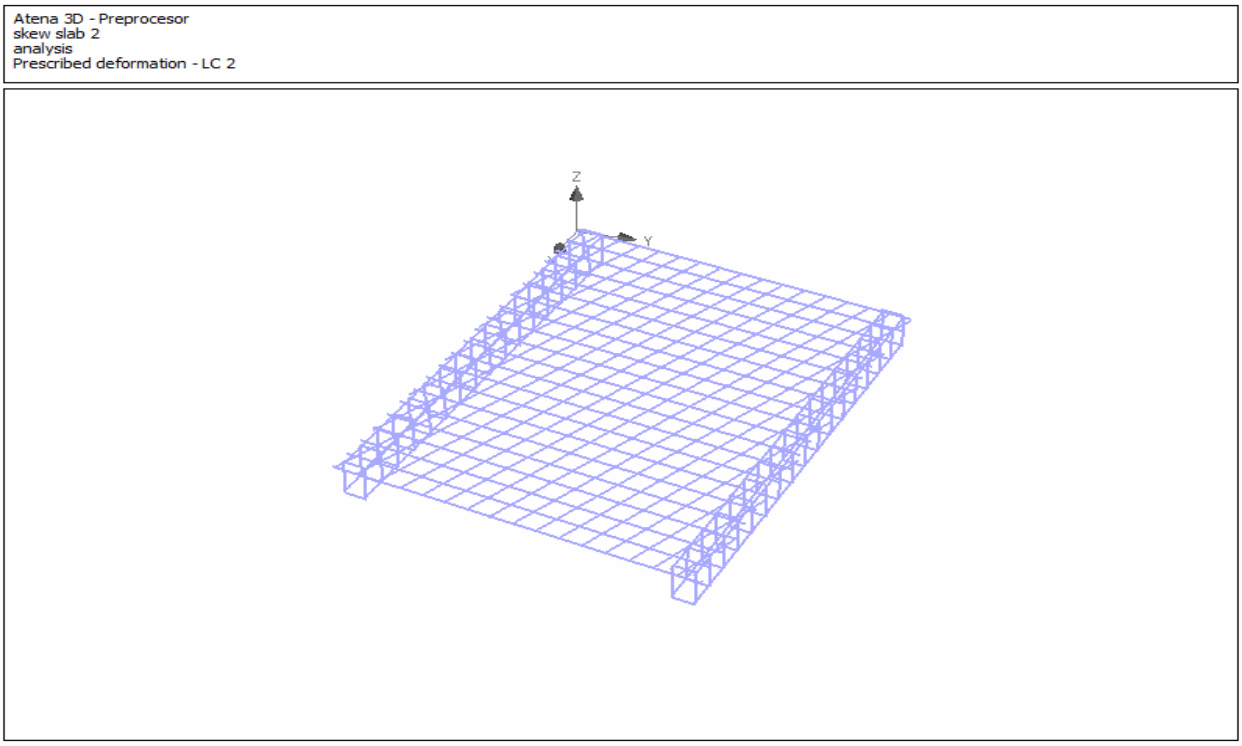

Figure 3.20, reinforcement in skew slab specimen 2

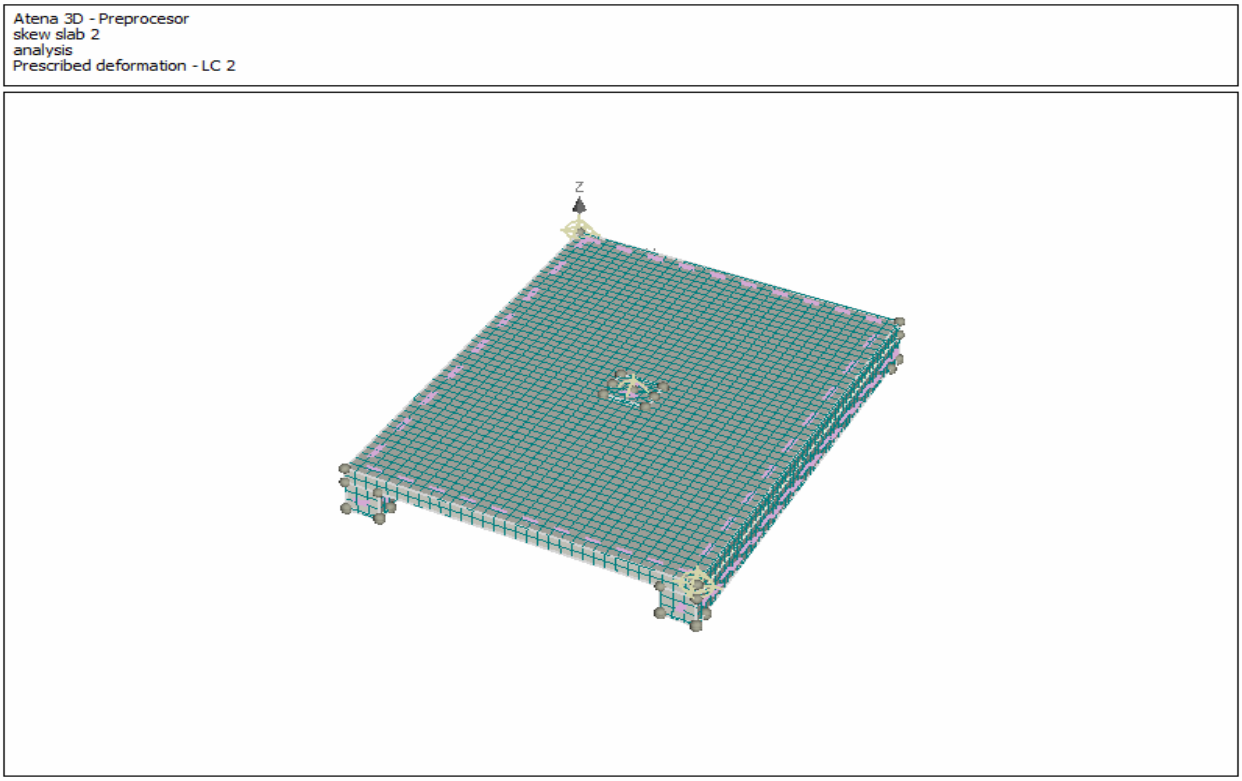

Figure 3.21, Modelling of skew slab specimen 2 with edge beam

CHAPTER 4, RESULTS AND DISCUSSIONS

This chapter presents the results of Finite Element modelling of Skew slabs with edge supports. Finite element modelling of skew slabs with edge supports under the static incremental loads has been performed using ATENA software. Subsequently these results are compared with experimental results of “Flexural behavior of reinforced cement concrete skew slabs" and " Finite Element modelling of RCC skew slab". This is followed by load deflection curve and Behavior of Up lift due to various changed sectional details as edge supports.

4.1 FE MODEL RESULTS OF SKEW SLAB

In the present study, non-linear response of RCC skew slab modelled as per details discussed in Chapter 3 (3.2 General Description of Structure) using FE Modelling under the incremental loading has been carried out. The objective of this study is to see the behavior of Uplift in the slab with edge supports, variation of load- displacement graph, load - uplift curve, the crack patterns, propagation of the cracks and the crack width at different values of the deflection.

4.1.1 LOAD V/S DEFORMATIONS OF SKEW SLAB SPECIMENS

In FE Model skew slabs specimen loads have been applied at the centre of the slabs represents resultant load due to self weight and applied uniform area load and concentrated live load due to different position of axles on the slab that will produce maximum bending in the slabs as done in case of experiment.

The load on the structure has been gradually increased in the steps till failure. When the FE non linear analysis is completed, the results are shown in third part of the ATENA i.e. Post processing. The load-deflection and uplifts values at every step have been recorded, further the crack pattern and cracks propagation at every step has been studied. The load v/s deflection and load/ uplift curves at both the slab specimens have been plotted and are presented in Figure 4.1 & 4.20.

Deflection/ uplifts of specimen 1

When the slab was free then these are the following graphical representation for the analytical and FE modelling behavior, which has been obtained by the previous reserches.

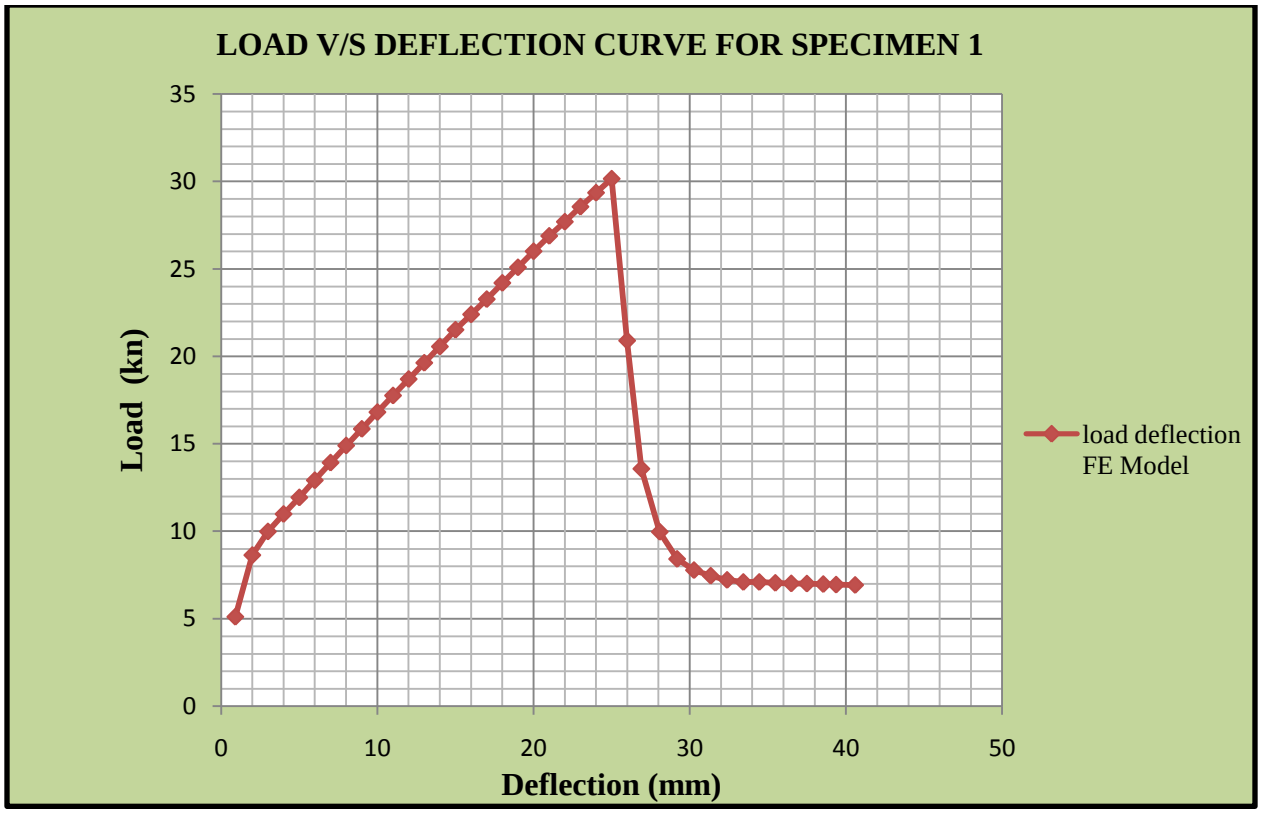

Figure 4.1, Load v/s Displacement of skew slab specimen 1 [1]

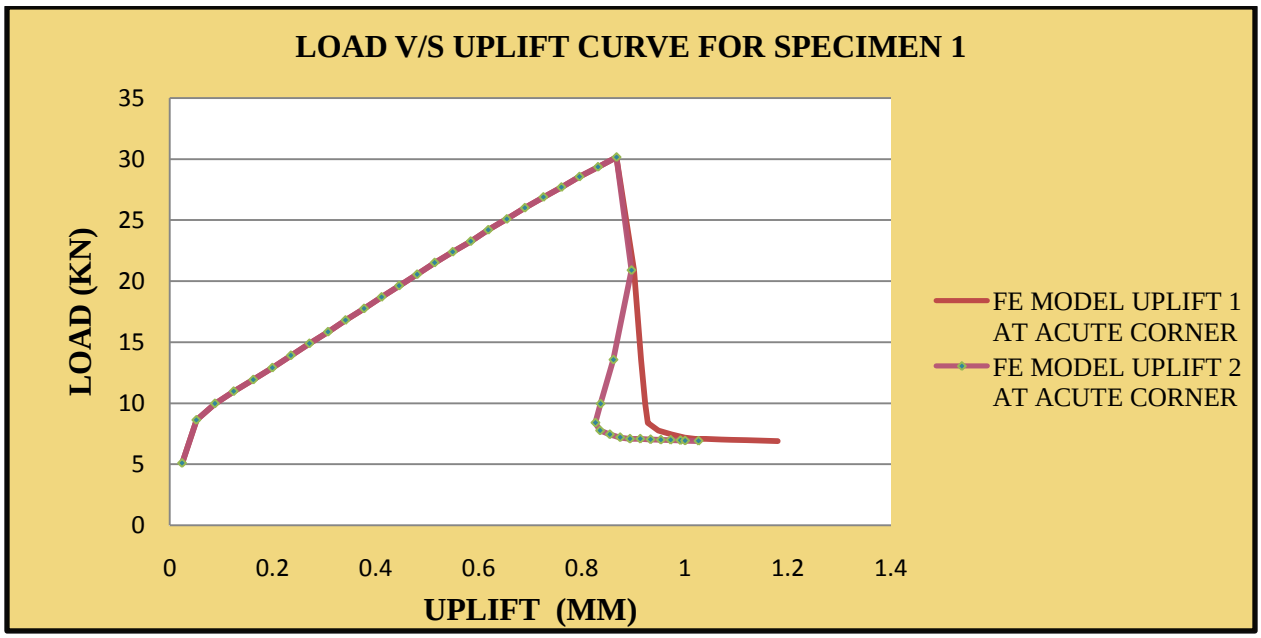

Figure 4.2, Load v/s Uplifts at acute corners of skew slab specimen 1[1]

Based on the previsions studies, to prevent the up lift the physical behavior for a slab with edge supports has been introduced and the results are as under:-

The deflection at skew slab specimen 1 in which the short diagonal of slab is less than its span along the traffic. It is clear from figure 4.3. Focusing on the behavior of slab specimen 1, deflection at skew slab specimen 1with 130x150mm edge supports has been plotted in Figure 4.3. It can be seen from that the structure behaved linearly elastic up to the value of load sheer 73.92 KN. At this point the minor cracks started to get generated at bottom part (tensile zone) of the slab. After this point there is slight decrement in curvature in the plot and deflection started increasing. When the deflection reached to the value of 21.01 mm, the graph depicted non-linearity in its behavior and crack widened and extended up to the free edges. It is clear from the Figure 4.4 after load 73.92 KN; increase in deflection is more with uplift occurred at acute corners. As the load increases uplifts at acute corners started increasing. The maximum uplift at acute corners has been observed to be 1.18 mm. As the uplifts increases there is a rapid increase in displacement is observed.

It has been depicted through the figure 4.4 it can be observed that there were some uplifts at skew slab acute corners of specimen 1. It can be seen from that the structure behaved linearly elastic up to the value of load 73.92 KN. After this point, as the uplifts increases at the both acute corners, load started decreases. There is sudden fall in curvature as the load decreases and constantly reduces gradually with no change in both the sides. The load deflection and uplifts at acute corners of skew slab specimen 1 have been tabulated in tables 4.1, 4.2&4.3

Sr. no.	Load In KN	Deflection In MM	Uplift 1 (MM) at Acute Corner	Uplift 2 (MM) at Acute Corner
1	16.13	1.00	0.04	0.04
2	21.33	2.00	0.08	0.08
3	25.01	3.00	0.13	0.13
4	28.58	4.00	0.18	0.18
5	32.05	5.00	0.23	0.22
6	35.49	6.00	0.28	0.27
7	38.87	7.01	0.33	0.32
8	42.02	8.01	0.38	0.37
9	45.09	9.01	0.44	0.43
10	48.21	10.01	0.50	0.49
11	51.15	11.01	0.57	0.56

12	54.11	12.02	0.63	0.62
13	57.05	13.02	0.69	0.68
14	59.89	14.02	0.76	0.75
15	62.62	15.02	0.83	0.82
16	65.46	16.02	0.89	0.88
17	68.02	17.03	0.96	0.95
18	70.53	18.03	1.02	1.01
19	72.25	19.03	1.08	1.07
20	73.37	20.02	1.14	1.13
21	73.92	21.01	1.18	1.18
22	73.31	22.39	1.22	1.21
23	71.67	23.70	1.23	1.22
24	69.50	24.88	1.22	1.23
25	65.58	25.94	1.21	1.20
26	62.17	26.93	1.18	1.17
27	59.75	27.97	1.14	1.13
28	57.94	29.02	1.11	1.10
29	56.19	30.07	1.07	1.06
30	55.22	31.10	1.04	1.03
31	54.77	32.17	1.02	1.01
32	54.72	33.24	1.01	1.00
33	57.90	34.28	1.00	0.98
34	54.87	35.30	0.99	0.97
35	55.38	36.28	0.99	0.97
36	55.96	37.28	0.99	0.97
37	56.44	38.27	0.99	0.97
38	56.91	39.27	0.99	0.78
39	57.36	40.27	1.00	0.98
40	57.67	41.26	1.01	0.99

Table 4.1 F.E results of skew slab specimen 1 [1]

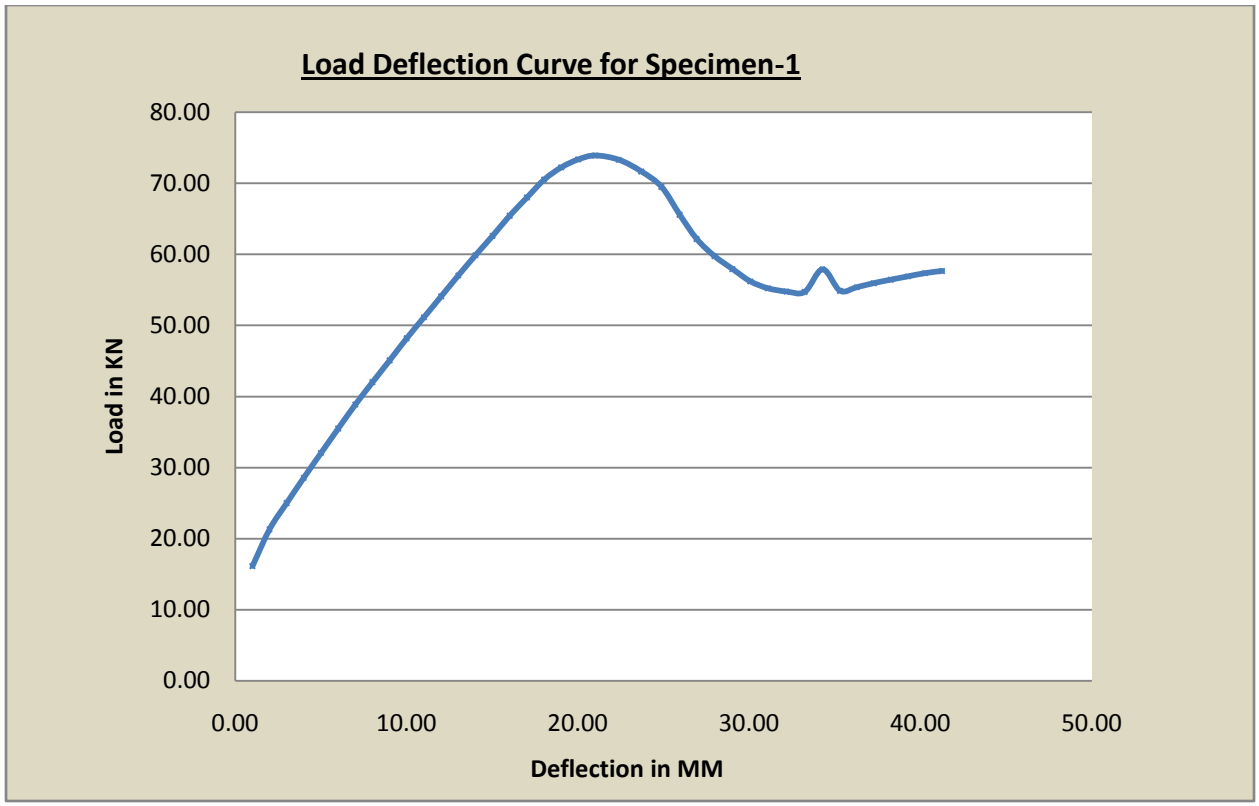

Figure 4.3, Load v/s Displacement of skew slab specimen 1 (130x150mm edge support)

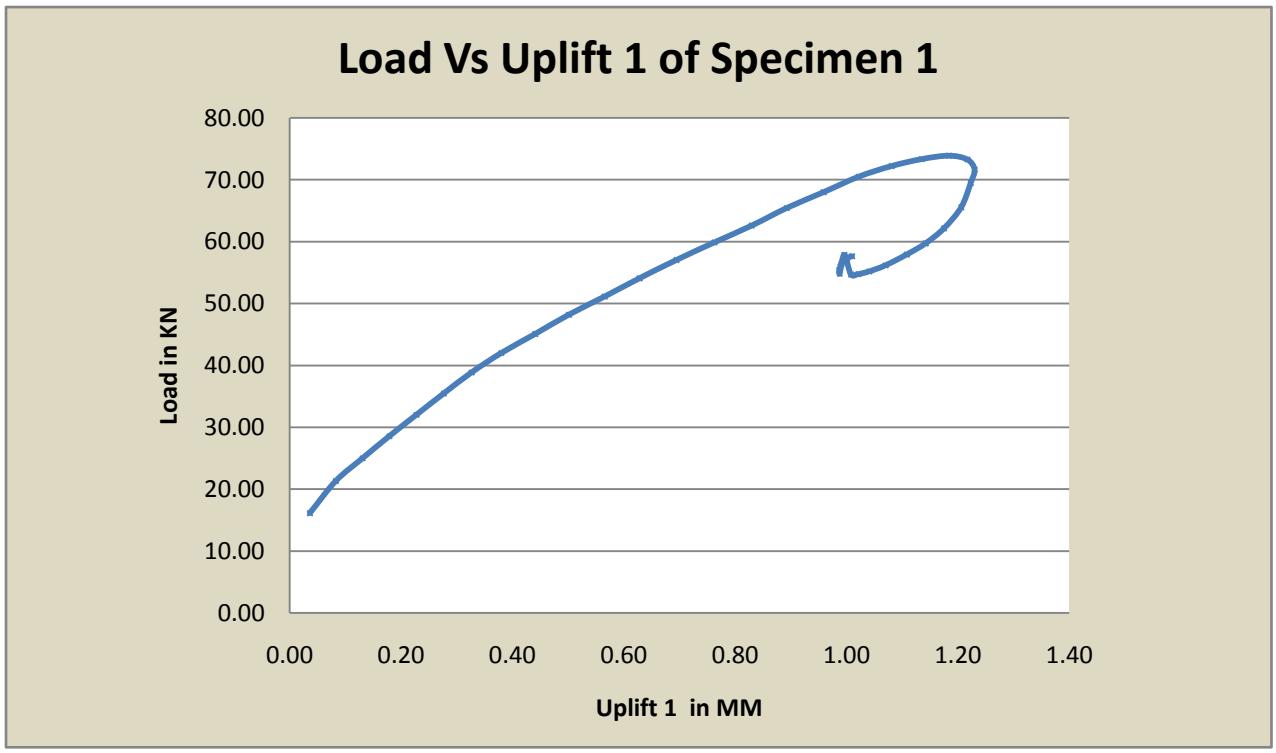

Figure 4.4, Load v/s Uplifts of skew slab specimen(130x150mm edge support)

Figure

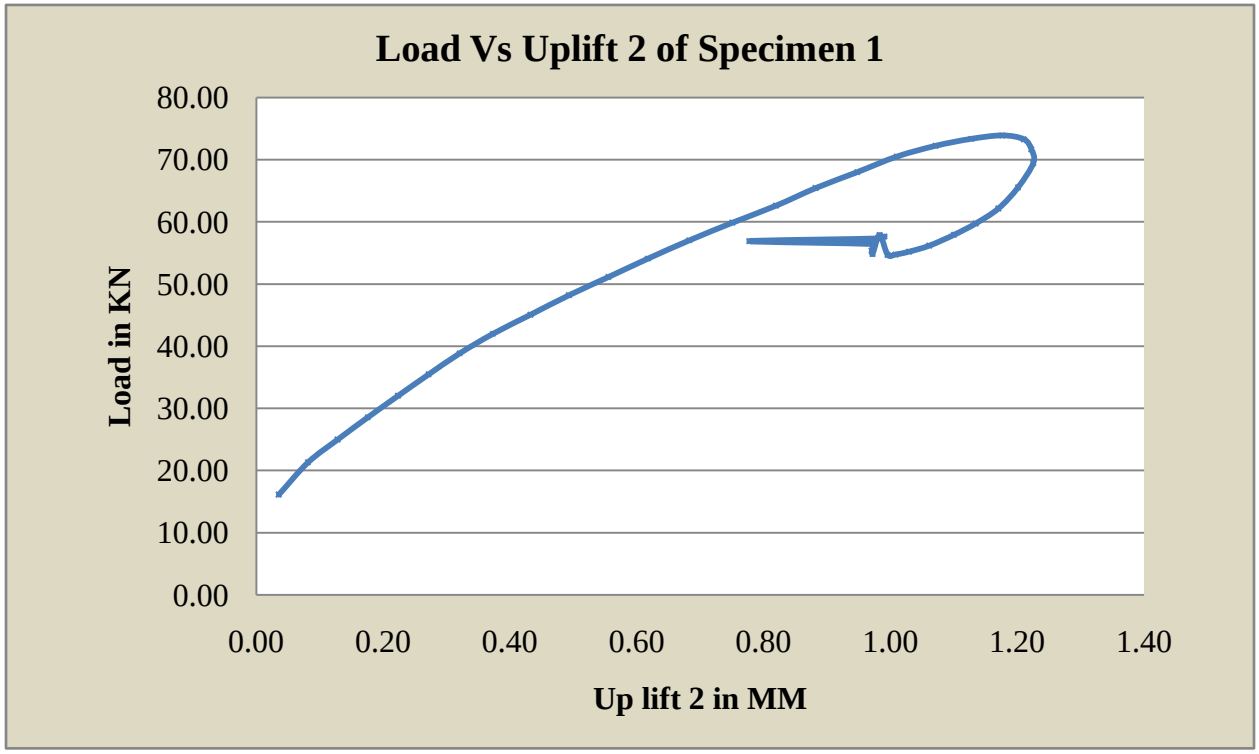

Figure 4.5, Load v/s Uplifts of skew slab specimen (130x150mm edge support)

From Table 4.1(A). Focusing on the behavior of slab specimen 1, deflection at skew slab specimen 1with 100x150mm edge supports has been plotted in Figure 4.6. It can be seen from that the structure behaved linearly elastic up to the value of load sheer 79.97 KN. At this point the minor cracks started to get generated at bottom part (tensile zone) of the slab. After this point there is slight decrement in curvature in the plot and deflection started increasing. When the deflection reached to the value of 21.88 mm, the graph depicted non-linearity in its behavior and crack widened and extended up to the free edges. It is clear from the Figure 4.7 & 4.8 after load 79.97 KN; increase in deflection is more with uplift occurred at acute corners. As the load increases uplifts at acute corners started increasing. The maximum uplift at acute corners has been observed to be 1.14 mm. As the uplifts increases there is a rapid increase in displacement is observed.

It has been depicted through the Table 4.1(A), it can be observed that there were some uplifts at skew slab acute corners of specimen 1. It can be seen from that the structure behaved linearly

elastic up to the value of load 79.97 KN. After this point, as the uplifts decreases at the both acute corners, load started decreases. There is sudden fall in curvature as the load decreases and constantly reduces gradually with no change in both the sides.

Table 4.1(A) FE results for Skew slab Specimen 1 with 100x150 mm beams supports

Sl no	Load In KN	Deflection In MM	Uplift 1 (MM) at Acute Corner	Uplift 2 (MM) at Acute Corner
1	20.30	1.00	0.03	0.03
2	26.10	2.00	0.07	0.07
3	30.72	3.00	0.12	0.12
4	35.07	4.00	0.17	0.16
5	39.12	5.01	0.22	0.21
6	43.13	6.01	0.27	0.27
7	46.58	7.01	0.34	0.33
8	50.18	8.01	0.40	0.39
9	53.81	9.02	0.47	0.46
10	60.83	11.02	0.60	0.59
11	64.15	12.02	0.66	0.65
12	67.50	13.03	0.73	0.72
13	70.77	14.03	0.80	0.78
14	73.92	15.03	0.86	0.85
15	77.05	16.03	0.92	0.91
16	78.89	17.04	0.99	0.97
17	80.10	18.04	1.05	1.03
18	81.19	19.43	1.10	1.08
19	81.21	20.74	1.14	1.12
20	79.97	21.88	1.15	1.14
21	77.57	22.99	1.15	1.14
22	73.10	24.02	1.12	1.10
23	67.94	25.02	1.06	1.04
24	64.46	26.04	1.00	0.98

25	62.22	27.13	0.95	0.94
26	60.36	28.25	0.91	0.90
27	59.35	29.35	0.88	0.87
28	58.82	30.39	0.86	0.85
29	58.62	31.45	0.84	0.83
30	58.69	32.52	0.83	0.82
31	58.78	33.60	0.82	0.81
32	59.13	34.63	0.81	0.80
33	59.55	35.63	0.81	0.80
34	60.29	36.59	0.81	0.80
35	61.30	37.56	0.81	0.80
36	62.45	38.55	0.82	0.81
37	63.64	39.54	0.83	0.83
38	64.78	40.54	0.84	0.84
39	65.76	41.57	0.85	0.85

Table 4.1(A) FE results for Skew slab Specimen 1 with 100x150 mm beams supports

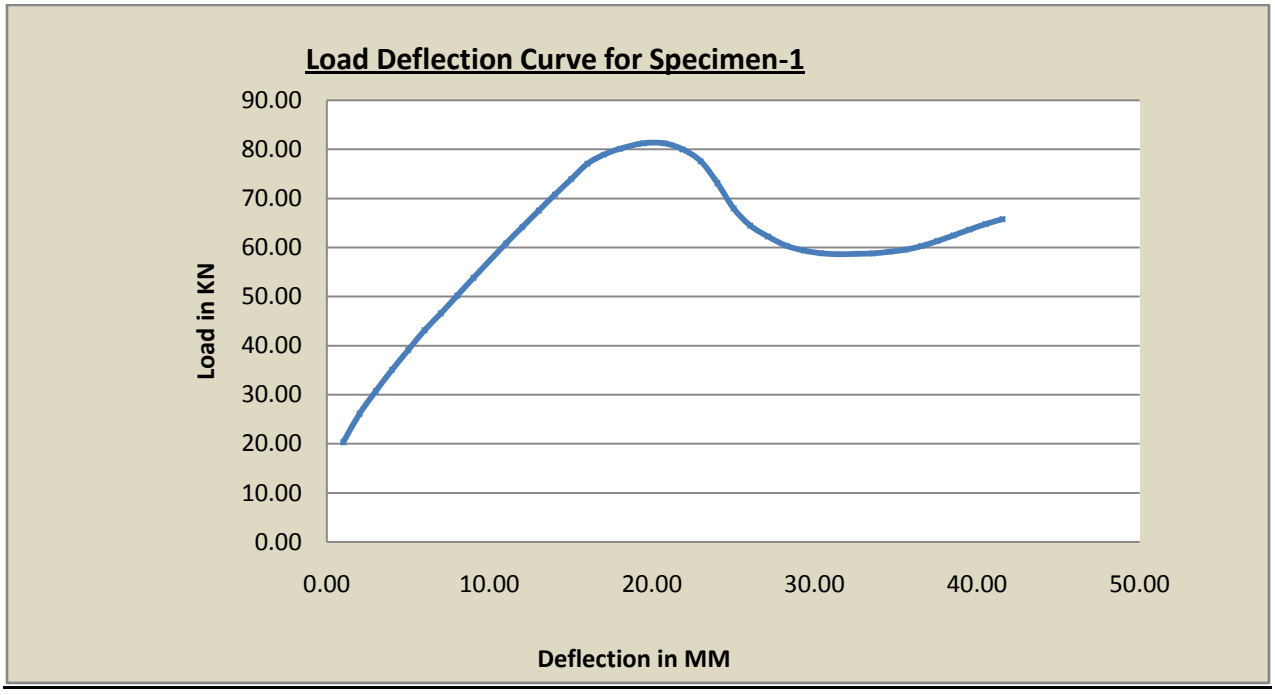

Figure 4.6, Load v/s Displacement of skew slab specimen 1 (100x150mm edge support)

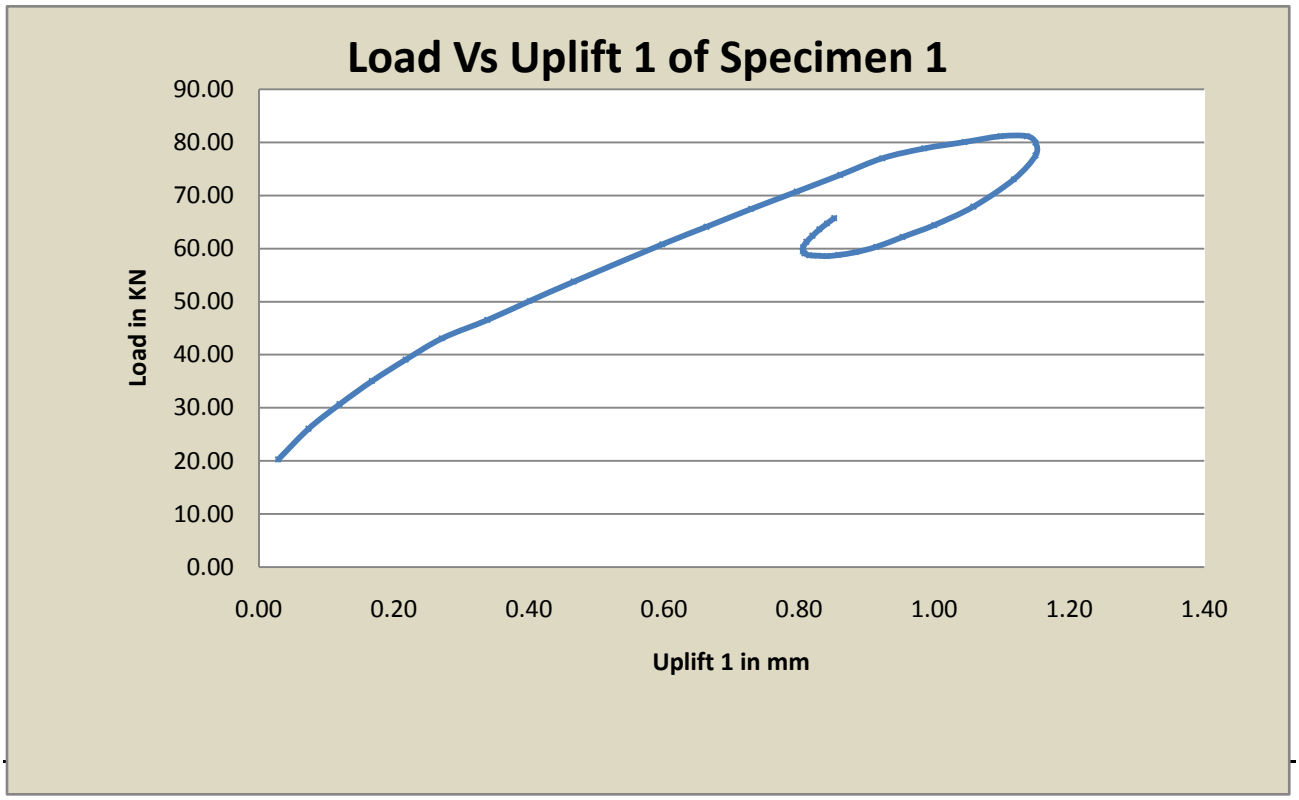

Figure 4.7, Load v/s Uplift of skew slab specimen 1 (100x150mm edge support)

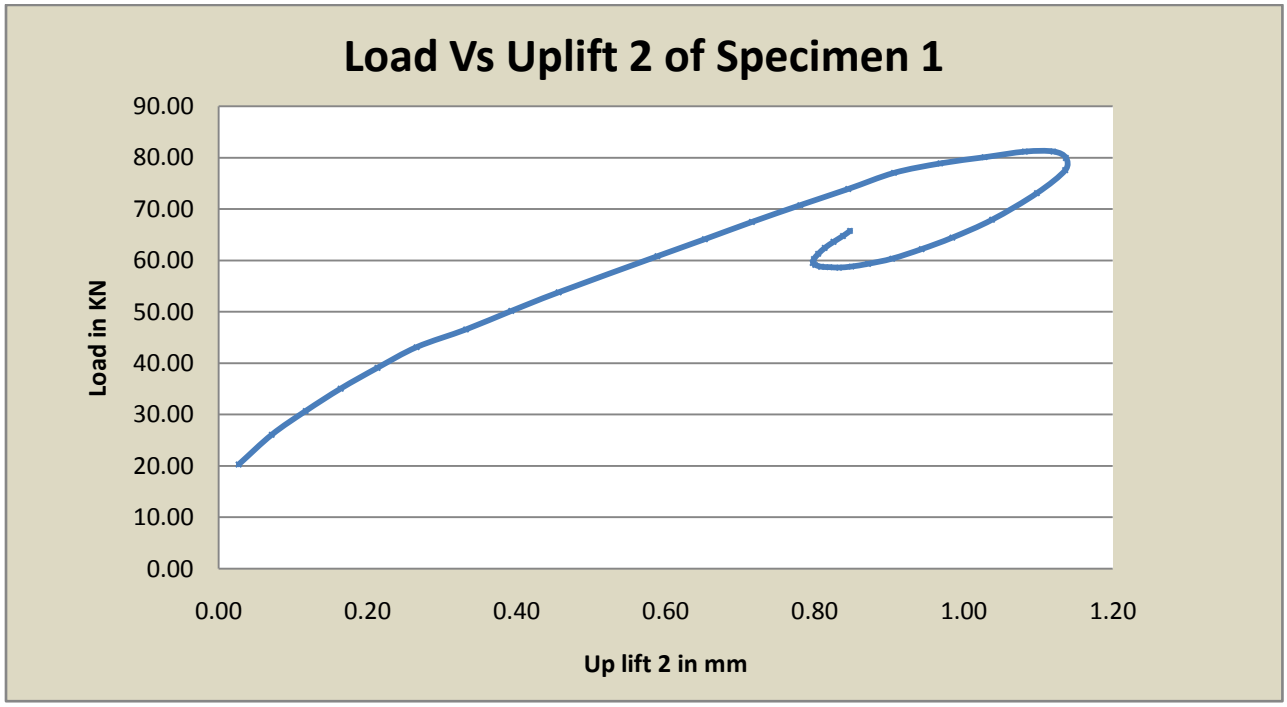

Figure 4.8, Load v/s Uplift of skew slab specimen 1 (100x150mm edge support)

From Table 4.1(B). Focusing on the behavior of slab specimen 1, deflection at skew slab specimen 1with 150x150mm edge supports has been plotted in Figure 4.9. It can be seen from that the structure behaved linearly elastic up to the value of load sheer 86.14 KN. At this point the minor cracks started to get generated at bottom part (tensile zone) of the slab. After this point there is slight decrement in curvature in the plot and deflection started increasing. When the deflection reached to the value of 21.88 mm, the graph depicted non-linearity in its behavior and crack widened and extended up to the free edges. It is clear from the Figure 4.10 & 4.11 after load 86.14 KN; increase in deflection is more with uplift occurred at acute corners. As the load increases uplifts at acute corners started increasing. The maximum uplift at acute corners has been observed to be 1.11 mm. As the uplifts increases there is a rapid increase in displacement is observed. It has been depicted through the Table 4.1(B), it can be observed that there were some uplifts at skew slab acute corners of specimen 1. It can be seen from that the structure behaved linearly elastic up to the value of load 86.14 KN. After this point, as the uplifts decreases at the both acute corners, load started decreases. There is sudden fall in curvature as the load decreases and constantly reduces gradually with no change in both the sides.

Table 4.1(B) FE results for Skew slab Specimen 1 with 150x150 mm beams supports

Table 4.1(B) FE results for Skew slab Specimen 1 with 150x150 mm beams supports				
Sl no	Load In KN	Deflection In MM	Uplift 1 (MM) at Acute Corner	Uplift 2 (MM) at Acute Corner
1	23.22	1.00	0.02	0.02
2	29.25	2.00	0.07	0.07
3	34.71	3.00	0.11	0.11
4	39.40	4.00	0.16	0.16
5	43.65	5.01	0.22	0.22
6	47.61	6.01	0.29	0.28
7	51.59	7.01	0.35	0.35
8	55.55	8.01	0.42	0.42
9	59.38	9.02	0.49	0.48
10	63.28	11.02	0.56	0.55
11	67.26	12.02	0.62	0.61

12	71.00	13.03	0.69	0.68
13	74.57	14.03	0.76	0.74
14	78.19	15.03	0.82	0.80
15	81.38	16.03	0.89	0.86
16	82.84	17.35	0.95	0.93
17	84.63	18.65	1.01	0.99
18	85.86	19.85	1.07	1.03
19	86.17	21.04	1.11	1.08
20	85.44	22.17	1.14	1.11
21	81.84	22.17	1.14	1.11
22	76.24	23.30	1.10	1.06
23	70.08	24.44	1.02	0.99
24	64.53	25.61	0.92	0.90
25	59.69	26.78	0.84	0.82
26	56.76	27.90	0.78	0.76
27	55.28	29.03	0.74	0.72
28	54.49	30.11	0.71	0.69
29	54.22	31.18	0.68	0.67
30	54.30	32.21	0.67	0.66
31	55.07	33.21	0.67	0.66
32	56.78	34.18	0.68	0.67
33	57.78	35.16	0.69	0.67
34	58.92	36.14	0.69	0.68
35	60.05	37.12	0.70	0.68
36	61.20	38.12	0.71	0.69
37	62.38	39.12	0.72	0.70
38	63.47	40.12	0.73	0.71
39	64.50	41.12	0.74	0.72
40	65.35	42.10	0.75	0.73

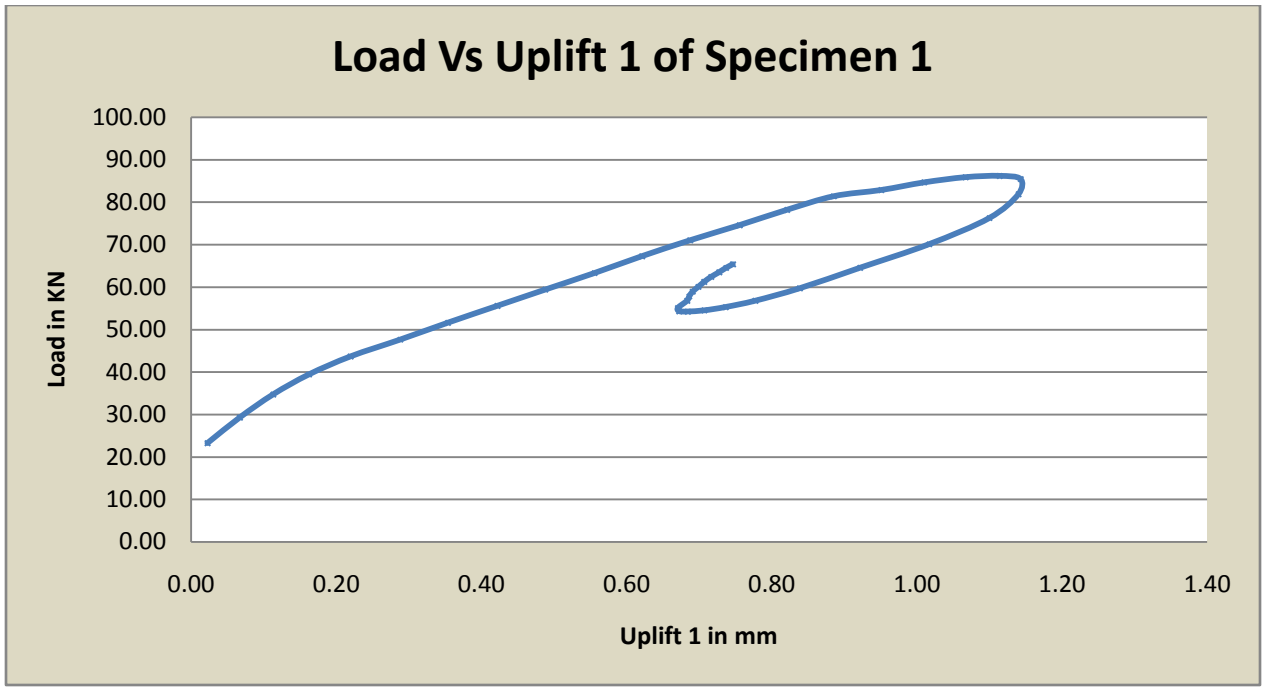

Figure 4.10, Load v/s Uplift of skew slab specimen 1 (150x150mm edge support)

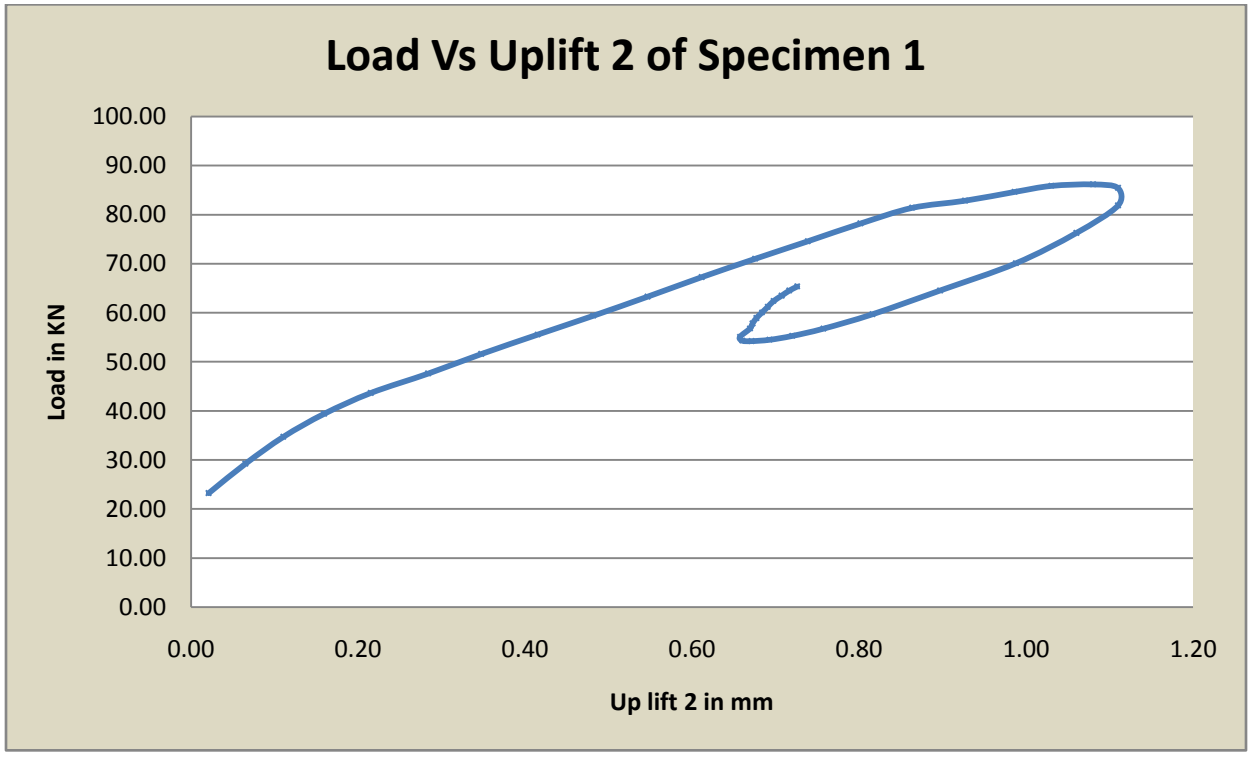

Figure 4.11, Load v/s Uplift of skew slab specimen 1 (150x150mm edge support)

Deflection /uplift at specimen 2

The deflection at skew slab specimen 2 in which the short diagonal of slab is greater than its span along the traffic. It is clearly specified from Table 4.2, Focusing on the behaviour of slab specimen 2. Deflection at skew slab specimen 2 has been plotted in Figure 4.12. It can be seen from that the structure behaved linearly elastic up to the value of load sheer 27.94 KN. At this point the minor cracks started to get generated at bottom part (tensile zone) of the slab. After this point there is a slight decrement in curvature in the plot and deflection started increasing. When the deflection reached to the value of 30.29 mm, the graph depicted non-linearity in its behavior and crack widened and extended up to the free edges. It is clear from the Figure 4.4 after load 38.77 KN, increase in deflection is more with uplifts occurred at acute corners. As the load increases uplifts at acute corners started increasing. The maximum uplift at acute corners has been observed to be 1.47 mm and other side as 0.38. As the uplifts increases there is a rapid increase in displacement is observed.

The load deflection and uplifts at acute corners of skew slab specimen 2 have been tabulated in table 4.2.

Table 4.2. FE results for Skew slab Specimen 2 with 100x150 mm beams supports

Sl no	Load In KN	Deflection In MM	Uplift 1 (MM) at Acute Corner	Uplift 2 (MM) at Acute Corner
1	4.48	1.01	-1.138	-0.18
2	8.96	2.02	-0.227	-0.36
3	11.93	3.03	-0.267	-0.46
4	13.40	4.04	-0.230	-0.47
5	14.22	5.05	-0.157	-0.46
6	14.84	6.06	-0.246	-0.43

7	15.52	7.07	0.006	-0.41
8	16.06	8.08	0.097	-0.37
9	16.68	9.09	0.113	-0.34
10	17.32	10.10	0.267	-0.31
11	17.94	11.11	0.355	-0.28
12	18.49	12.12	0.448	-0.24
13	19.09	13.13	0.535	-0.20
14	19.64	14.14	0.627	-0.17
15	20.21	15.15	0.631	-0.13
16	20.76	16.16	0.657	-0.10
17	21.25	17.17	0.721	-0.06
18	21.71	18.18	0.783	-0.02
19	22.20	19.19	0.843	0.01
20	22.75	20.20	0.890	0.04
21	23.20	21.21	0.917	0.08
22	23.74	22.22	0.939	0.11
23	24.26	23.23	0.980	0.15
24	24.78	24.24	0.993	0.18
25	25.31	25.25	1.003	0.21
26	25.83	26.26	1.111	0.24
27	26.33	27.27	1.312	0.28

28	26.88	28.27	1.356	0.31
29	27.42	29.28	1.360	0.34
30	27.94	30.29	1.470	0.38

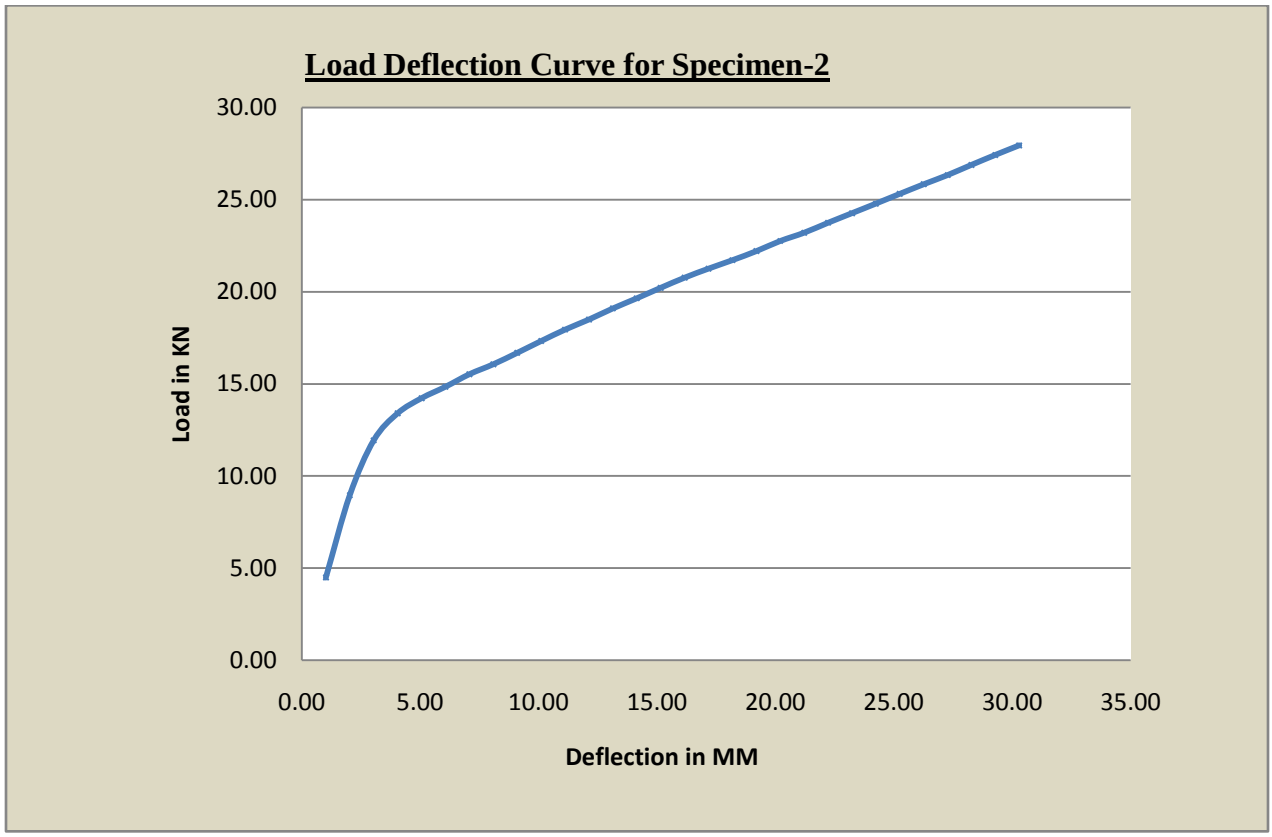

Figure 4.12, Load v/s Displacement of skew slab specimen 2(100x150mm edge supports)

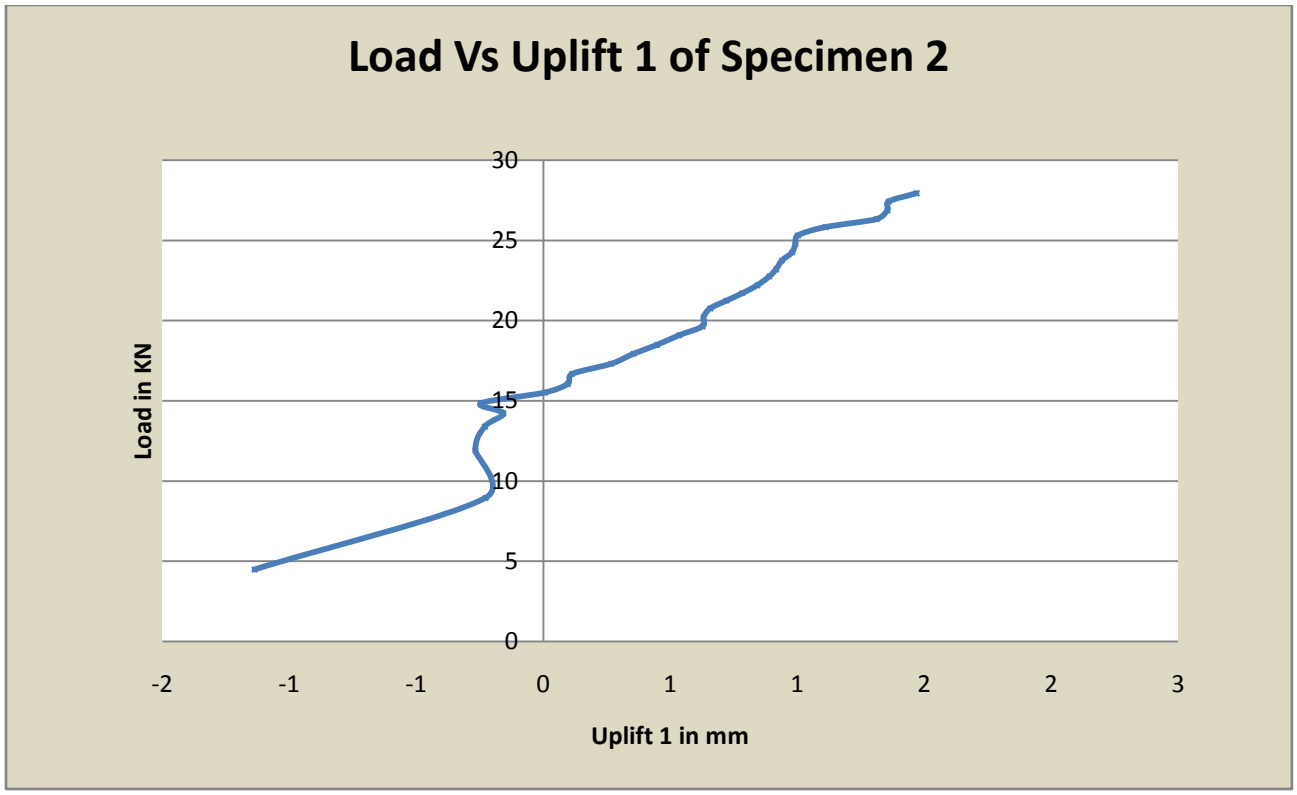

Figure 4.13, Load v/s Uplift of skew slab specimen 2 (100x150mm edge support)

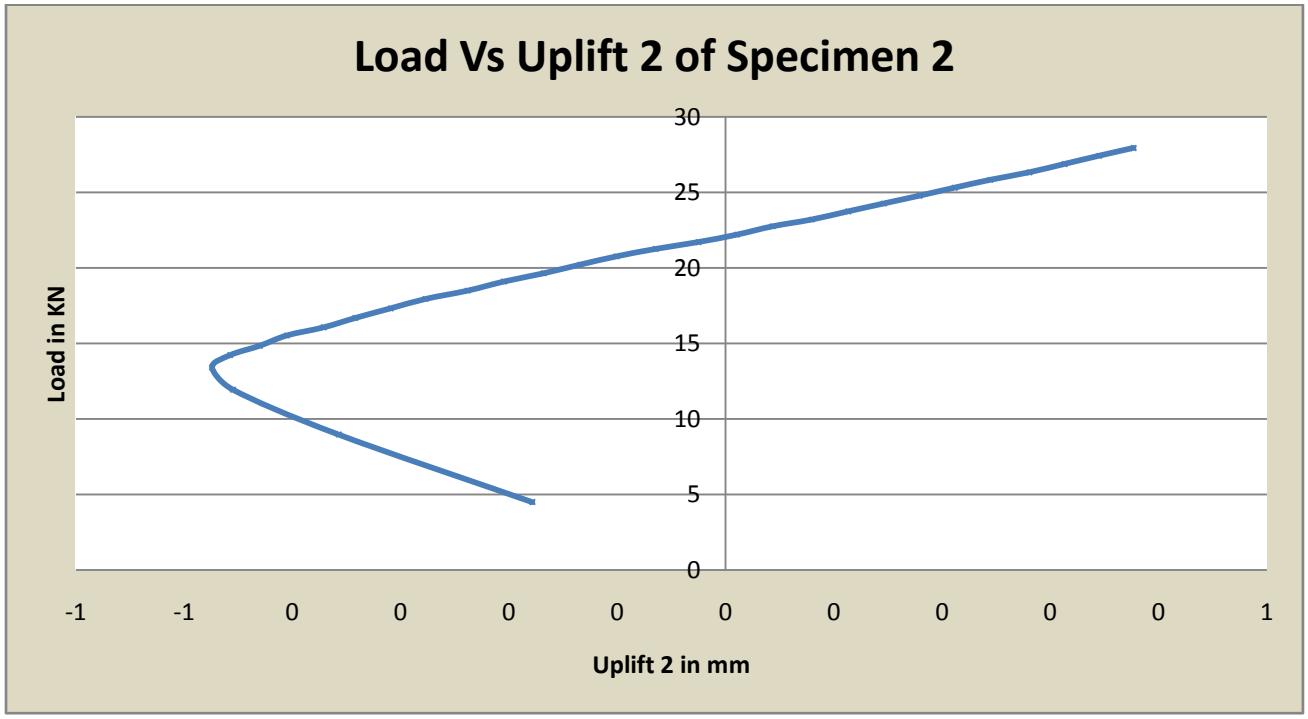

Figure 4.14, Load v/s Uplift of skew slab specimen 2 (100x150mm edge support

From Table 4.2(A). Focusing on the behavior of slab specimen 2, deflection at skew slab specimen 1with 130x150mm edge supports has been plotted in Figure 4.15. It can be seen from that the structure behaved linearly elastic up to the value of load sheer 57.70 KN. At this point the minor cracks started to get generated at bottom part (tensile zone) of the slab. After this point there is slight decrement in curvature in the plot and deflection started increasing. When the deflection reached to the value of 20.08 mm, the graph depicted non-linearity in its behavior and crack widened and extended up to the free edges. It is clear from the Figure 4.16 & 4.17 after load 57.70 KN; increase in deflection is more with uplift occurred at acute corners. As the load increases uplifts at acute corners started increasing. The maximum uplift at acute corners has been observed to be .46 mm. As the uplifts increases there is a rapid increase in displacement is observed.

It has been depicted through the Table 4.2(A), it can be observed that there were some uplifts at skew slab acute corners of specimen 2. It can be seen from that the structure behaved linearly elastic up to the value of load 57.70 KN. After this point, as the uplifts decreases at the both acute corners, load started decreases. There is sudden fall in curvature as the load decreases and constantly reduces gradually with no change in both the sides.

Table 4.2(A). FE results for Skew slab Specimen 2 with 130x150 mm beams supports

Sl no	Load In KN	Deflection In MM	Uplift 1 (MM) at Acute Corner	Uplift 2 (MM) at Acute Corner
1	14.38	1.00	-0.241	-0.24
2	23.09	2.00	-0.349	-0.35
3	27.44	3.00	-0.361	-0.36
4	29.55	4.00	-0.313	-0.31
5	31.66	5.05	-0.274	-0.27
6	33.79	6.01	-0.236	-0.23
7	35.83	7.01	-0.194	-0.19
8	37.92	8.01	-0.156	-0.15
9	40.02	9.01	-0.117	-0.11
10	42.08	10.01	-0.077	-0.05
11	43.99	11.01	-0.033	-0.02

12	46.06	12.02	0.006	0.02
13	47.94	13.03	0.052	0.07
14	49.94	14.04	0.093	0.11
15	51.93	15.04	0.138	0.15
16	53.86	16.05	0.181	0.20
17	55.37	17.06	0.233	0.25
18	56.35	18.06	0.298	0.31
19	57.35	19.07	0.363	0.38
20	57.70	20.08	0.447	0.46
21	56.60	21.08	0.570	0.58
22	53.03	22.09	0.780	0.76
23	41.03	23.60	0.812	0.81
24	33.33	24.95	0.878	0.86
25	28.93	26.19	0.928	0.90
26	26.29	27.37	0.945	0.94
27	24.75	28.57	0.956	0.97
28	23.44	29.73	0.973	0.99
29	22.57	30.85	0.981	1.03
30	22.09	31.94	0.987	1.08

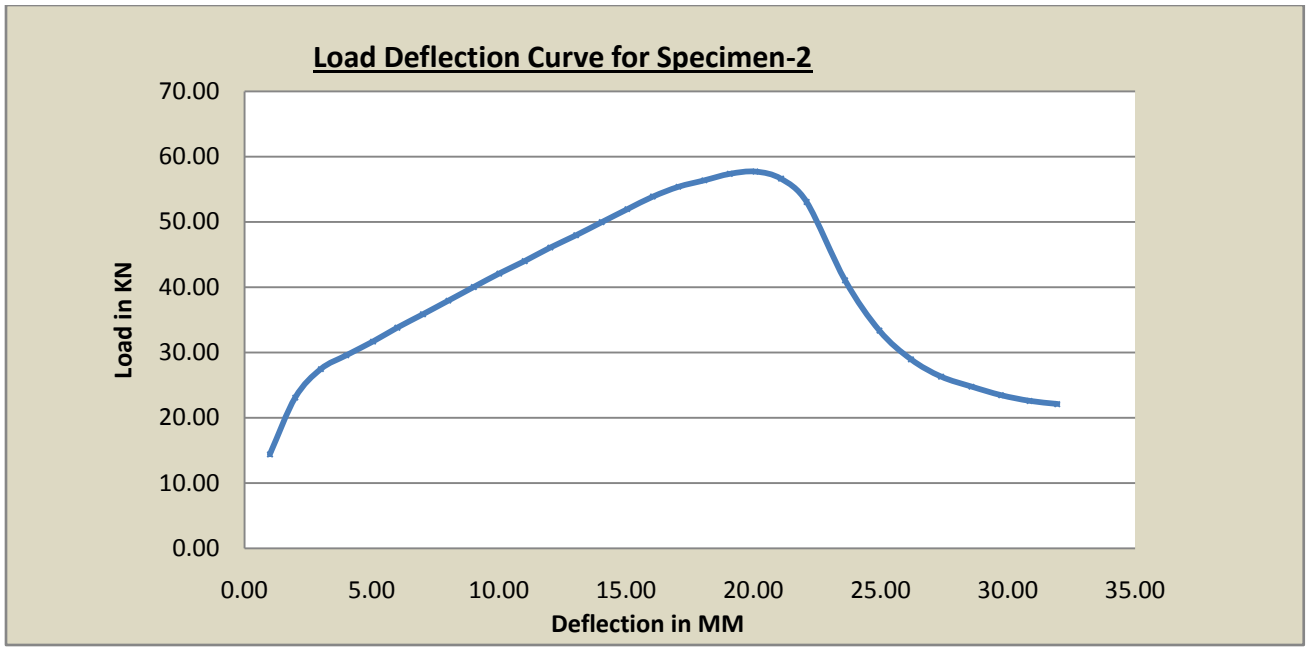

Figure 4.15, Load v/s Displacement of skew slab specimen 2(130x150mm edge supports)

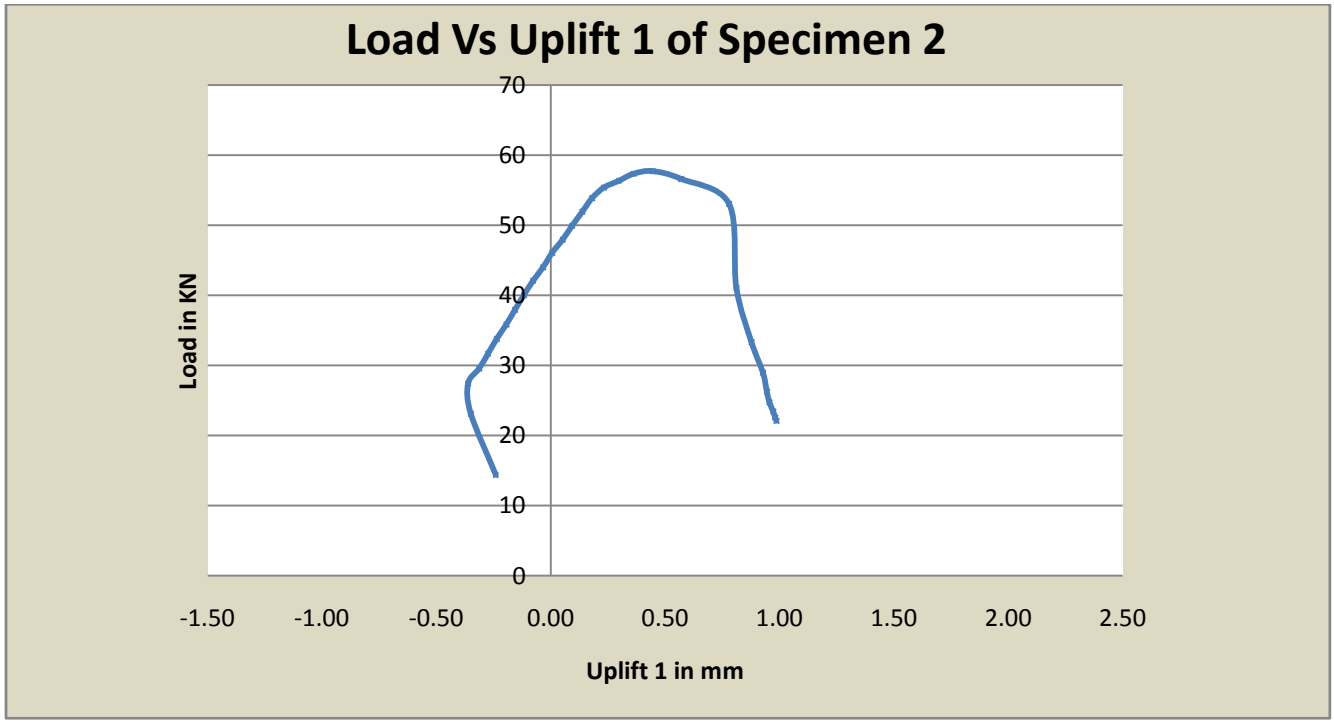

Figure 4.16, Load v/s Uplift of skew slab specimen 2(130x150mm edge supports)

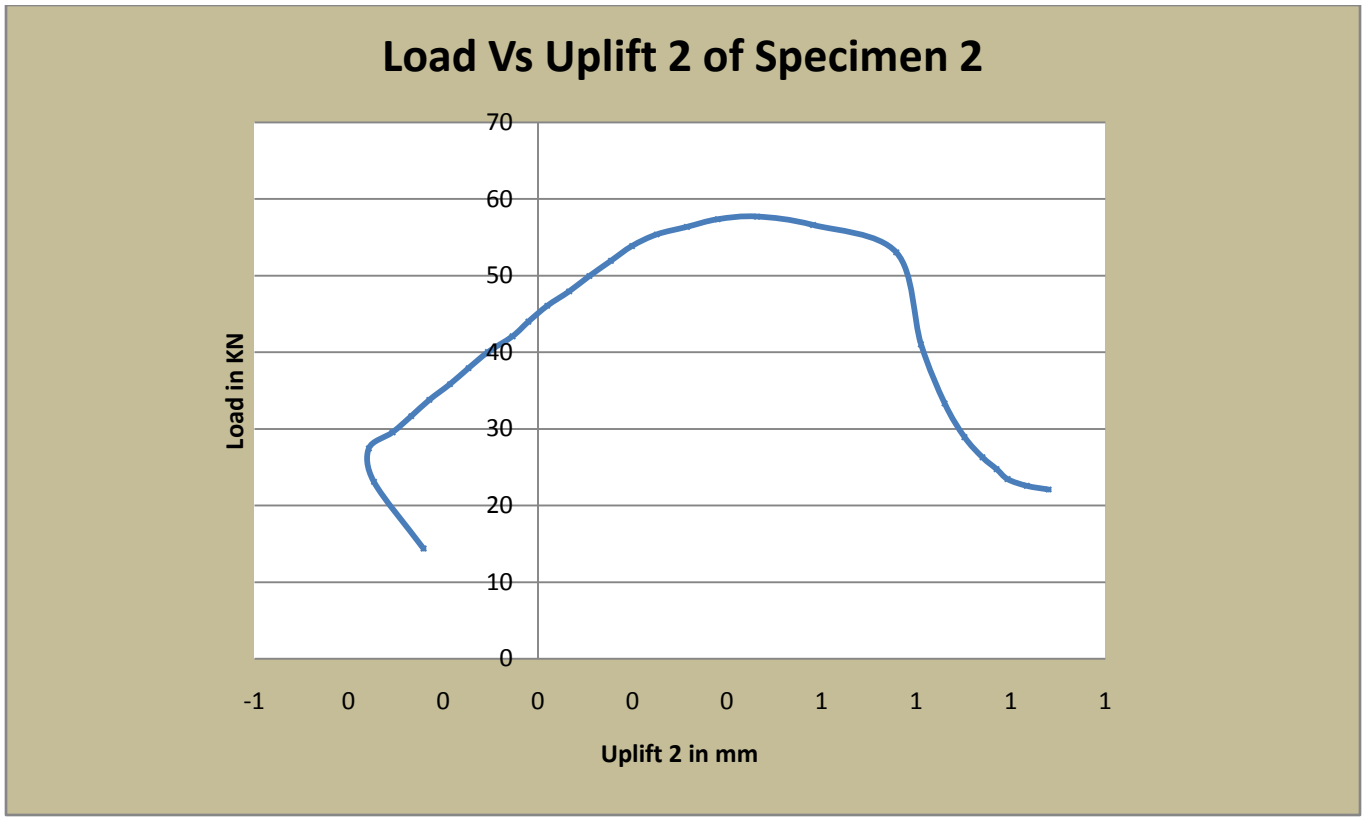

Figure 4.17, Load v/s Uplift of skew slab specimen 2(130x150mm edge supports)

From Table 4.2(B). Focusing on the behavior of slab specimen 2, deflection at skew slab specimen 2with 150x150mm edge supports has been plotted in Figure 4.15. It can be seen from that the structure behaved linearly elastic up to the value of load sheer 57.05 KN. At this point the minor cracks started to get generated at bottom part (tensile zone) of the slab. After this point there is slight decrement in curvature in the plot and deflection started increasing. When the deflection reached to the value of 19.19 mm, the graph depicted non-linearity in its behavior and crack widened and extended up to the free edges. It is clear from the Figure 4.16 & 4.17 after load 57.05 KN; increase in deflection is more with uplift occurred at acute corners. As the load increases uplifts at acute corners started increasing. The maximum uplift at acute corners has been observed to be .448 mm. As the uplifts increases there is a rapid increase in displacement is observed.

It has been depicted through the Table 4.2(B), it can be observed that there were some uplifts at skew slab acute corners of specimen 2. It can be seen from that the structure behaved linearly

elastic up to the value of load 57.05 KN. After this point, as the uplifts incresing at the both acute corners, load started decreases. There is sudden fall in curvature as the load decreases and constantly reduces gradually with no change in both the sides.

Table 4.2(B). FE results for Skew slab Specimen 2 with 150x150 mm beams supports

Sl no	Load In KN	Deflection In MM	Uplift 1 (MM) at Acute Corner	Uplift 2 (MM) at Acute Corner
1	15.33	1.00	-0.266	-0.27
2	25.46	1.99	-0.412	-0.41
3	27.44	3.00	-0.399	-0.40
4	29.24	4.04	-0.356	-0.35
5	31.64	5.05	-0.315	-0.31
6	33.90	6.06	-0.275	-0.27
7	36.10	7.07	-0.233	-0.22
8	38.25	8.08	-0.204	-0.20
9	40.92	9.09	-0.153	-0.14
10	42.57	10.10	-0.107	-0.10
11	44.57	11.11	-0.066	-0.06
12	46.77	12.12	-0.023	-0.01
13	48.84	13.13	0.016	0.03
14	51.02	14.14	0.060	0.07
15	53.00	15.15	0.108	0.12
16	54.79	16.16	0.167	0.18
17	56.02	17.17	0.235	0.24
18	56.98	18.18	0.329	0.34
19	57.05	19.19	0.448	0.46
20	56.08	20.20	0.633	0.63
21	52.70	21.78	1.087	1.05
22	41.75	23.08	1.496	1.46
23	31.69	24.36	1.760	1.72
24	26.62	25.56	1.950	1.91
25	23.95	26.74	2.100	2.06

26	22.50	27.89	2.230	2.19
27	21.80	29.02	2.350	2.30
28	20.97	30.13	2.460	2.42
29	20.65	31.24	2.570	2.52
30	20.40	32.32	2.670	2.63

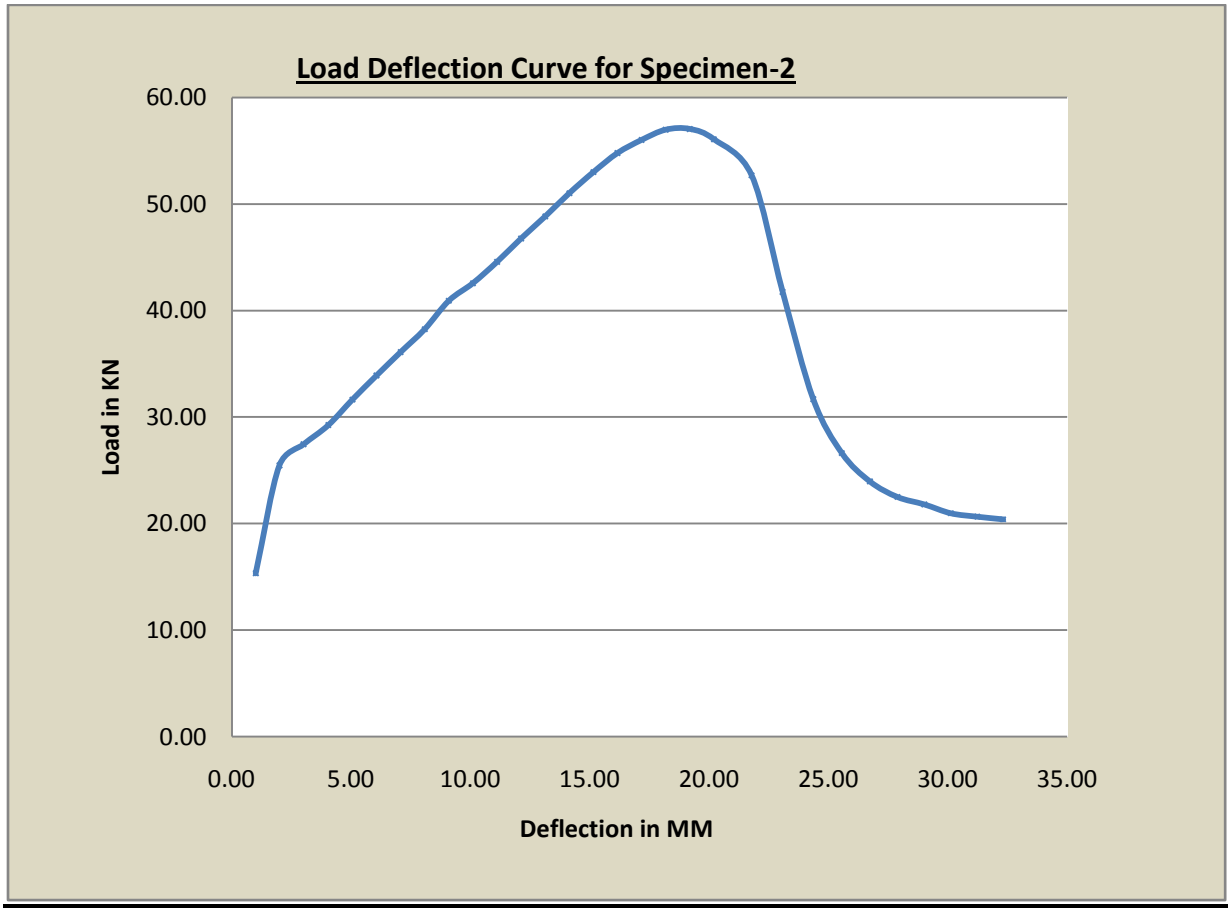

Figure 4.18, Load v/s Displacement of skew slab specimen 2(150x150mm edge supports)

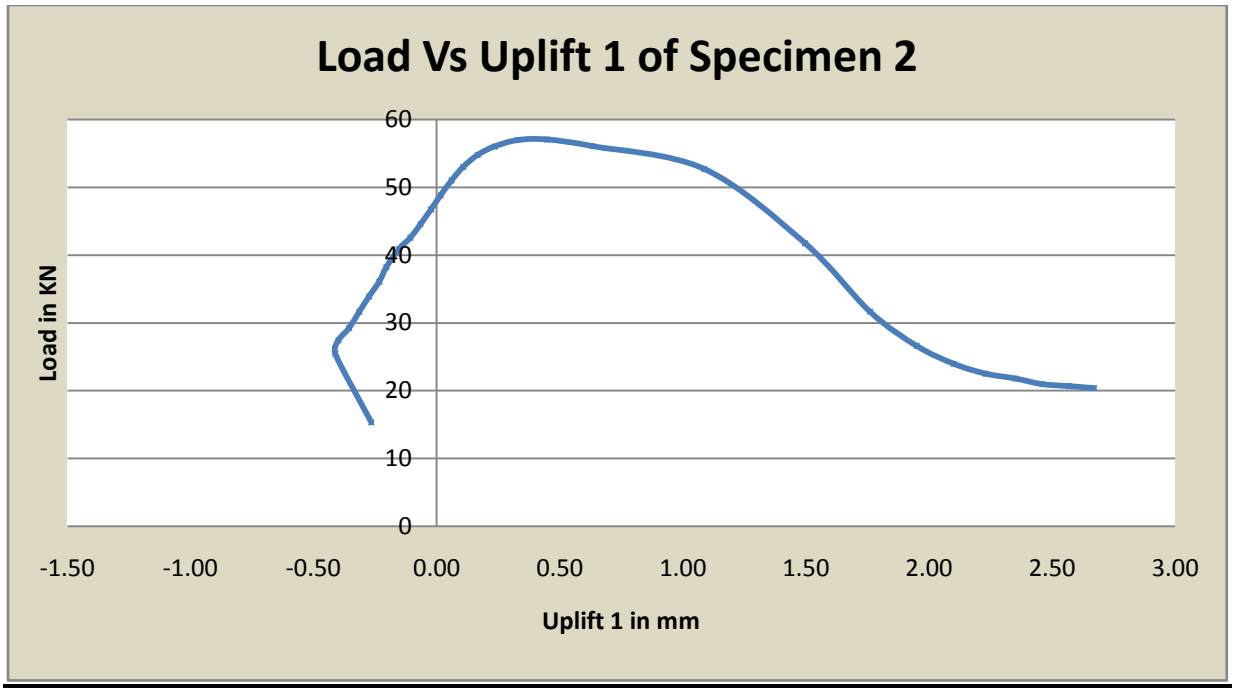

Figure 4.19 Load v/s Uplift of skew slab specimen 2(150x150mm edge supports)

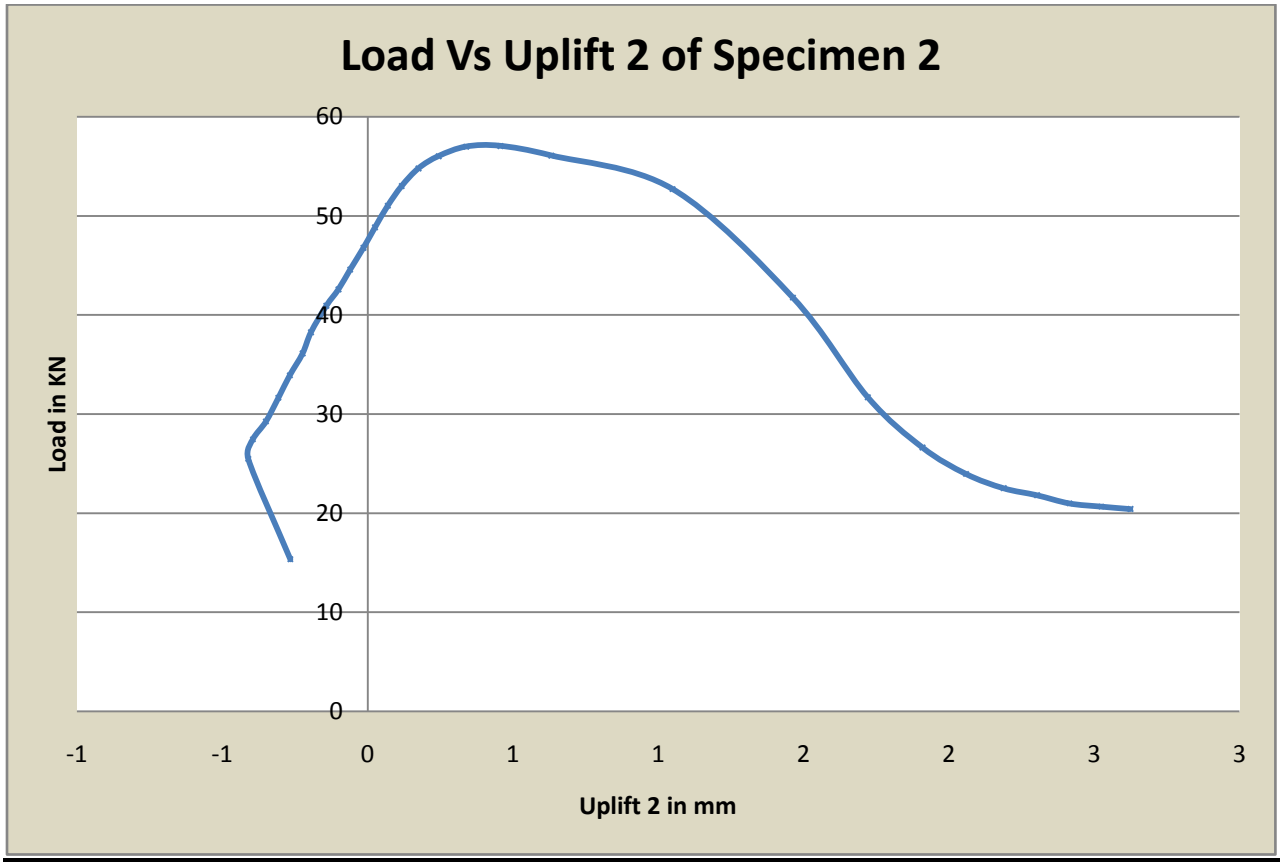

Figure 4.20, Load v/s Uplift of skew slab specimen 2(150x150mm edge supports)

Where as in the previous studies The Load deflection And the Load Uplift Curves are plotted as below.

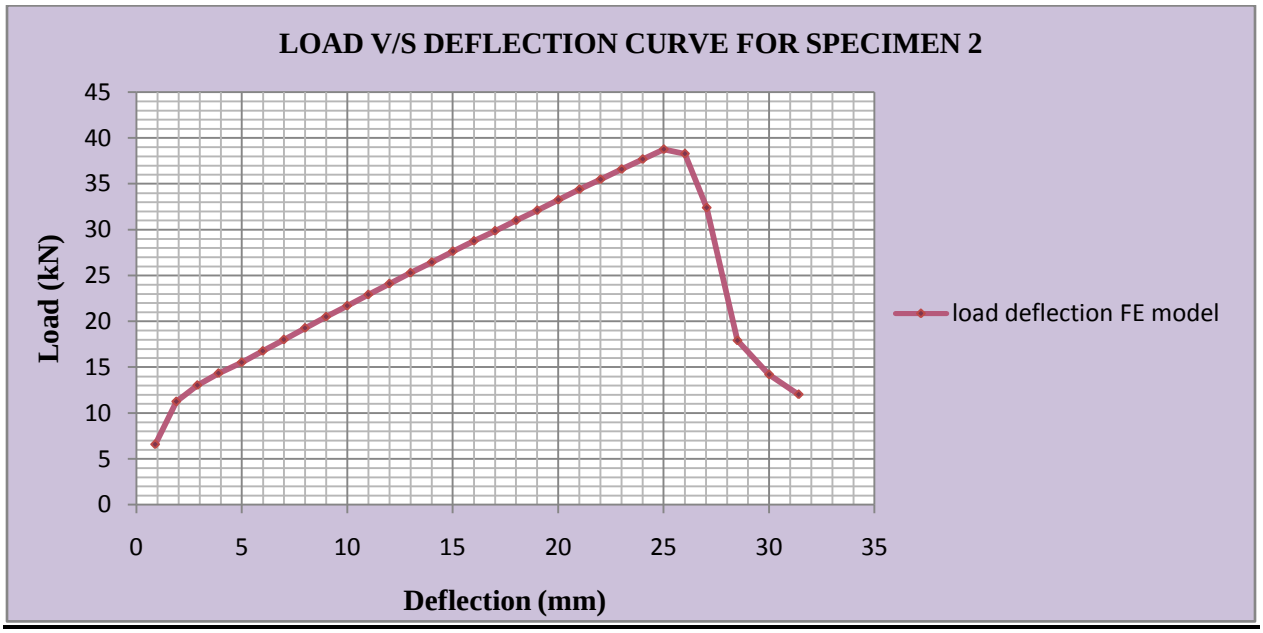

Figure 4.21, Load v/s Displacement of skew slab specimen 2 as per The previous Studies

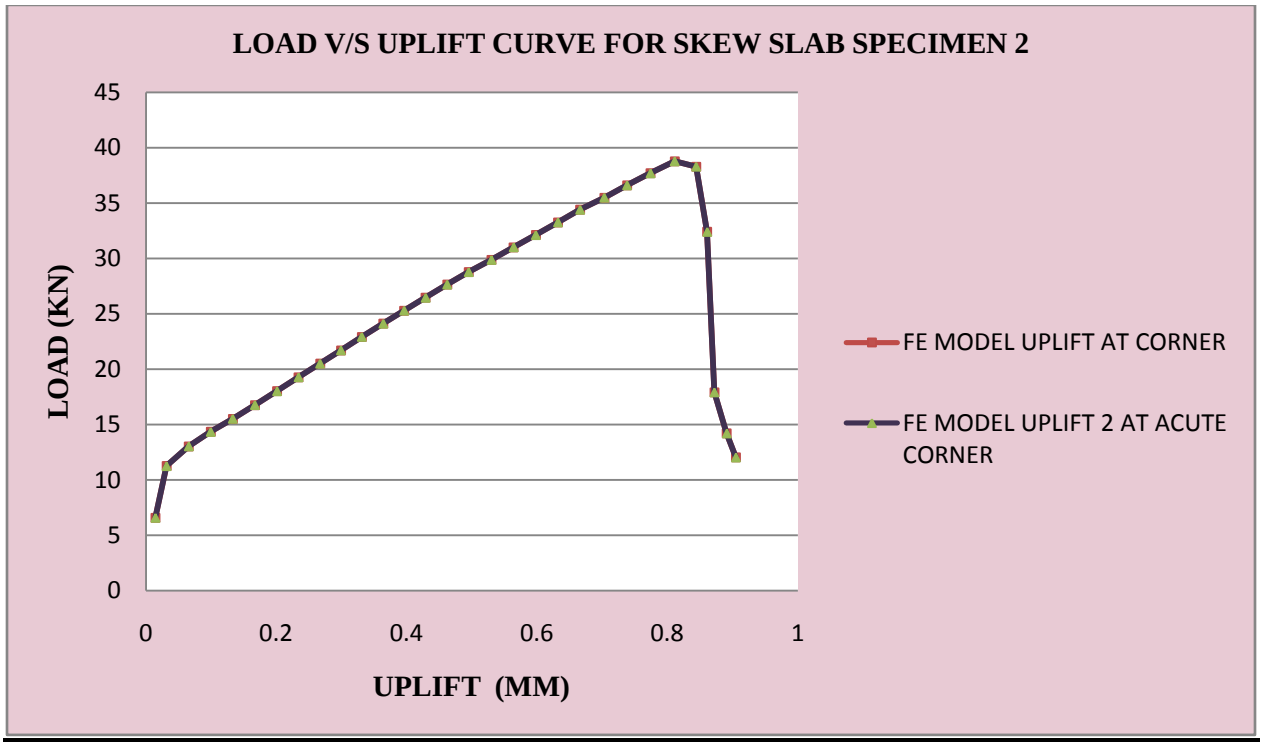

Figure 4.22, Load v/s Uplift at acute corners of skew slab specimen 2 as per previous studies

4.1.2 CRACK PATTERNS

The variations of crack pattern have been taken out from the post processer of ATENA and are plotted in Figure 4.23 to 4.17. A discussion on crack pattern plotted here has been presented here.

The shape of un-deformed and deformed structure has been shown in Figure 4.5 & 4.6. In the deformed shape of skew slab specimens drift in the Z direction (direction of loading) at upper levels is clearly visible.

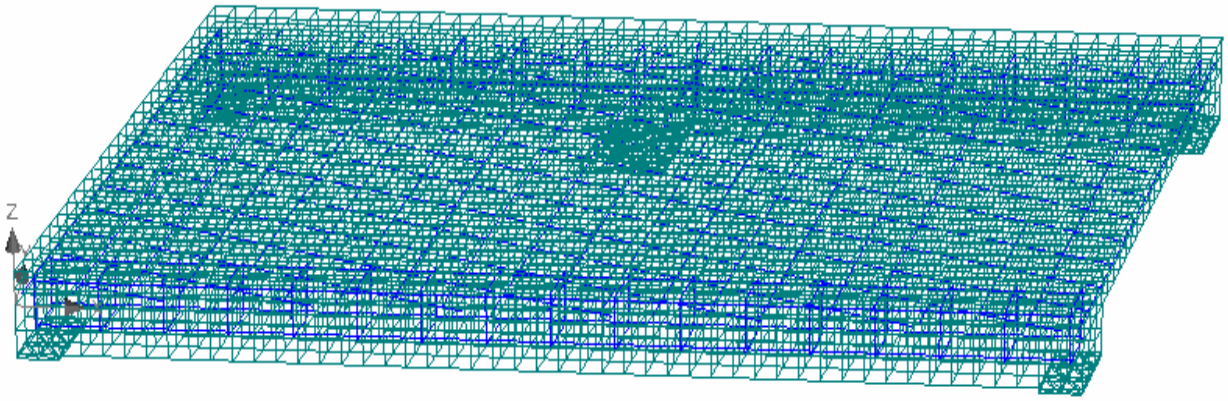

Figure 4.23, Undeformed shape of specimen 1

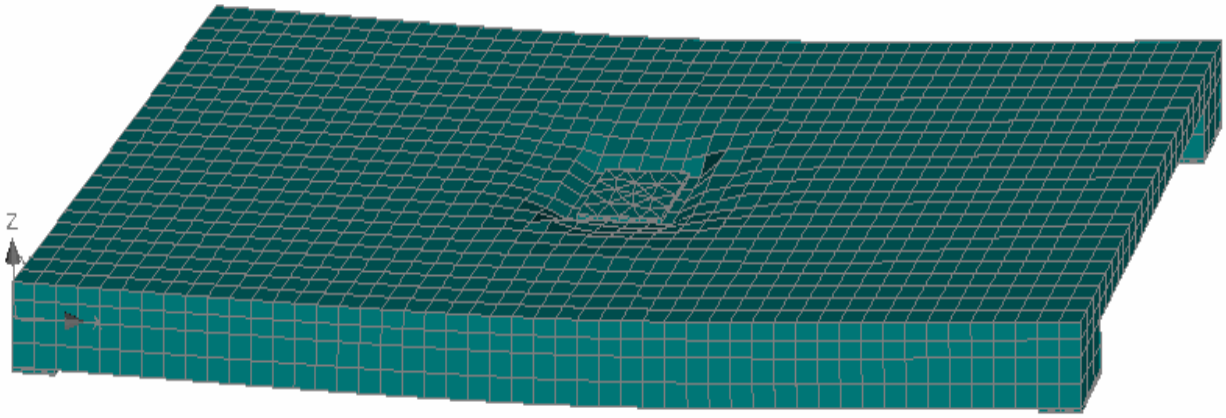

Figure 4.24, deformed shape of specimen 1

4.1.2.1 CRACK PATTERNS OF SKEW SLAB SPECIMEN 1

For the skew slab specimen1 in general, at the early stages of loading the behavior was elastic until the appearance of the first crack. Invariably, the crack was initiated at the centre of the skew slab and the cracks gradually propagate towards the end of the free edge on the tension face side as the loading progressed.

Edge Support 130x150

CRACK PATTERNS AT STEP- 2

It can be observed from Figure 4.25 that micro-cracks appeared in the structure when skew slab is in linear zone. The appearance of initial crack has been observe as **Maximum width=7.87E-05 minimum width =1.05E-08** and keeps on increasing as the load and the deflection increases

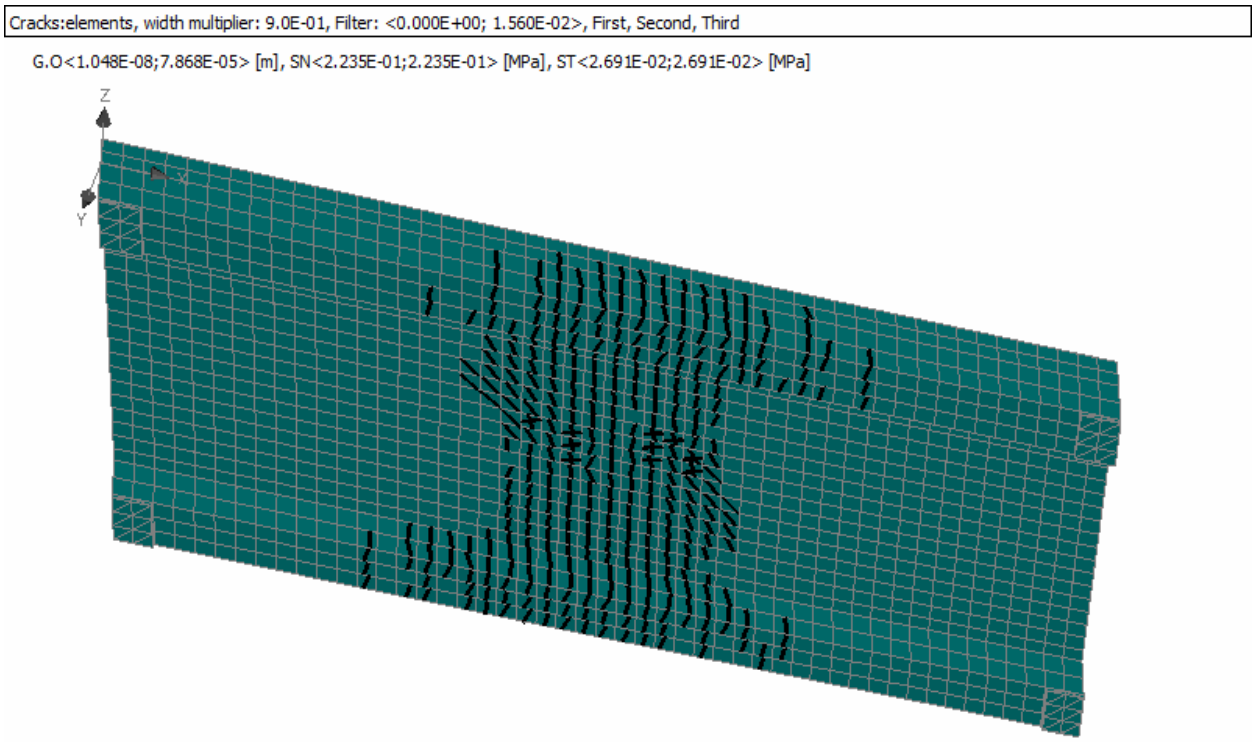

Figure 4.25 Crack pattern at As in Initial stage

CRACK PATTERNS AT STEP- 40

At the 40th step cracks propagate in tension face moves towards the centre to free edge of specimen shown in fig 4.8. The maximum crack width is **max =1.56E-02 Min= 0**

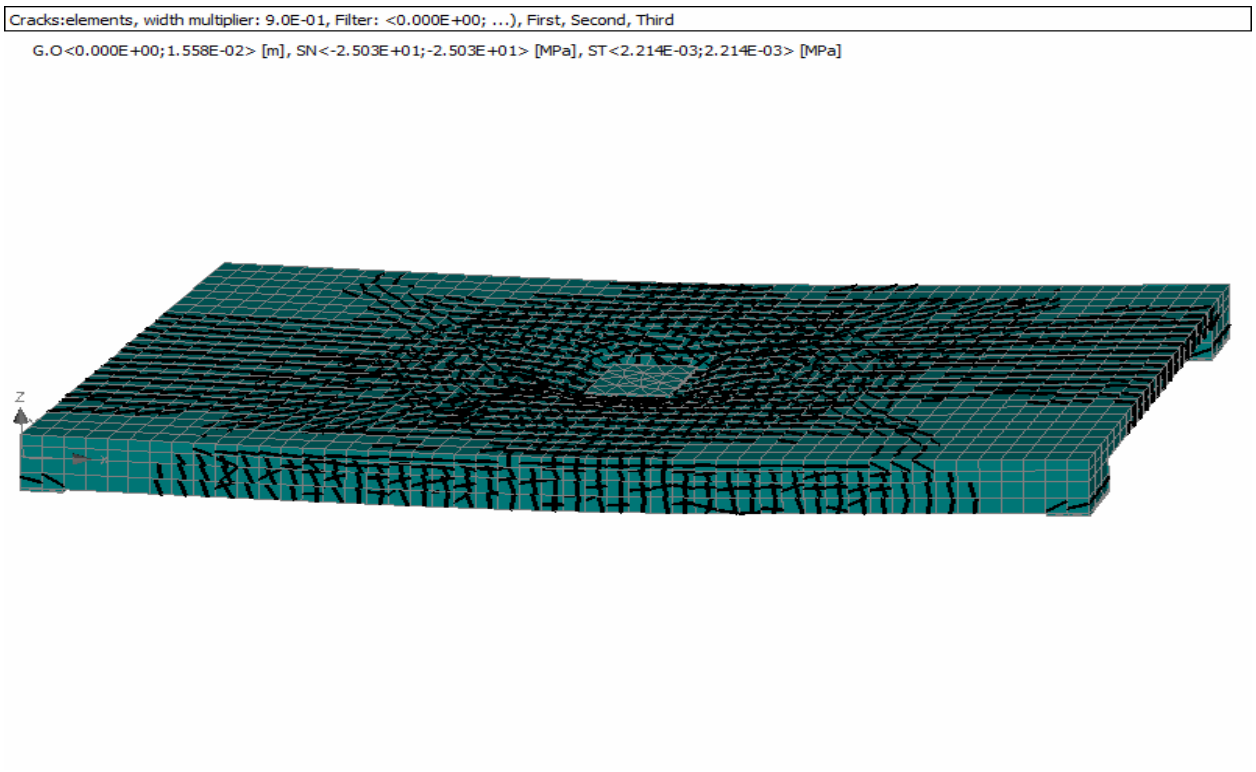

Figure 4.26, Crack pattern at step 40

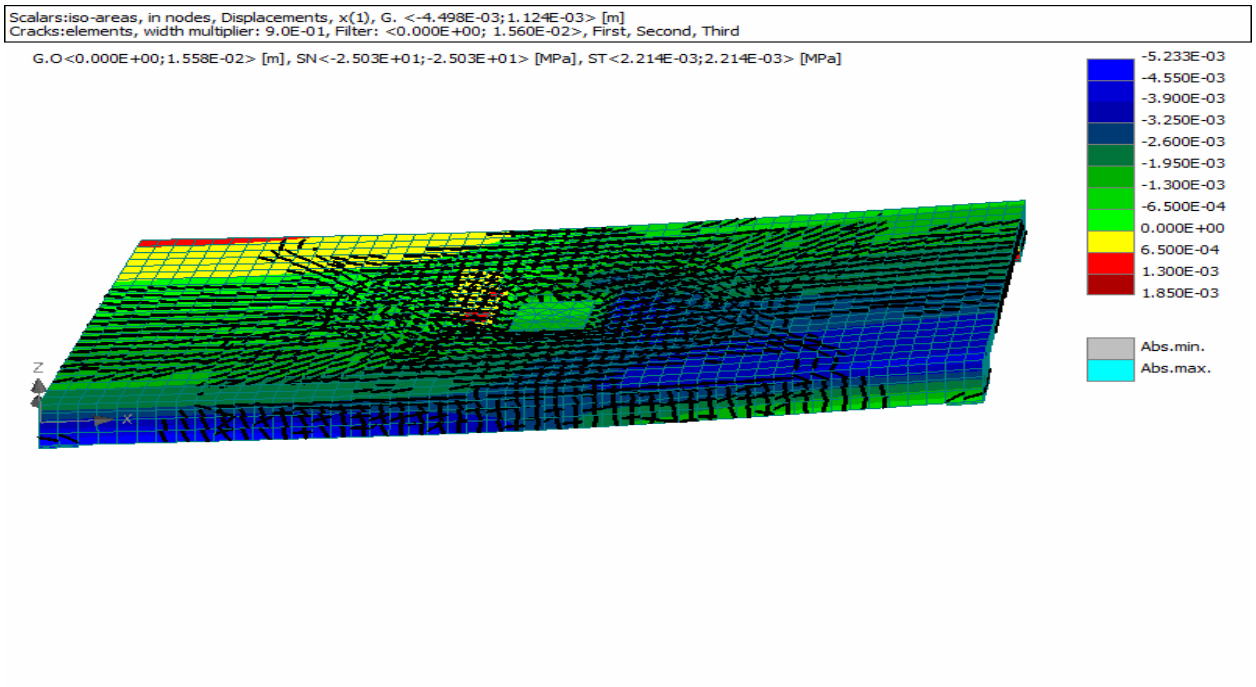

Figure 4.27, Iso areas of displacement of specimen 1 (130x150)

Edge Support 150x150

CRACK PATTERNS AT STEP- 2

At the step cracks propagate in tension face moves towards the centre to free edge of specimen shown in fig 4.27. The maximum crack width is **max =1.12e-04 Min= 9.15e-09 ,**

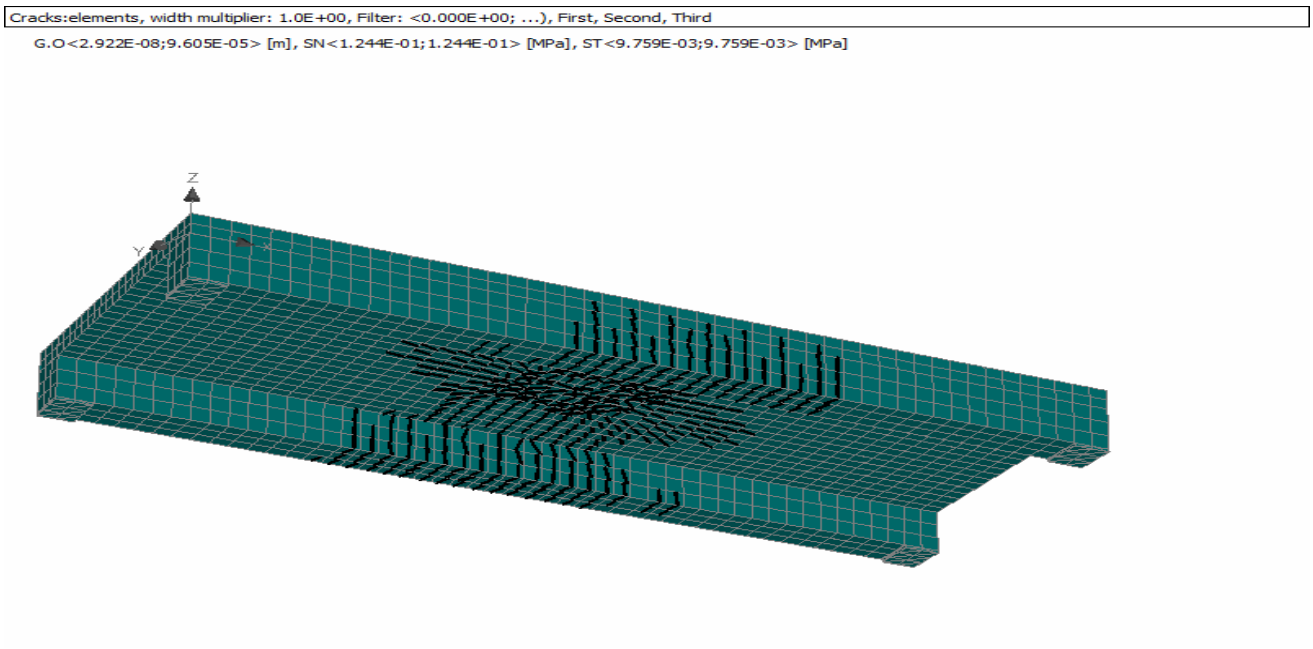

Figure 4.28, Crack pattern at step 6

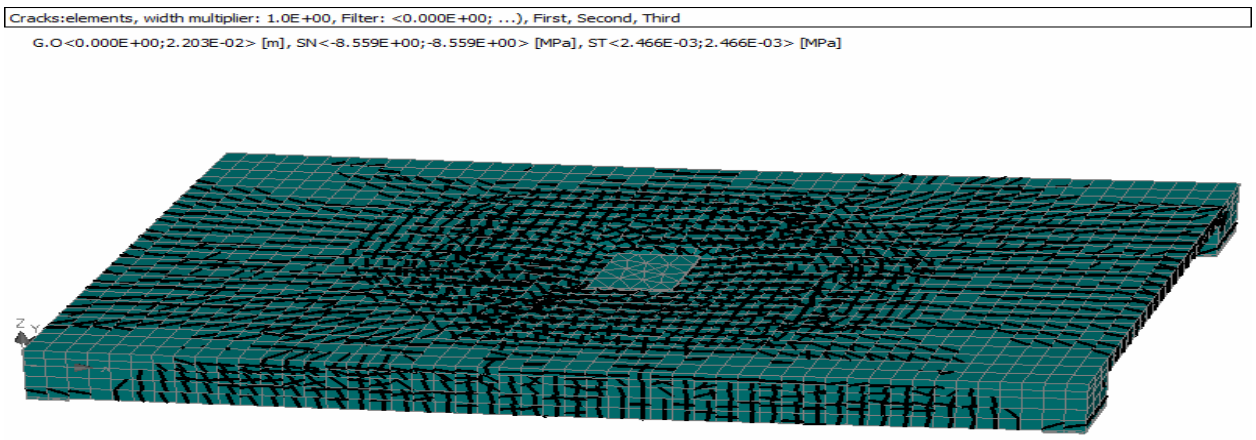

Figure 4.29, Crack pattern at step 40

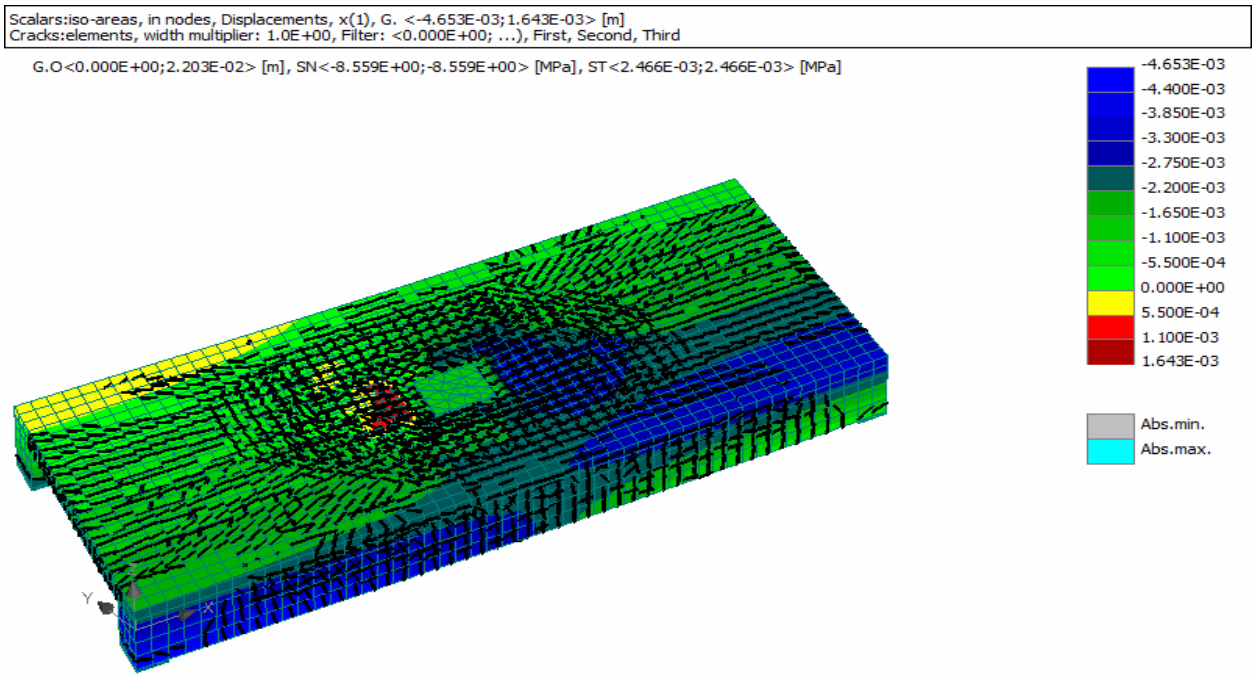

Figure 4.30, Iso areas of displacement of specimen 1 (150x150)

Edge Support 100x150

CRACK PATTERNS AT STEP- 2

At the step cracks propagate in tension face moves towards the centre to free edge of specimen shown in fig 4.31. The maximum crack width is **Min=0 max=2.20e-02**

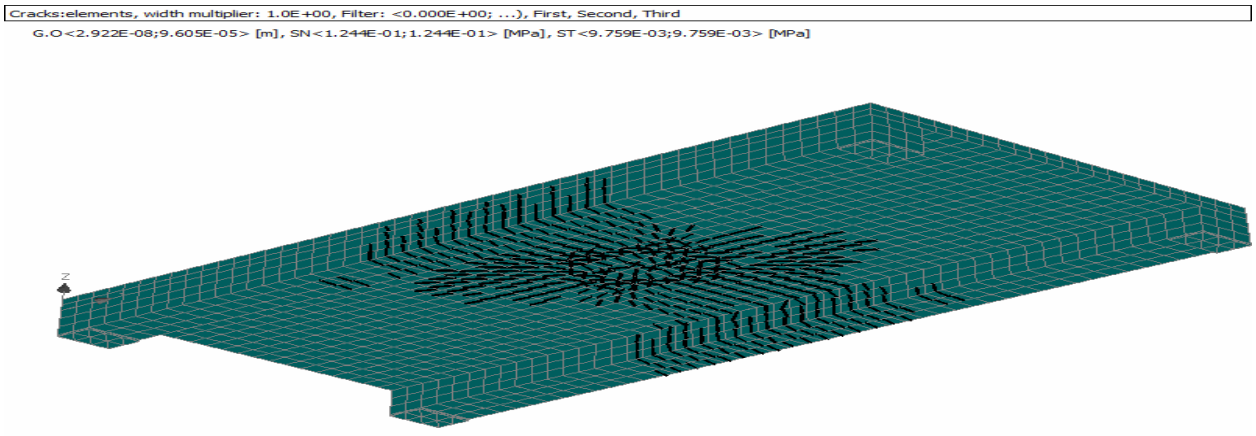

Figure 4.31, Crack pattern at step 2

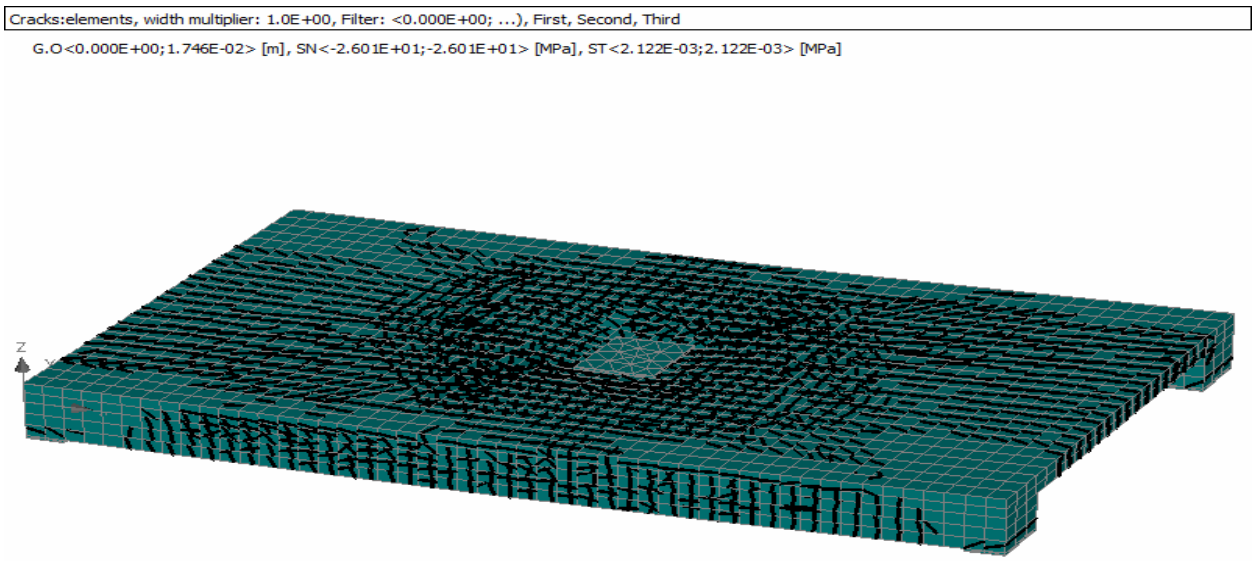

Figure 4.32, Crack pattern at 40

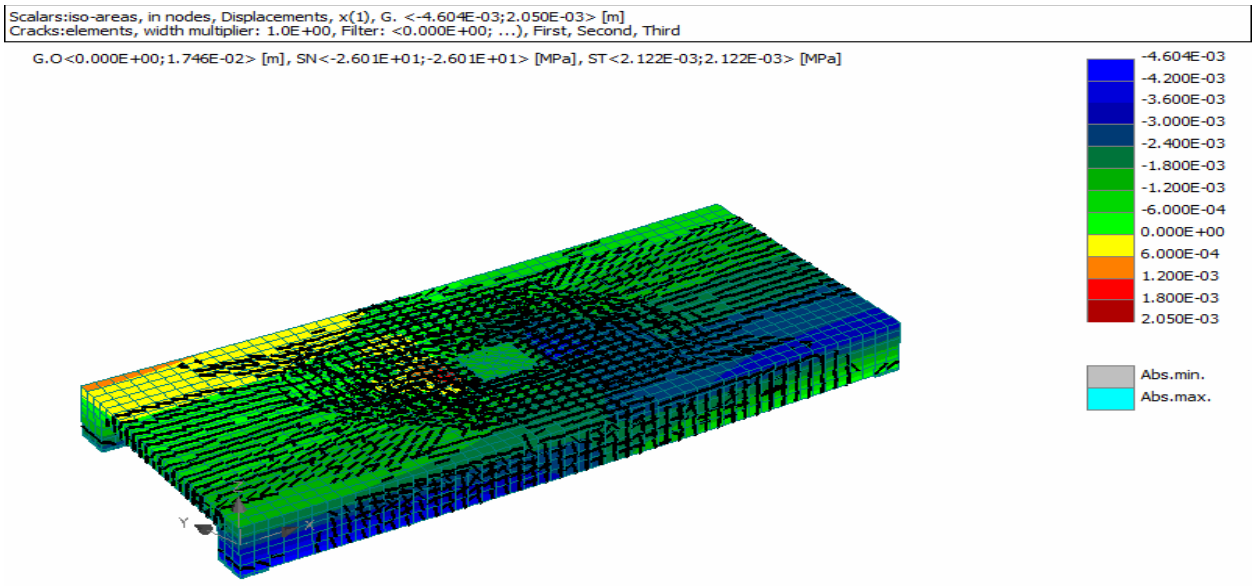

Figure 4.33, Iso areas of displacement of specimen 1 (100x150)

4.1.2.2 CRACK PATTERNS OF SKEW SLAB SPECIMEN 2

For the skew slab specimen 2 in general, For **EDGE support 100x150** at the early stages of loading the behaviour was elastic until the appearance of the first crack. Invariably, the crack was initiated at the centre of the skew slab and the cracks gradually propagate towards the end of the free edge on the tension face side as the loading progressed. Crack **MIN 2.55E-09 MAX 6.62E -05**

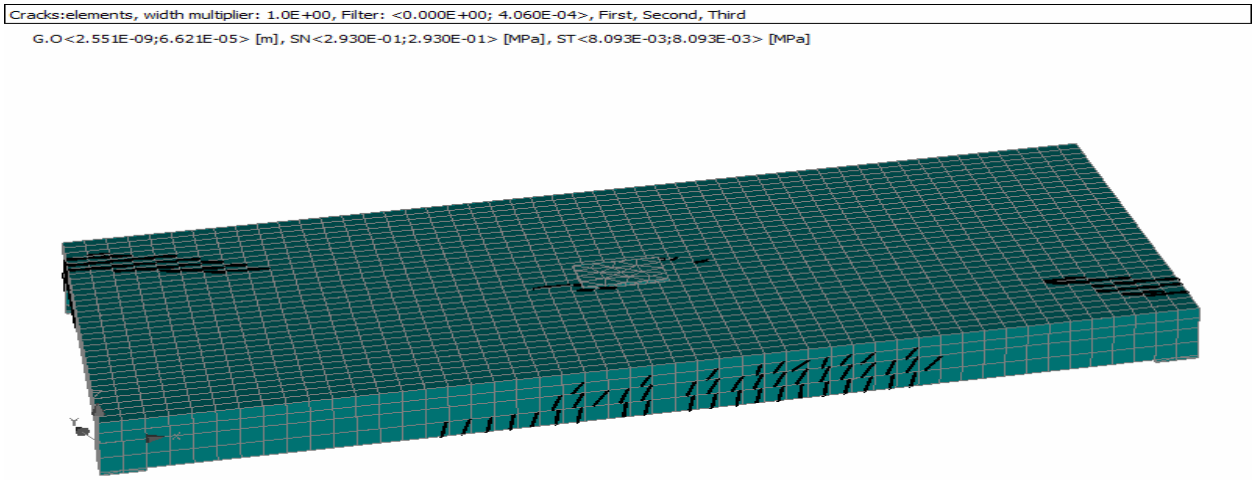

Figure 4.34, Crack pattern at step 5

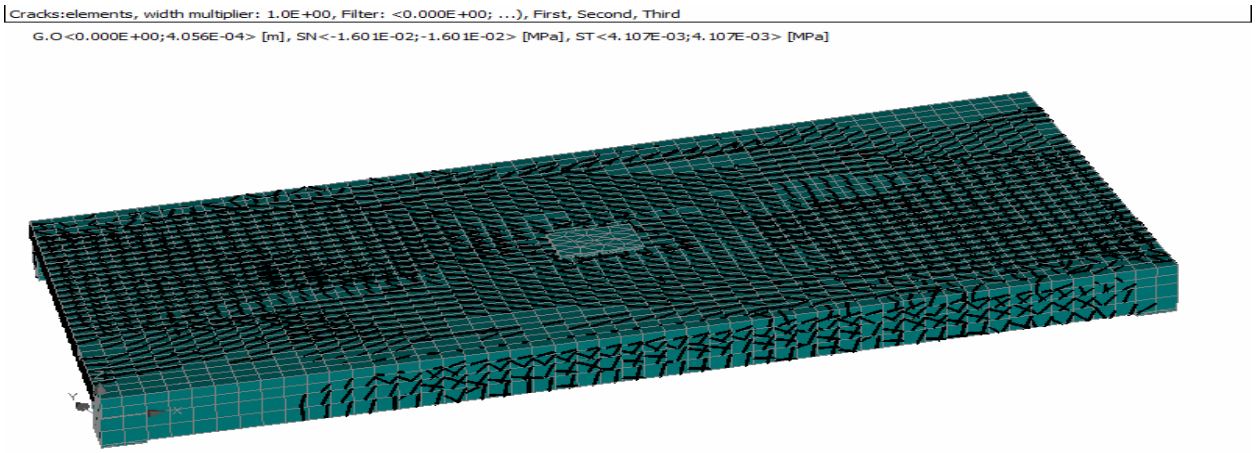

Figure 4.35, Crack pattern at step 30

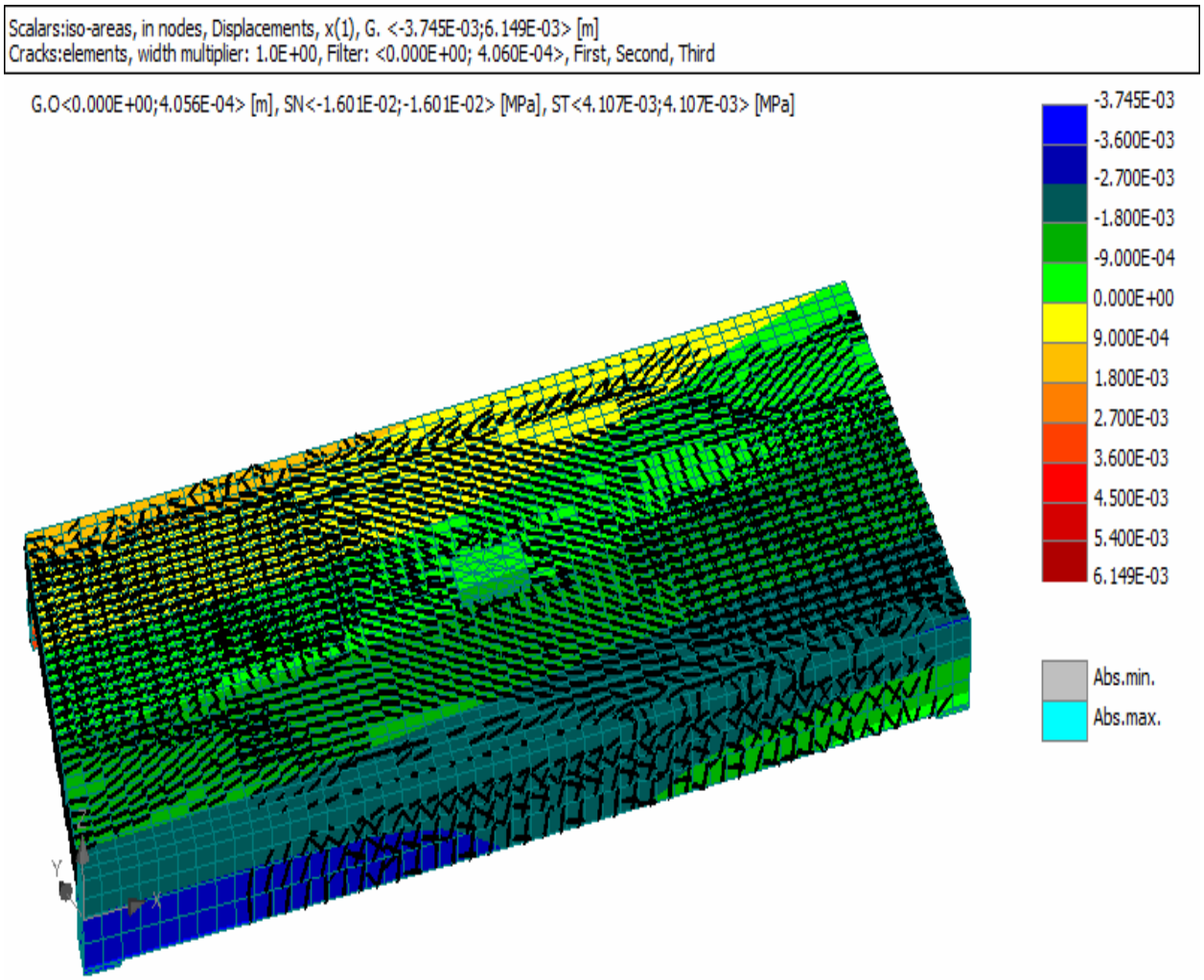

Figure 4.36, Iso areas of displacement of specimen 2 (100x150)

For the skew slab specimen 2, , For **EDGE support 130x150** at the early stages of loading the behaviour was elastic until the appearance of the first crack. Invariably, the crack was initiated at the centre of the skew slab and the cracks gradually propagate towards the end of the free edge on the tension face side as the loading progressed. Crack **min=2.92e-09 max= 8.40e-05**

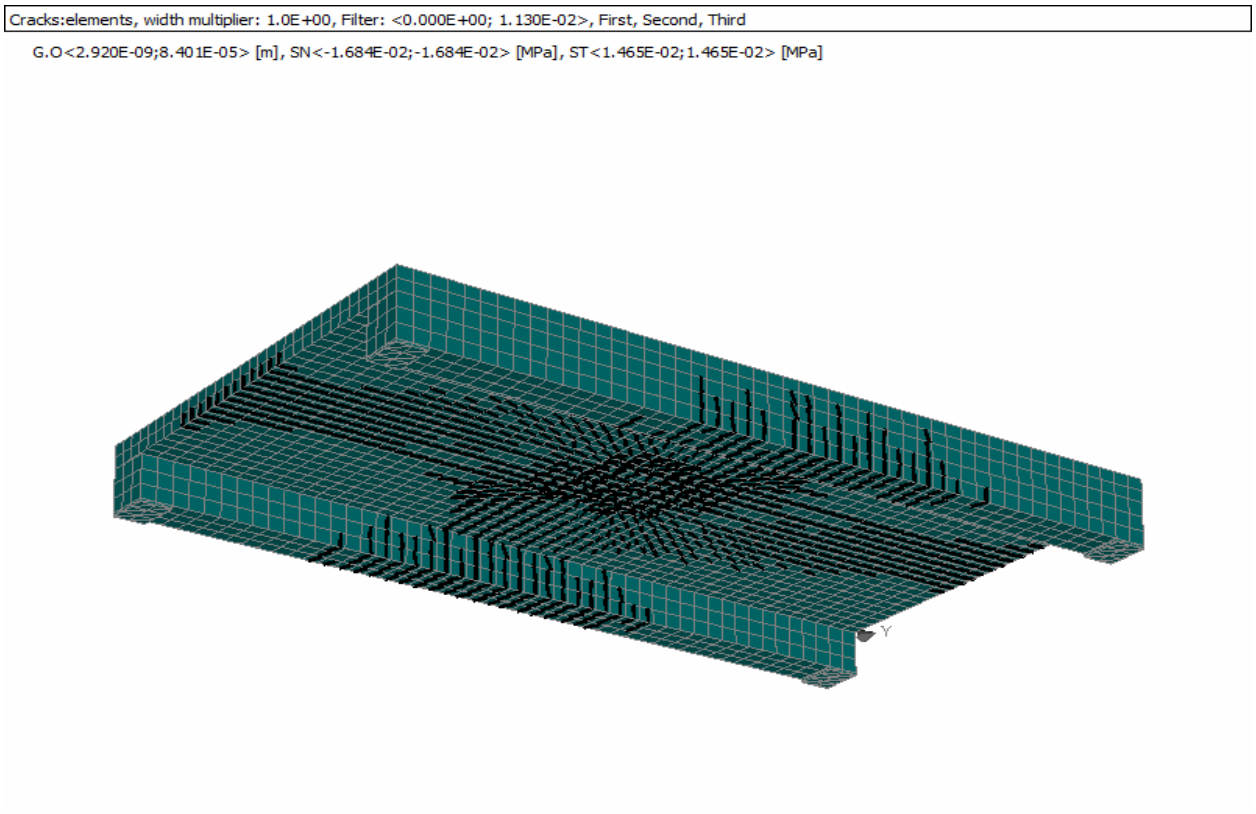

Figure 4.37, Crack pattern at 3

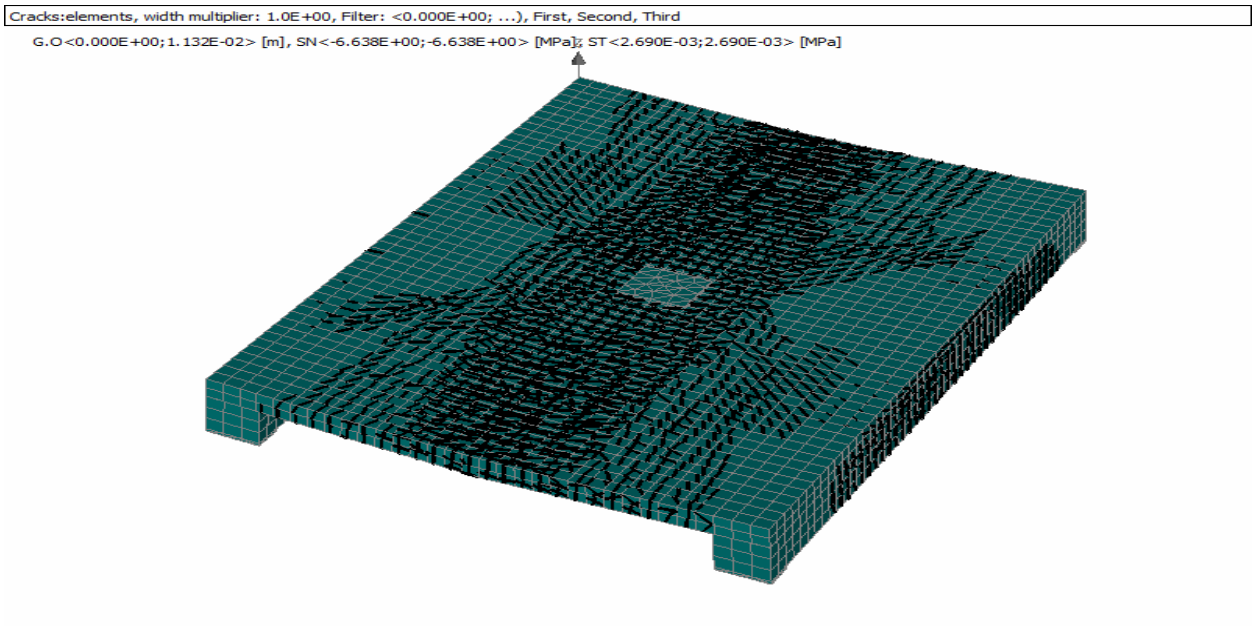

Figure 4.38, Crack pattern at 30

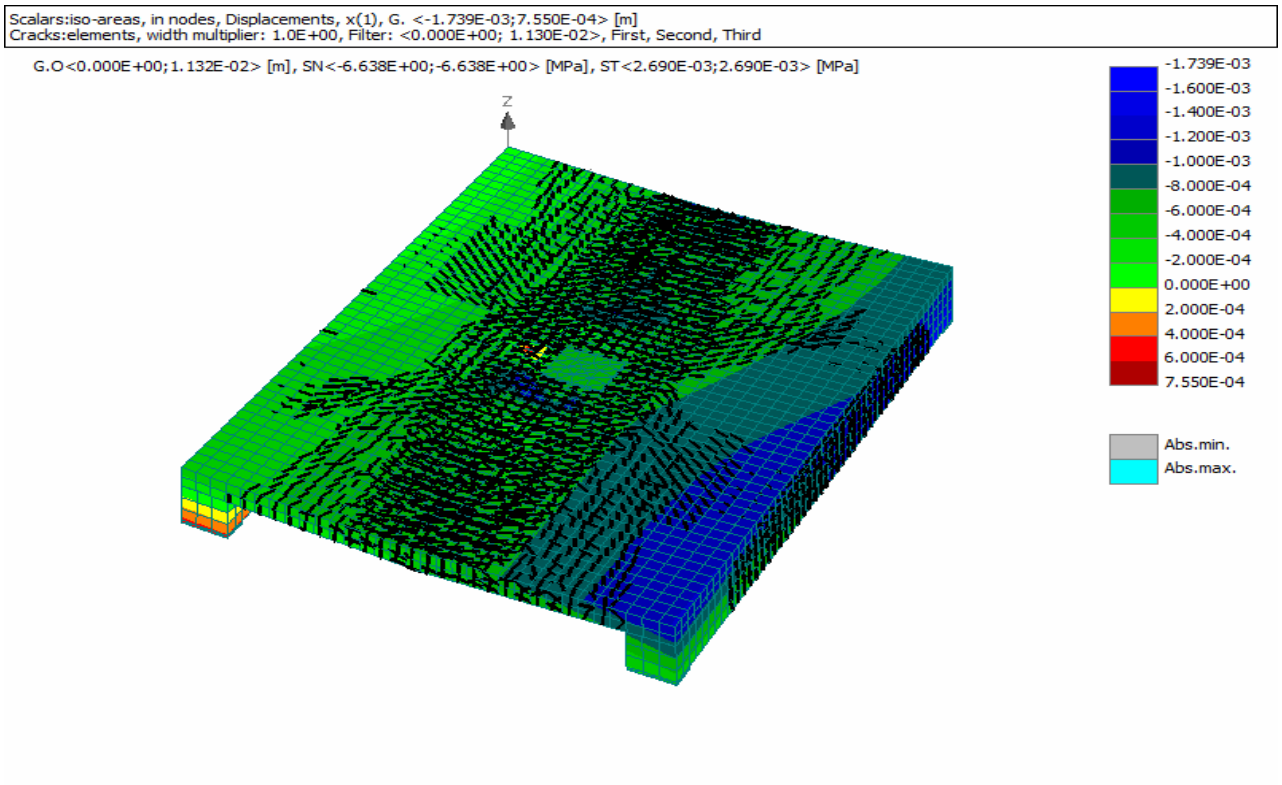

Figure 4.39, Iso areas of displacement of specimen 2 (130x150)

For **EDGE support 150x150,** It can be observed from Figure 4.40 that micro-cracks appeared in the structure when slab is in linear zone. The crack width is **min -0.00 max- 9.62e-030.14 m.**

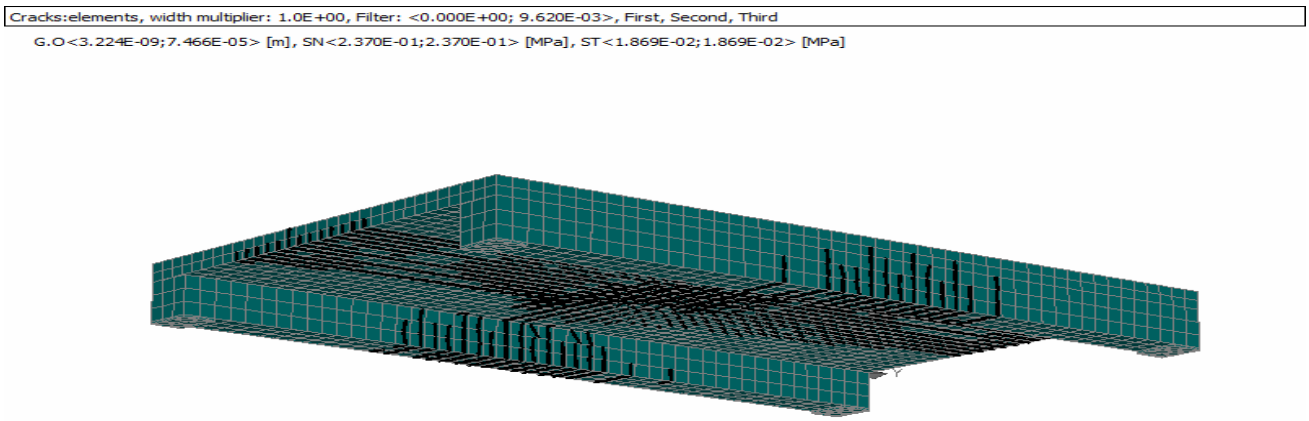

Figure 4.40, Crack pattern at step 3

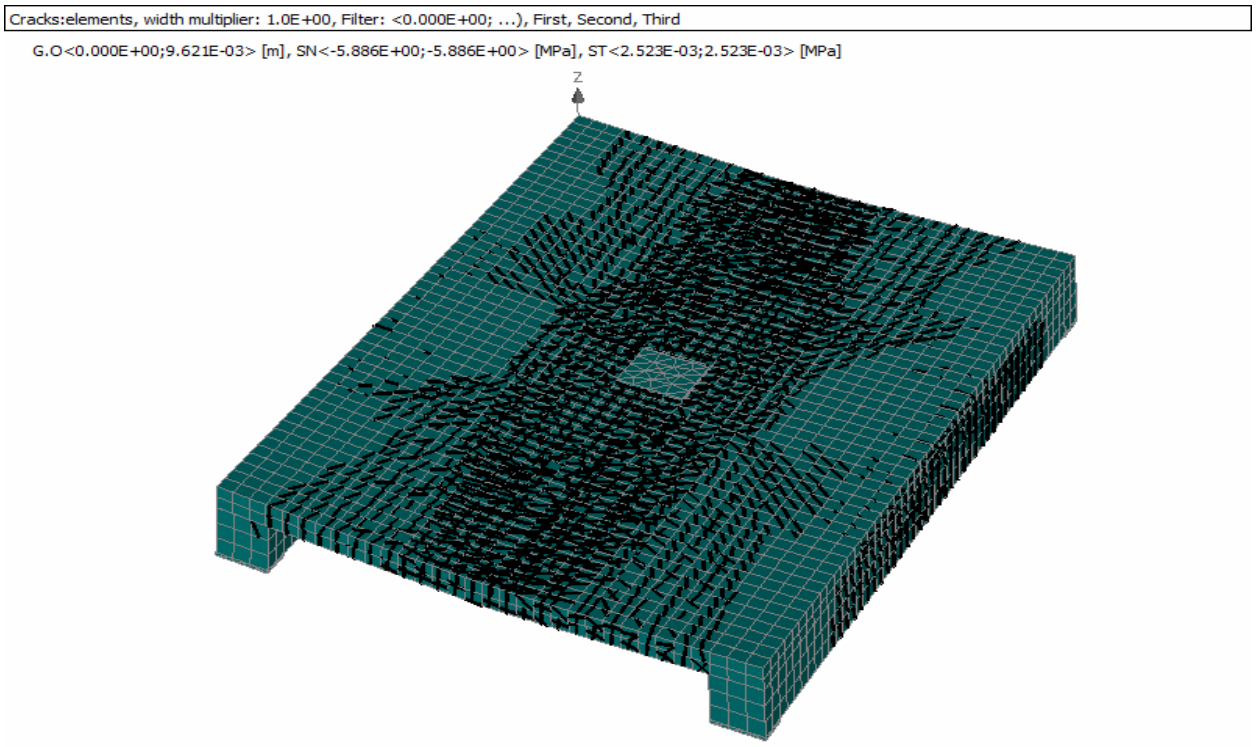

Figure 4.41, Crack pattern at step 30

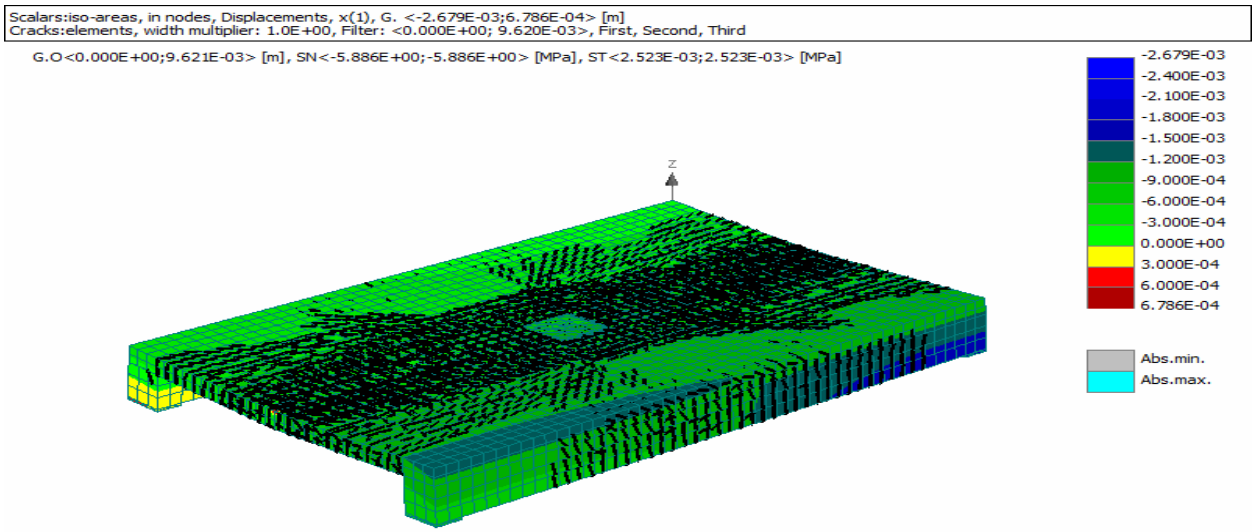

Figure 4.42, Iso areas of displacement of specimen 2 (150x150)

4.2 COMPARISON BETWEEN THE FE MODELS, THE EXPERIMENTAL RESULTS OF THE RCC SKEW SLABS AND THE SKEW SLAB WITH EDGE SUPPORTS

4.2.1 EXPERIMENTAL RESULTS OF RCC SKEW SLAB SPECIMEN 1 [(24)]

The load was applied gradually at the centre of the test specimen and deflection of the slab at the centre and uplift at the acute corner have been at different load as given in table 4.3

Table 4.3, Experimental results for skew slab specimen -1 [(24)]

S.No	Load applied at the centre of gravity (KN)	Deflection at the centre (mm)	Uplift at acute corners (mm)
1	5	5.5	0
2	10	7.7	0.3
3	15	17.0	0.1
4	20	24.7	1.0
5	25	29.3	1.22
6	25	40.0	1.65

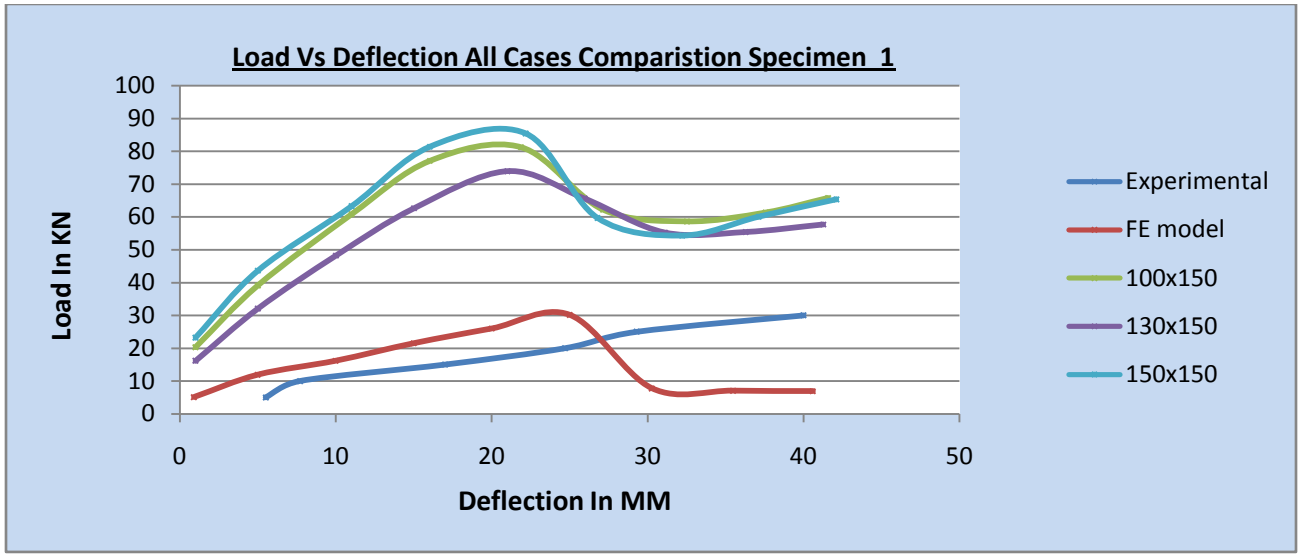

Figure 4.43, Load v/s deflection curve for skew slab specimen 1

Table 4.4, F.E Modelling result of skew slab specimen 1 [1]

S.No.	Load (kN)	Deflection (mm)	Uplift 1 (mm)at acute corner	Uplift 2(mm) at acute corner
1	5.10	0.90	0.0238	0.0238
5	11.93	5.00	0.162	0.162
10	16.81	10.00	0.341	0.341
15	21.52	15.00	0.514	0.514
20	26.01	20.00	0.689	0.689
25	30.16	25.00	0.867	0.867
30	7.77	30.27	0.948	0.835
35	7.04	35.48	1.07	0.933
40	6.92	40.59	1.18	1.026

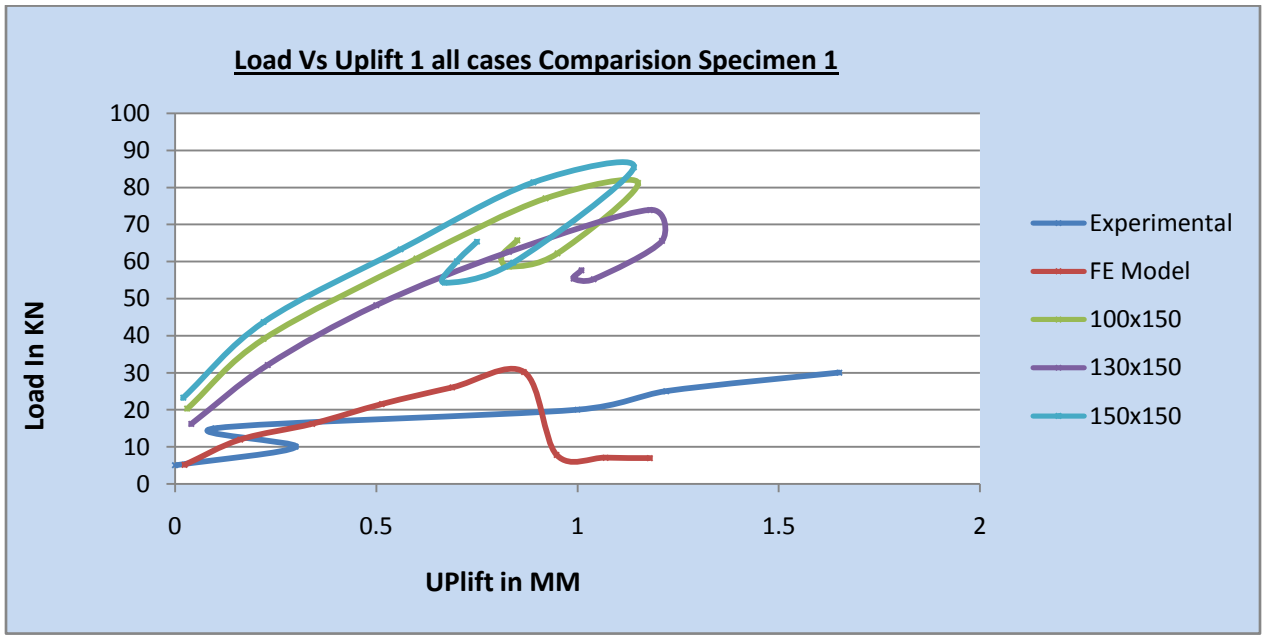

Figure 4.44, Load v/s uplifts at acute corner curve for skew slab specimen 1

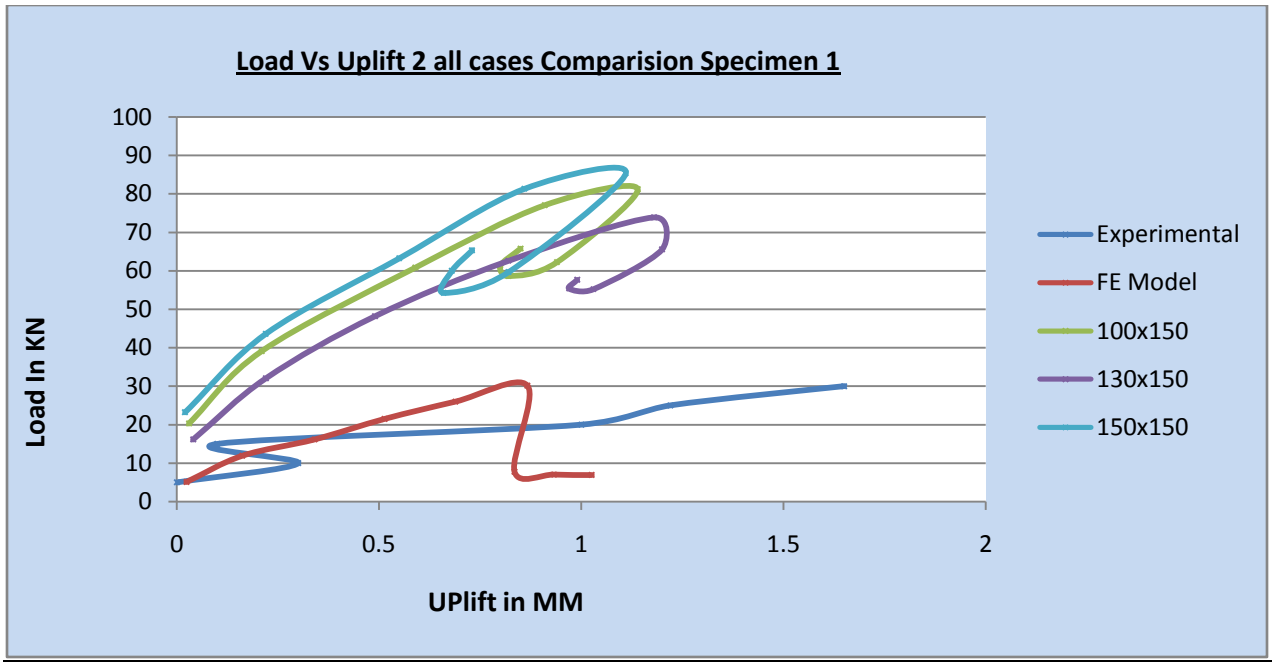

Figure 4.45, Load v/s uplifts at acute corner 2, curve for skew slab specimen 1

From above all the data and graph, the result came from the analytical data vary as compared to the experimental data and modeled data

4.2.2 EXPERIMENTAL RESULTS OF RCC SKEW SLAB SPECIMEN 2 [(24)]

The load was applied gradually at the centre of the test specimen and deflection of the slab at the centre and uplift at the acute corner have been at different load as given in table 4.5

Table 4.5 Experimental results for skew slab specimen -2 [(24)]

S.No	Load applied at the centre of gravity (KN)	Deflection at the centre (mm)	Uplift at acute corners (mm)
1	5	4.9	0
2	10	5.6	0
3	15	11.4	0
4	20	16.6	0
5	25	22.2	0
6	30	26.7	0
7	35	30.5	0

Table 4.6, F. E. results for skew slab specimen -2[1]

S.No.	Load (KN)	Deflection (mm)	Uplift 1 (mm) at acute corner	Uplift 2 (mm) at acute corner
1	6.58	0.90	0.0144	0.0144
5	15.52	5.00	0.133	0.133
10	21.70	10.00	0.299	0.299
15	27.64	15.01	0.462	0.462
20	33.26	20.01	0.632	0.632
25	38.77	25.01	0.811	0.811
30	12.03	31.40	0.905	0.905

These are the comparative study which shows the variation in the Load carrying capacity and the uplift with respect to the Load application.

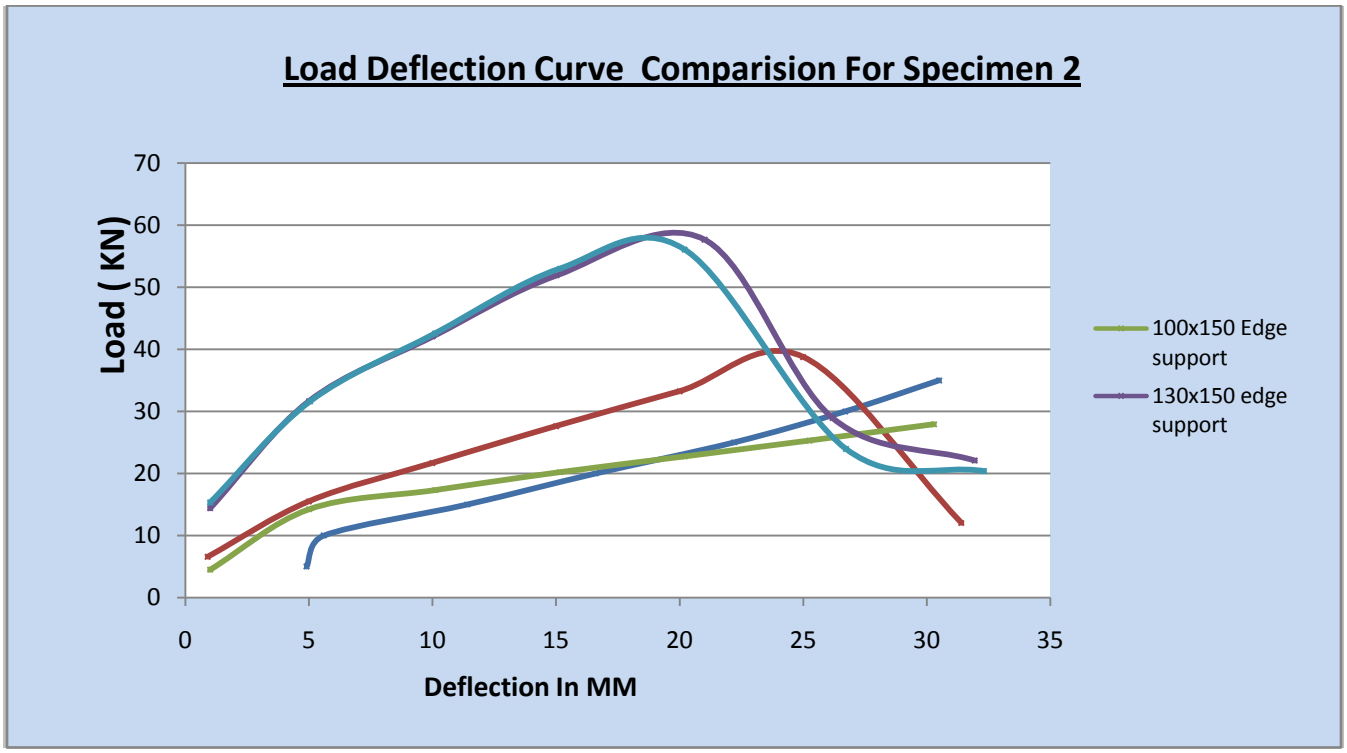

Figure 4.46, Load v/s deflection curve for skew slab with Edge support specimen 2

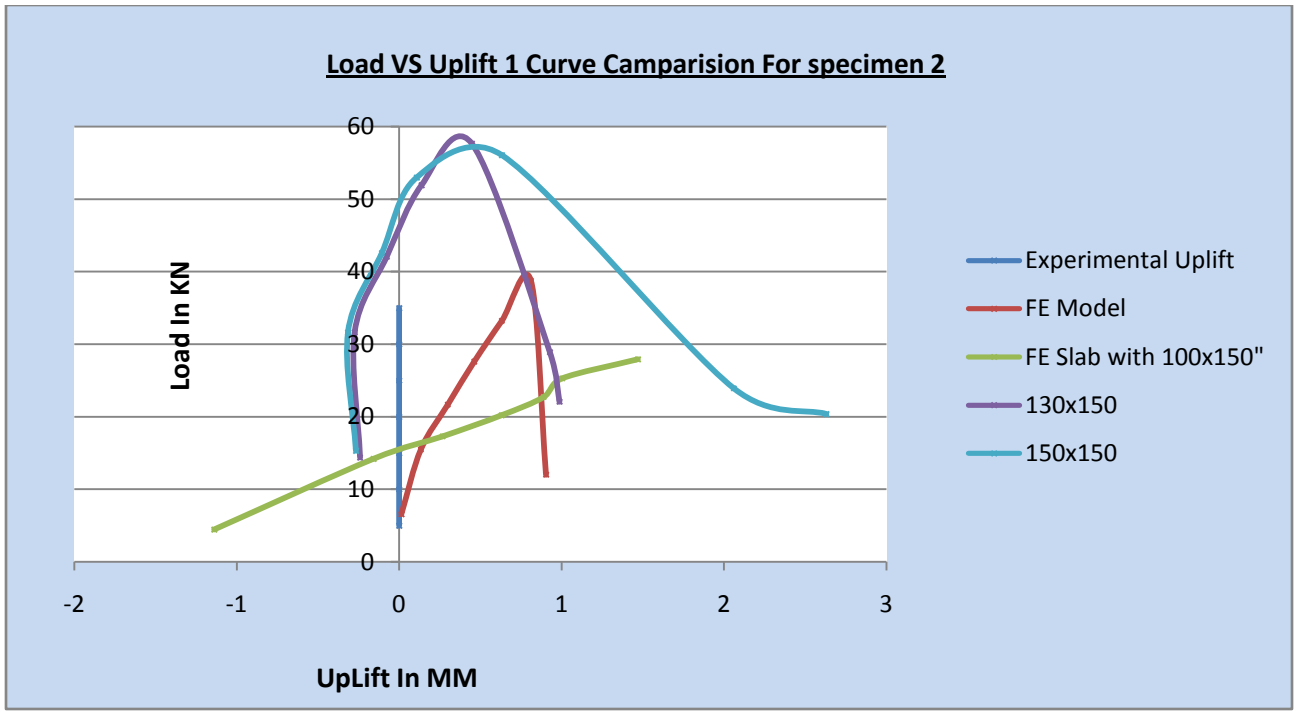

Figure 4.47, Load v/s uplifts at acute corner curve for skew slab specimen 2

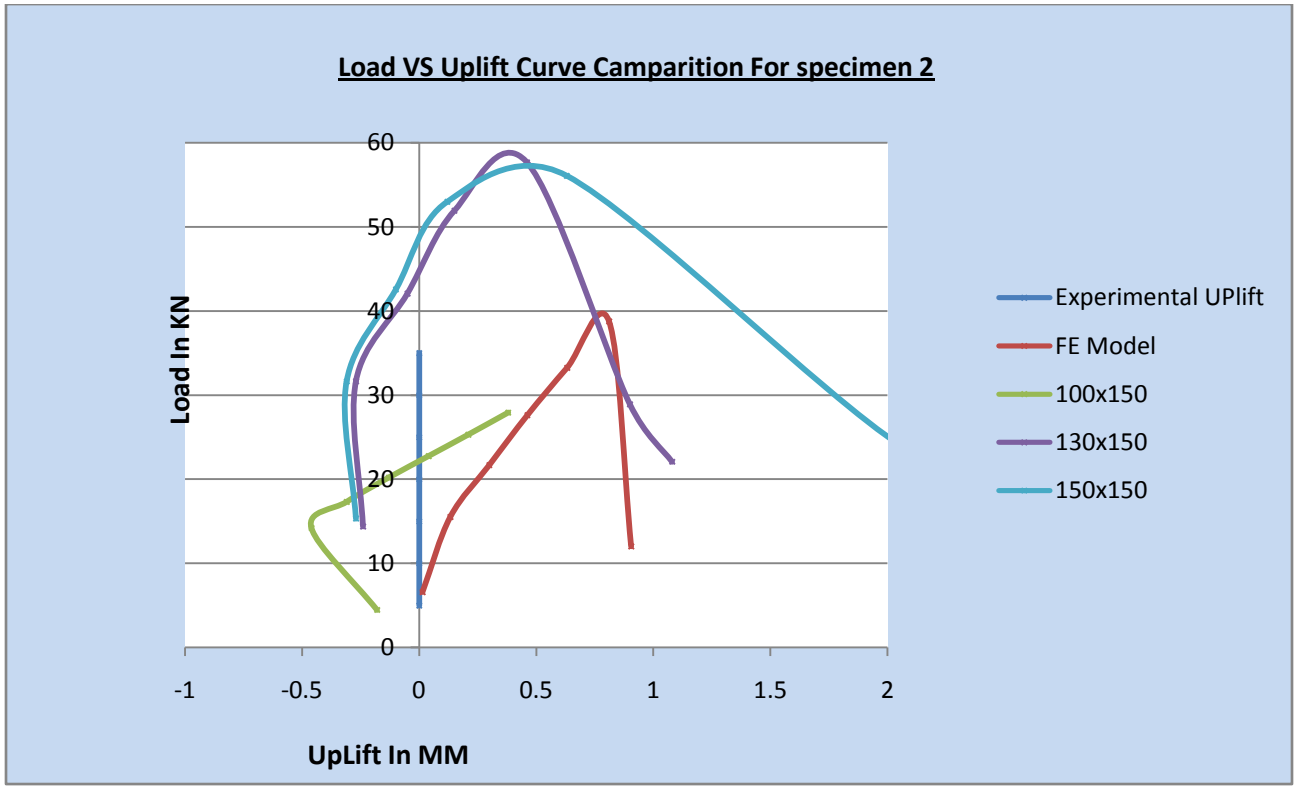

Figure 4.48, Load v/s uplifts at acute corner curve for skew slab specimen 2

4.3 COMPARISON BETWEEN THE FE MODEL ,THE EXPERIMENTAL AND SKEW SKAB WITH DIFFRENT TYPE OF EDGE SUPPORTS

RESULTS OF THE SKEW SLABS

A) Specimen - 1

1. The skew slab specimen 1 behaved linearly elastic up to a load of around 81.21 KN,73.92KN & 85.44KN in the respective 3 different edge supports model. Which is almost 2.5 times greater than the load carrying value as compare to FE Model specimen and the Experimental specimen. After this value of load, it depicted non-linearity in its behavior. Increase in deflection has been observed to be more with load decrements. It has reached to the value of 32.52 mm, 31.1 mm and 32.21mm respectively when load is 58.62 KN, 55.22 KN & 54.3 KN. After this value of load, plastic behavior has been observed by the skew slab as a constant increase in deflection has been observed, after the value of load 58.62 KN, 55.22 KN & 54.3 KN. After this point there is constant increase in deflections and plot has become almost flat. Subsequently deflection started increasing without any significant decrement in load; it has reached to the value of 40 mm with the load value 41.57 KN, 41.26 KN & 42.1 KN.
2. It can be observed that there were some uplifts at skew slab acute corners of specimen 1. It can be seen from that the structure behaved linearly elastic up to the value of load 81.21 KN,73.92KN & 85.44KN. After this point, as the uplifts increases at the both acute corners, load started decreases. There is sudden fall in curvature after the value of uplift 1.15 mm,1.18mm & 1.14mm. At these point of Load value, both the uplifts shows slight difference from each other in all the three edge support specimen. The maximum uplifted has been noticed 1.15 mm,1.18mm & 1.14mm at acute corner 1 and 1.14 mm, 1.18 mm & 1.11mm 1.026 at acute corner 2. Subsequently uplifts started decreasing with the significant decrement in load; it has reached to the value of uplift Less than 1 at both the corners at 40 mm deflection at centre with the load value 65.76 KN, 57.67KN and 65.35 KN.

Table- 4.7 ***SKEW SLAB SPECIMEN 1 LOAD V/S DIFFLECTION COMPARISION***

	LOAD					Deflection				
Sr No	**Experimental Data**	**FE Model**	**Model with EDGE Support**			**Experimental Data**	**FE Model**	**Model with EDGE Support**		
			100x150	**130x150**	**150x150**			**100x150**	**130x150**	**150x150**
1	5	5.1	20.3	16.13	23.22	5.5	0.9	1	1	1
2	10	11.93	39.12	32.05	43.65	7.7	5	5	5	5.01
3	15	16.18	60.83	48.21	63.28	17	10	11.02	10.01	11.02
4	20	21.52	77.05	62.62	81.38	24.7	15	16.03	15.02	16.03
5	25	26.01	81.21	73.92	85.44	29.3	20	21.88	21.01	22.17
6	30	30.16	62.22	65.58	59.69	40	25	27.13	25.95	26.78
7		7.77	58.62	55.22	54.3		30.27	32.52	31.1	32.21
8		7.04	61.3	55.38	60.05		35.48	37.56	36.28	37.12
9		6.92	65.76	57.67	65.35		40.59	41.57	41.26	42.1

TABLE - 4.8 SKEW SLAB SPECIMEN 1 LOAD V/S UPLIFT AT ACUTE CORNER 1 COMPARISION

	LOAD					Uplift 1				
Sr No	**Experimental**	**FE Model**	**Model with EDGE Support**			**Experimental**	**FE Model**	**Model with EDGE Support**		
			100x150	**130x150**	**150x150**			**100x150**	**130x150**	**150x150**
1	5	5.1	20.3	16.13	23.22	0	0.024	0.03	0.04	0.02
2	10	11.93	39.12	32.05	43.65	0.3	0.162	0.22	0.23	0.22
3	15	16.18	60.83	48.21	63.28	0.1	0.341	0.6	0.5	0.56
4	20	21.52	77.05	62.62	81.38	1	0.514	0.92	0.83	0.89
5	25	26.01	81.21	73.92	85.44	1.22	0.689	1.15	1.18	1.14
6	30	30.16	62.22	65.58	59.69	1.65	0.867	0.95	1.21	0.84
7		7.77	58.62	55.22	54.3		0.948	0.83	1.04	0.67
8		7.04	61.3	55.38	60.05		1.07	0.81	0.99	0.7
9		6.92	65.76	57.67	65.35		1.18	0.85	1.01	0.75

TABLE 4.9 SKEW SLAB SPECIMEN 1 LOAD V/S UPLIFT AT ACUTE CORNER 2 COMPARISION

	LOAD					Uplift 2				
Sr No	**Experimental**	**FE Model**	**Model with EDGE Support**			**Experimental**	**FE Model**	**Model with EDGE Support**		
			100x 150	130x 150	150x 150			100x 150	130x 150	150x 150
1	5	5.1	20.3	16.13	23.22	0	0.0238	0.03	0.04	0.02
2	10	11.93	39.12	32.05	43.65	0.3	0.162	0.21	0.22	0.22
3	15	16.18	60.83	48.21	63.28	0.1	0.341	0.59	0.49	0.55
4	20	21.52	77.05	62.62	81.38	1	0.514	0.91	0.82	0.86
5	25	26.01	81.21	73.92	85.44	1.22	0.689	1.14	1.18	1.11
6	30	30.16	62.22	65.58	59.69	1.65	0.867	0.94	1.2	0.82
7		7.77	58.62	55.22	54.3		0.835	0.82	1.03	0.66
8		7.04	61.3	55.38	60.05		0.933	0.8	0.97	0.68
9		6.92	65.76	57.67	65.35		1.026	0.85	0.99	0.73

B) Specimen-2

1. The deflection at skew slab specimen 2 in which the short diagonal of slab is greater than its span along the traffic. It can be seen from that the structure behaved linearly elastic up to the value of load sheer 57.7 KN, 56.08 KN in the two specimen where as the Specimen with 100x 150 edge support, the load keeps on increasing and reaches 27.94 KN. At this point the minor cracks started to get generated at bottom part (tensile zone) of the slab. After this point there is a slight decrement in curvature in the plot and deflection started increasing. When the deflection reached to the value of 20.2 mm, 21.01 mm & 20.2 respectively, the graph depicted non-linearity in its behavior and crack widened and extended up to the free edges. After these load points, increase in deflection is more with uplifts occurred at acute corners. As the load increases uplifts at acute corners started increasing. The uplift at acute corners has been observed to be 0.89mm, 0.447mm &0 .633 mm. As the uplifts increases there is a rapid increase in displacement is observed. When the deflection reached to these value mm there is sudden decrement in load.. Subsequently deflection started increasing with significant decrement in load; it has reached to the value of 30.29mm, 31.94mm & 32.32mm with the load value 27.94 KN, 22.09 KN & 20.4 KN.

2. It can be observed that there were some uplifts at skew slab acute corners of specimen 2. It can be seen from that the structure behaved linearly elastic up to the value of load 57.7 KN, 56.08 KN . After this point as the uplifts increases at the both acute corners, load started decreases. There is sudden fall in curvature after the value of uplift 0.811 mm. both the uplifts started increasing without any slight difference. Maximum uplifts have been noticed 1.47mm,.987mm & 2.63mm at one corner and .38mm, 1.08mm & 2.63mm at other corner of slab.

Table- 4.10 ***SKEW SLAB SPECIMEN 2 LOAD V/S DIFFLECTION COMPARISION***

	LOAD					Deflection				
Sr No	**Experimental**	**FE Model**	**Model with EDGE Support**			**Experimental**	**FE Model**	**Model with EDGE Support**		
			100x150	**130x150**	**150x150**			**100x150**	**130x150**	**150x150**
1	5	6.58	4.48	14.38	15.33	4.9	0.9	1	1	1
2	10	15.52	14.22	31.66	31.64	5.6	5	5	5	5.05
3	15	21.7	17.32	42.08	42.57	11.4	10	10.1	10.01	10.1
4	20	27.64	20.21	51.93	53	16.6	15	15.15	15.02	15.15
5	25	33.26	22.75	57.7	56.08	22.2	20	20.2	21.01	20.2
6	30	38.77	25.31	28.93	23.95	26.7	25	25.25	26.19	26.74
7	35	12.03	27.94	22.09	20.4	30.5	31.4	30.29	31.94	32.32

TABLE - 4.11 SKEW SLAB SPECIMEN 2 LOAD V/S UPLIFT AT ACUTE CORNER 1 COMPARISION

	LOAD					Uplift 1				
Sr No	**Experimental**	**FE Model**	**EDGE Support**			**Experimental**	**FE Model**	**EDGE Support**		
			100x150	**130x150**	**150x150**			**100x150**	**130x150**	**150x150**
1	5	6.58	4.48	14.38	15.33	0	0.014	-1.138	-0.241	-0.266
2	10	15.52	14.22	31.66	31.64	0	0.133	-0.157	-0.274	-0.315
3	15	21.7	17.32	42.08	42.57	0	0.299	0.267	-0.077	-0.107
4	20	27.64	20.21	51.93	53	0	0.462	0.631	0.138	0.108
5	25	33.26	22.75	57.7	56.08	0	0.632	0.89	0.447	0.633
6	30	38.77	25.31	28.93	23.95	0	0.811	1.003	0.928	2.06
7	35	12.03	27.94	22.09	20.4	0	0.905	1.47	0.987	2.63

TABLE - 4.12 SKEW SLAB SPECIMEN 2 LOAD V/S UPLIFT AT ACUTE CORNER 2 COMPARISION

	LOAD					Uplift 2				
Sr No	**Experimental**	**FE Model**	**EDGE Support**			**Experimental**	**FE Model**	**EDGE Support**		
			100x150	**130x150**	**150x150**			**100x150**	**130x150**	**150x150**
1	5	6.58	4.48	14.38	15.33	0	0.0144	-0.18	-0.24	-0.27
2	10	15.52	14.22	31.66	31.64	0	0.133	-0.46	-0.27	-0.31
3	15	21.7	17.32	42.08	42.57	0	0.299	-0.31	-0.05	-0.1
4	20	27.64	20.21	51.93	53	0	0.462	-0.13	0.15	0.12
5	25	33.26	22.75	57.7	56.08	0	0.632	0.04	0.46	0.63
6	30	38.77	25.31	28.93	23.95	0	0.811	0.21	0.9	2.06
7	35	12.03	27.94	22.09	20.4	0	0.905	0.38	1.08	2.63

CHAPTER - 5, CONCLUSIONS & RECOMMENDATIONS

In the present work, F.E. model for skew slabs with any degree of skew angle and aspect ratio developed using ATENA. The non-linear response of RCC skew slab specimens using FE Modelling under the incremental loading has been carried out with the intention to study the relative importance of several factors in the non-linear finite element analysis of RC skew slabs.

5.1 CONCLUSIONS

Skew slab bridges may be required to maintain the geometry of the road or keep the road straight at crossing or for any other reason. Design-aids and plans for skew bridges suggested by IRC are applicable for skew angle 15^0, 30^0, 45^0, and 60^0 and for some selective spans only. Various researchers have used the yield criterion for normal and skew slabs, for predicting the collapse load. It has been noticed that the skew slabs using bridges with short diagonal less than its span causes lifting of acute corners under loading, whereas other does not. The study of skew slabs simply supported on two opposite rigid supports revealed the following fact.

Skew slab simply supported on two opposite sides can be devided into two types depending on the shape and behavior of slabs.

1. Skew slab with ratio of short diagonal to span less than unity.
2. Skew slab with ratio of short diagonal to span greater than unity.

Skew slabs with ratio of short diagonal to its span less than unity shows lifting of acute corners therefore these are not recommended for the construction and it is suggested that skew slabs with ratio of short diagonal greater than unity should be constructed and preferred by selection of suitable geometrical parameters.

The conclusions drawn are summarized below:

Conclusion Specimen - 1:-

- .Finite element analysis using non-linear models of cracked concrete, steel bars is used to
    - Predict the behaviour of skew slab. It is verified that the finite element analysis can accurately predict the load deformation, load capacity and cracking behavior process similar to the experiment.

- The results of FE model of the skew slabs have found to be higher by 5% of the experimental results. So it can be concluded that FE model results holds good with the experimental results though they are on slightly higher side.

- By introducing Edge supports in the skew slab the load carrying capacity has significantly increased and the Uplifts has been minimized to a greater extent. The Load carrying capacity has been almost increased by 2.5 times.

Conclusion specimen 2 :-

- The general behavior of the finite element models with three different edge supports represented by the load-deflection curves show that the load carrying capacity of the skew slab has been increased. This increase has initiated some uplift at corners which is within the permissible limits.

5.2 RECOMMENDATIONS

The literature review and analysis procedure utilized in this thesis has provided useful insight for future application of a finite element method for analysis. FEM model helps in comparing the results with experimental results data. Modelling the RCC skew slab specimens in FEM based ATENA software gives good results which can be included in future research.

5.3 FUTURE SCOPE

Skew slab with short diagonal /span < 1 show lifting of acute corners. Therefore it is required to anchor the acute corners with the supports and that changes its yield pattern and axis of rotation. Also two negative yield lines will generate at supports thereby changing and increasing its collapse load in this case of fixed supports. Further, it is required to design special anchorage or joint with the abutment that restrict lifting but allows expansion or contraction of the slab due to temperature at the same time.

REFERENCES;

1. **Madhu Sharma, (2011**)." *Finite element modelling of RCC skew slab,"*From Thapar University Panjab M.E.Thises.

2. **Kassahun K. Minalu, (2005),"***Finite element modelling of skew slab-girder bridges,"*From Technical university of deft

3. **S. B.Tamsekar and K. S. Jangde.,** "*guidelines for bridge design."* Designs Circle, Konkan Bhavan,Navi Mumbai

4. **Kwak, H.G., Fillipou, C.F**.(1990) *" Finite Element Analysis of Reinforced Concrete Structures Under Monotonic Loading***"** Structural Engineering Mechanics and Materials**,** Report no. UCB/ SEMM-90/14.

5. **Mohammad, Khaleel and Rafik.** *"Live load moment for continuous skew bridges".* September 1990, Journal of Structural Engineering, pp. 1-13.

6. **Mabsout. et. al. "***Finite Element Analysis of Steel Girder Highway Bridges."* s.l. : Journal of Bridge Engineering,1(3), 1997.

7. **Mirzabozorg, Khaloo and.** s.l."*.Load Distribution Factors in Simply Supported Skew bridges."* Journal of bridge engineering © ASCE, July/August 2003, Vols. 8, No 4.

8. **Huang, Shenton, and Chajes.** s.l."*Load Distribution for a Highly Skewed Bridge"* Journal of Bridge Engineering, , November, 2004, Vols. Vol. 9, No. 6.

9. **Maher Shaker Qaqish**, " *Effect of skew angle on distribution of bending moments in bridge slab*." Journal of applied sciences., pp, 366-372 ,2006.

10. **Menassa, Mabsout, Tarhiniand Frederick. "***Influence of Skew Angle on Reinforced Concrete Slab Bridge."*. : the Journal of Bridge Engineering, March 1, 2007, Vols. Vol. 12, No. 2.

11. **Misra, Trilok Gupta and Anurag. "***Effect on support reactions of t-beam skew bridge decks."* s.l. : ARPN Journal of Engineering and Applied Sciences, FEBRUARY 2007, Vols. VOL. 2, NO. 1.

12. **Sawko, F. and Cope, R. J**., "*The Analysis of Skew Bridge Decks - a New Finite Element Approach*," The Structural Engineer, vol. 47, pp. 215–224, June 1969.

13. **Cusens, A. R. and Besser, I. I**., "*Elastic Stress Parameters in Simply Supported Skew Plates in Flexure*," Journal of Strain Analysis, vol. 15, no. 2, pp. 103–111, 1980

14. **Barzegar, F. and Maddipudi, S**., "*Generating Reinforcement in FE Modeling of Concrete Structures*," ASCE Journal of the Structural Division, vol. 120, pp. 1656– 1662, May 1994

15. **James A. Kankam and Habib J. Dagher**, " *Nonlinear FE analysis of RC Skewed slab Bridges*," Journal of structural engineering, vol 121, No. 9, 1995

16. **Denton S.R. and Burgoyne C.J**.' *The assessment of reinforced concrete slabs*.' Journal of structural engineer. Vol. 74.pp 147-152, May (1996)

17. **Bruce W. Golley.**, "*Shear and Reaction distributions in continuous skew composite bridges,*" Journal of Bridge engineering, vol. 1, No. 4, 1998

18. **Phuvoravan, K. and Sotelino, E. D**., "*Nonlinear Finite Element for Reinforced Concrete Slabs*," ASCE Journal of the Structural Division, vol. 131, pp. 643–649, April 2005.

19. **Hossain, K. M. A and Olufemi, O.O**., " *Design Optimization of simply supported concrete slabs by finite element modeling*," ASCE Journal of the Structural Division, vol. 124, pp.76-88, January 2005.

20. **Jain S.C., Kennedy**, "*Yield Criterion for reinforced Concrete Slabs*", Journal of structural division, ASCE,pp 631-664,Vol.100,No.ST3,March1973.

21. **Baur,D. and Redwood, R.G**., "*Numerical Method for Lower –Bound Solution of the rigid-Plastic Limit Analysis Problem*", Journal of Engineering Mechanics, pp1075-1081, Vol127, No. 4, 1987

22. **Valentin Quintas** , ' *Two main Methods for Yield Line Analysis of Slabs* ', Journal of Engineering Mechanics, pp 223-231, Vol. 129. No.2, 2003.

23. **Johansen K.W**., "*Yield Line Theory*", Cement and Concrete Association London, 1967.

24. **Sharma B.R.** (2009). Report on "*Flexural Behaviour of Reinforced Cement Concrete Skew Slabs***"** Pg 1-48.

25. **Singhal, H.** (2009), **"***Finite Element Modeling of Retrofitted RCC Beams"* M.E. Thesis, Thapar University, Patiala.

26. *ATENA theory manual, part 1 from* **Vladimir Cervenka, Libor Jendele and Jan Cervenka**.

27. **AASHTO. _2003_**. *Standard specifications for highway bridges*, Washington,D.C.

28. **Dagher.H. Elgaaly, M., Kankam, J.A., Comstock, L."** *Skewed slab bridges with integral slab abutments*, vol. 1 to VI ," Prepared for Maine DOT, Dept. of civil engrg; University of Maine, Orono. (1991)

29. **Mawenya, A.S., and Davis, J. D**." *Finite Element bending analysis of Multilayer plates*." Lnt.J. Numer methods Engrg., 8, 215-225. 1974.

30. *Standard Plans for highway bridges*, vol- ll(concrete slab bridge) published by IRC, **ministry of shipping and transport**, Gol.

31. **ATENA 3D** and ATENA WIN "*finite element software manuals"*.